

IL
NUOVO CIMENTO

ORGANO DELLA SOCIETÀ ITALIANA DI FISICA

SOTTO GLI AUSPICI DEL CONSIGLIO NAZIONALE DELLE RICERCHE

VOL. XII, N. 6

Serie nona

1° Dicembre 1954

████████████████████

ENRICO FERMI

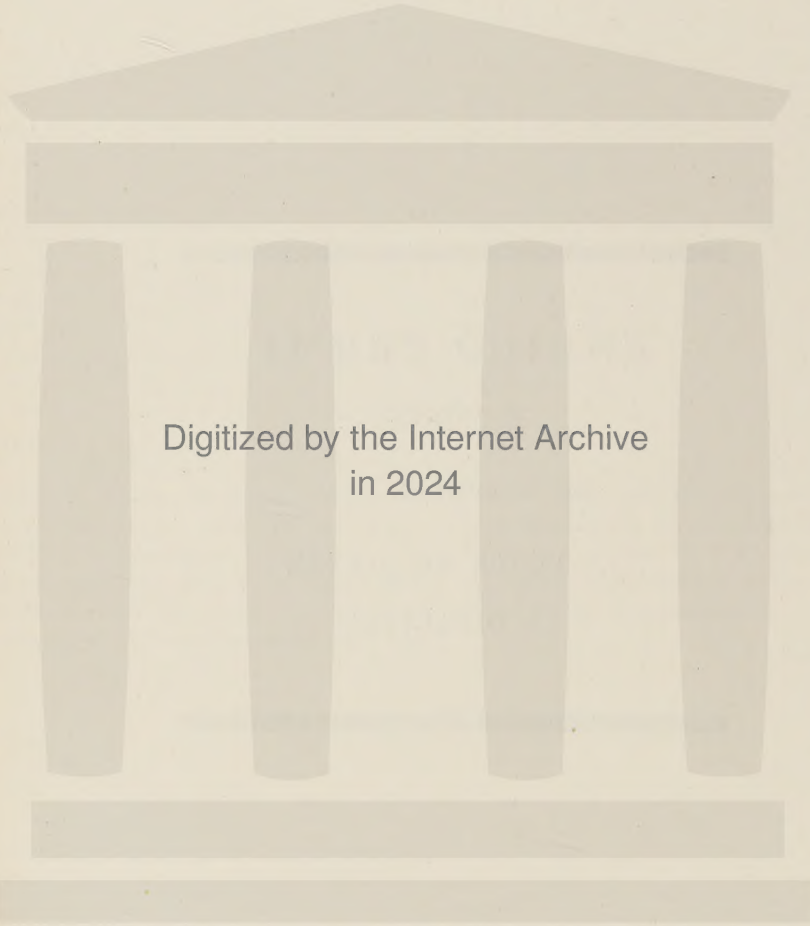
È MORTO

28 NOVEMBRE 1954

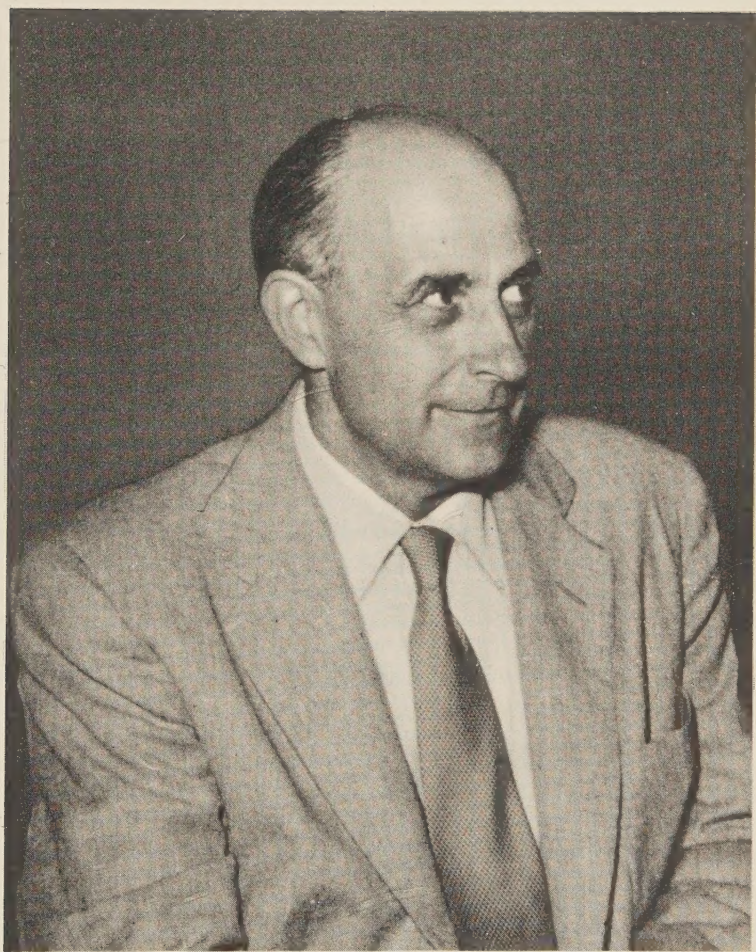
LA FISICA NE PIANGE

LA DIPARTITA

████████████████████



Digitized by the Internet Archive
in 2024



Enrico Fermi

Questo quartino va preposto alla pag. 825.

Conformal Geometry and Elementary Particles.

R. L. INGRAHAM

Institute for Advanced Study, Princeton, New Jersey

(ricevuto il 2 Settembre 1954)

Summary. — The kinematical consequences of basing (classical or quantum) field theory on the conformal geometry are examined in this paper. The space in question is that of all spheres in R_4 (flat 4-space of signature $(+++ -)$); the fundamental invariant, the angle under which two spheres intersect. In the mathematical preliminaries (§ 1) a convenient inhomogeneous formalism is developed, permitting the sphere to be treated as a point in a 5-dimensional Riemannian space of constant unit curvature whose length element is the infinitesimal angle between two neighboring spheres. The conformal group (proper Lorentz transformations, translations, uniform dilations, and inversions in spheres) is just the 15-parameter group of motions (metric-preserving transformations) of this space. In § 2 the spheres are interpreted as finite (non localized) test particles. Physical fields are thus defined on test particles rather than (e.g. in position space) on the events occupied by these test particles alone. The spheres can be labelled either with the 5-position (test particle's space-time position and *size*) in a q -frame, or with the 5-momentum (test particle's 4-momentum and rest mass) in a p -frame. There exists a motion transforming q - into p -space and conversely (in other words, q - and p -observers are physically equivalent), in virtue of which any conformal theory is shown to exhibit an automatic *Born-reciprocity* between q - and p -space. The 5-position and 5-momentum satisfy an uncertainty-relation type equation; i.e., the non-localizations in q - and p -space are in an inverse relation with Planck's \hbar measuring the intrinsic correlation. All the other motions can be built up from subgroups taking q - and p -space into themselves. These are systematically interpreted as changes of frame. Those involving relative motion represent *uniform* relative accelerations of Lorentz observers (Lorentz group \longleftrightarrow zero accelerations). Test particle mass and size are invariant under the Lorentz group but non-uniformly renormalized by the accelerative motions. In § 3 the geodesics of sphere space (motion equations of (elementary) test particles) are

shown to describe uniform motion in the present (force-free) case. Test particles tend to dislocalize in q space with increasing time and in p -space with increasing energy. The time-constancy of the 5-momenta, their inter-dependence as given by special relativity dynamics follow from these motion equations. Free elementary particles are shown to maintain a state of uniform velocity under all motions, in particular the accelerative ones. This contradicts ordinary relativity and suggests an experiment capable in principle of choosing between the conformal and Lorentz geometries for physics.

1. - Introduction.

This paper is an attempt to indicate the common features of all physical theories based on the conformal group in Minkowski space as fundamental group. By fundamental group is understood that group of coordinate transformations under which the field laws are form-invariant, or, equivalently stated, that group connecting the preferred coordinate systems representing the physically equivalent observers of the theory. The fundamental group of the standard classical and quantized field theories of today is (at most) the ten-parameter one of Lorentz transformations and space-time translations; to attain the fifteen-parameter conformal group one adjoins the uniform dilations and inversions in space-time hyperspheres⁽¹⁾. The last-mentioned transformations are non-linear and, roughly speaking, it is to their presence in the fundamental group that most of the novel features are due. Our subject is thus pure kinematics, independent of the particular form of the field laws considered. Already at this stage much with physical content can be said. The physical interpretation of the geometry (2·3) shows that the finite size of test (elementary) particles takes its place alongside space-time as a bona-fide dimension of physical space, for example. This new degree of freedom naturally brings with it the appearance of another fundamental dimensional constant, Planck's h , alongside c in the angle metric. Again, any such theory must exhibit a perfect reciprocity between position and momentum space (2·3). The five independent dimensions in the latter picture are test particle momentum, energy, and rest mass. Or again, free particle behavior is determinable at this stage (3·2). The persistence of uniform motion under certain accelerative changes of frame, contradicting relativity kinematics, suggests a simple experiment capable of choosing between the conformal and Lorentz geometries for physics.

A sequel to this paper treats the consequences of a particular set of (linearized) field laws in this geometry. Gravitation, electron, and light in particular are described.

(1) Our terminology will in general ignore signature. Thus a space-time «hyper-sphere» is a hyperboloid as a real locus.

The conformal group is actually a group of projective transformations on the X_5 ⁽²⁾ of spheres in Minkowski space, in which the events themselves are represented as null spheres. Physical fields get 6^p components with respect to the six homogeneous (« hexaspherical ») coordinates of these spheres and a convenient tensor formalism in which the fundamental group is represented by linear transformations with constant coefficients is usable (2.1). An equivalent inhomogeneous formalism of tensors with 5^p components is developed (2.2) and used in preference to the homogeneous formalism because of its more immediate physical meaning. Because of their relative unfamiliarity in physics, these necessary mathematical preliminaries are worked out systematically at some length. In the conventional treatment ⁽³⁾ one thus has various differential laws for homogeneous 6-tensors whose domain of definition is restricted to the X_4 of null spheres. One essential difference of the present theory from the conventional treatment is that not only the null, but also the non-null, spheres form the domain of definition of the physical fields; i.e., the physical continuum from which we start is five-dimensional. (Indeed, this theory shows that the X_4 of null spheres, far from sufficing as the physical domain, plays a rather exceptional role.) We need the X_5 of all the spheres for both for mathematical and physical reasons. Mathematically, the force-free and weak field theories treated in this paper and the sequel resp. must be considered as a degenerate case of the rigorous theory, for which the proper curvilinear generalization of C_4 ⁽²⁾ is the geometrical framework. The unique correct generalization of C_4 (the prototype being the generalization of euclidean by Riemannian geometry) must start from an underlying X_5 ; the arguments, which are not directly relevant to this paper, cannot be given here ⁽⁴⁾. Previous attempts ⁽⁵⁾ to generalize the ordinary conformal geometry C_n invariably started from an underlying X_n and were on these grounds alone,

⁽²⁾ Alphabet conventions: late roman letters $k, l, m, \dots = 1, \dots, 4$; early greek letters $\alpha, \beta, \gamma, \dots = 1, \dots, 5$; late greek letters $\mu, \nu, \xi, \dots = 0, 1, \dots, 5$.

Notation: $X_n = n$ -dimensional manifold

$C_n =$	»	conformal geometry
$R_n =$	»	flat (Riemannian) space
$P_n =$	»	ordinary projective space
$V_n =$	»	Riemannian space.

⁽³⁾ E.g., P. DIRAC: *Ann. of Math.*, **37**, 429 (1936).

⁽⁴⁾ R. INGRAHAM: *Proc. Nat. Acad. Sci.*, **38**, 921 (1952); *Nuovo Cimento*, **9**, 886 (1952).

⁽⁵⁾ H. WEYL: *Sitz. d. Preuss. Akad. d. Wiss.*, 465 (1918), *Raum, Zeit, Materie* 5. Aufl. Berlin, 1923), §§ 40, 41; E. CARTAN: *Ann. Soc. Pol. Math.*, 171 (1923); T. Y. THOMAS: *Proc. Nat. Acad. Sci.*, **18**, 103 (1932); O. VELEN: *Proc. Nat. Acad. Sci.*, **21**, 168 (1935); J. A. SCHOUTEN and J. HAANTJES: *Math. Ann.*, **112**, 594 (1936); **113**, 568 (1936).

mathematically unsatisfactory. The lack of success of their application to physics is thus not surprising. The physical arguments, on the other hand, for the X_5 are what this paper aims, in part, to supply in some detail.

A final general remark: the necessary adjunction of a fifth dimension to space-time, the expansion of the standard class of equivalent observers, the tensors with 6^n components, etc., all the features that point toward the possibility of a real unification of physical fields flow automatically from the one assumption that the fundamental physical geometry is conformal. The unification is, so to speak, an incidental by-product of this assumption. It is not a question of examining impartially a whole spectrum of logical possibilities. Physicists who distrust the aimless formal adventuring of much of so-called « unified field » theory should take comfort from the fact that here the motivation is quite different.

2. — The Force Free-World.

2.1. *The sphere space M_5 .* — Let $g_{mn}(g_{11}=g_{22}=g_{33}=-g_{44}=1, g_{mn}=0 (m \neq n))$ be the metric referred to orthonormal cartesian coordinates $x^m (m=1, \dots, 4)$ of the R_4 ⁽²⁾ of special relativity. Then the sphere ⁽¹⁾ of center x^m and radius (real or pure imaginary) R can be assigned six homogeneous coordinates ⁽⁶⁾ $X^\mu (\mu=0, 1, \dots, 5)$ via

$$(2.1) \quad \begin{cases} \tau X^0 = 1, & \tau X^m = x^m, & \tau X^5 = \frac{1}{2}((x)^2 - R^2) \\ [(x)^2 \equiv g_{mn}x^m x^n, & \tau \neq 0 \text{ a proportionality const.}] \end{cases}$$

Since they are homogeneous, that is, under the modular group

$$(2.1)' \quad X^\mu \rightarrow \varrho X^\mu \quad [\varrho \neq 0, \text{ const.}]$$

the set of numbers X^μ goes into another set ϱX^μ representing the same sphere, the X^μ can be interpreted as cartesian (« preferred ») projective coordinates of a point in an ordinary five dimensional projective space P_5 ⁽²⁾. A transformation of cartesian coordinates in P_5

$$(2.2) \quad X^{\mu'} = A^{\mu'}_\nu X^\nu \quad [\text{Det } A^{\mu'}_\nu \neq 0, A^{\mu'}_\nu = \text{constants}]$$

corresponds to a linear change of sphere basis. In this P_5 the locus of the null spheres ($R=0$) is by (2.1) the quadric Q :

$$(2.3) \quad g_{mn}X^m X^n - 2X^0 X^5 = 0.$$

The quadric Q defines the projective tensor $G_{\mu\nu}$ ($\text{Det } G_{\mu\nu} \neq 0$) via

$$(2.4) \quad \sigma G_{mn} = g_{mn}, \quad \sigma G_{05} = -1, \quad \text{other } G_{\mu\nu} = 0; \\ [\sigma \neq 0 \text{ a proportionality const.}]$$

⁽⁶⁾ On polyspherical coordinates, see say F. KLEIN: *Vorlesungen über Höhere Geometrie*, 3 Aufl. (Berlin, 1926), p. 49.

that is, under the modular group

$$(2.4)' \quad G_{\mu\nu} \rightarrow \lambda G_{\mu\nu} \quad [\lambda \neq 0, \text{const.}]$$

the components $G_{\mu\nu}$ go into the components $\lambda G_{\mu\nu}$ representing the same quadric, and under the coordinate group (2.2) $G_{\mu\nu}$ transforms cogrediently to X^μ :

$$(2.5) \quad G_{\mu'\nu'} = A_{\mu'}^\rho A_{\nu'}^\xi G_{\rho\xi} \quad [A_{\nu'}^{\mu'} A_{\xi'}^\nu = A_{\xi'}^{\mu'} \equiv \delta_{\xi'}^{\mu'}].$$

The space P_5 falls into two disjoint regions Q^+ and Q^- , the exterior and interior of Q , resp.. X^μ non-null ε Q^+ or Q^- according as $\text{Sgn } G_{\rho\xi} X^\rho X^\xi = +1$ or -1 , resp.. Let X^μ and Y^ν be two non-null spheres in the same region; then the fundamental invariant, the angle θ_{xy} under which they intersect, is defined by

$$(2.6) \quad \left\{ \begin{array}{l} \cos \theta_{xy} \equiv \varepsilon \frac{G_{\mu\nu} X^\mu Y^\nu}{|(X)| |(Y)|} \\ [(X)^2 \equiv G_{\lambda\xi} X^\lambda X^\xi \neq 0, \text{ etc.}; \text{Sgn } (X)^2 = \text{Sgn } (Y)^2 = \varepsilon] \end{array} \right.$$

The invariance of (2.6) under the coordinate group (2.2) and both modular groups (2.1)' and (2.4)' shows that this angle is a well defined sphere geometrical concept. The classical sphere space of R_4 is now invariantly defined as the space P_5 with the tensor $G_{\mu\nu}$ representing the quadric of null spheres; its fundamental angle invariant is given by the formula (2.6).

The *flat Möbius space* M_5 used by the author is the same sphere space trivially generalized to allow the proportionality factors τ , ϱ , σ , and λ in (2.1), (2.1)', (2.4) and (2.4)' resp. to be (non-vanishing, differentiable) functions of the sphere (7). We shall be working exclusively in this geometry for the rest of the paper. We recall the connection of M_5 with conformal transformations of R_4 : every conformal (8) transformation $\bar{x}^m = f^m(x^\nu)$ in R_4 is represented by a constant linear sphere transformation $\bar{X}^\mu = P^\mu_\nu X^\nu$, where the P^μ_ν satisfy

$$(2.7) \quad G_{\mu\nu} P^{-1\mu}_\lambda P^{-1\nu}_\xi = \lambda G_{\rho\xi},$$

$$[\text{for some } \lambda; P^{-1\mu}_\lambda P^\lambda_\nu = \delta^\mu_\nu; \text{Det } P^\mu_\nu > 0],$$

in the sense that the null sphere $X^\mu \longleftrightarrow (x^m, R=0)$ via (2.1) goes into the null sphere $\bar{X}^\mu \longleftrightarrow (\bar{x}^m = f^m(x^\nu), \bar{R}=0)$ via (2.1). This correspondence between the

(7) The reason for this is that the curvilinear M_5 (cf. (4)) is defined as an X_5 provided with the variable tensor $G_{\mu\nu}(X^\rho)$ homogeneous of degree zero whose tangent spaces are classical sphere spaces as defined above. When coordinates X^ρ can be found for which $G_{\mu\nu}(X^\rho) = \sigma(X^\rho) g_{\mu\nu}$, $g_{\mu\nu}$ constants, σ homogeneous of degree zero, the space is said to be flat; in this case, all the tangent spaces can be identified. The resulting flat sphere space, M_5 , is then identical with the classical sphere space except for the difference mentioned above.

(8) Angle preservation in both sense and magnitude is implied.

conformal group and M , the group of sphere transformations P^μ_ν satisfying (2.7), is in fact an isomorphism. M will be called the group of *conformal sphere transformations* — by (2.7) and (2.6) the transformations of non-null spheres are conformal also in the sense that they preserve the angle⁽⁸⁾ between spheres. M is the group of *motions* of M_5 for by (2.7) it takes the tensor $G_{\mu\nu}$ into itself. M is thus also the fundamental group (see Introduction) of any physical theory built on the space M_5 .

The angle metric, which expresses the infinitesimal angle between two neighboring non-null spheres in terms of their coordinate differences, is arrived at in the following way. Suppose that X^μ and $X^\mu + dX^\mu$ are coordinates of the neighboring spheres in one point gauge, i.e., for some definite function $\tau(X^e)$ in (2.1). (Of course, it will have to be proved a posteriori that our result is independent of the point gauge, that is, invariant under the modular group (2.1)'). Then the application of (2.6) yields (App. I)

$$(2.8) \quad d\theta^2 = \gamma_{\mu\nu} dX^\mu dX^\nu,$$

where

$$(2.9) \quad \text{a) } \gamma_{\mu\nu} \equiv S_{\mu\nu} - X_\mu X_\nu, \quad \text{b) } S_{\mu\nu} \equiv \frac{G_{\mu\nu}}{(X)^2}, \quad \text{c) } X_\mu \equiv S_{\mu\epsilon} X^\epsilon$$

and $(X)^2$ has been defined in (2.6). We note at once the invariance of (2.7) against the coordinate and quadric-modular groups (2.2) and (2.4)' resp.. The less trivial invariance against the point-modular group (2.1)': $dX^\mu \leftrightarrow \varrho dX^\mu + d\varrho X^\mu$ follows from

$$(2.10) \quad \gamma_{\mu\nu} X^\nu = 0.$$

We shall call the tensor $\gamma_{\mu\nu}$ the *angle metric*. It is singular of rank 5 (cf. (2.10)), invariant under the group (2.4)', and under the group (2.1)', it gets the factor ϱ^{-2} . $S_{\mu\nu}$ is non-singular, invariant under the group (2.4)', gets the factor ϱ^{-2} under the group (2.1)', and satisfies the identity $S_{\mu\nu} X^\mu X^\nu = 1$. For the physical application only $S_{\mu\nu}$ and $\gamma_{\mu\nu}$ are relevant; no further mention need be made of $G_{\mu\nu}$ and its modular group (2.4)'.

Note the close analogy between the angle metric (2.8) and Riemannian length metric. In the next section we show that $d\theta^2$ is actually the element of length in a simple Riemannian space. Moreover this inhomogeneous formalism seems to be the most convenient for the physical interpretation.

2.2. The Riemannian formalism. — To express $d\theta^2$ in terms of a convenient set of inhomogeneous sphere coordinates, say x^m and $x^5 \equiv |R|$, let us go to

a point gauge in which $\tau=1$ in (2.1). In this point gauge

$$dX^0 = 0, \quad dX^m = dx^m, \quad dX^5 = x_m dx^m - \varepsilon x^5 dx^5 \quad [x_m \equiv g_{mn} x^n]$$

and

$$S_{\mu\nu} = \varepsilon(x^5)^{-2} g_{\mu\nu}, \quad X_\mu = \varepsilon(x^5)^{-2} g_{\mu\lambda} \xi^\lambda,$$

where ξ^λ and $g_{\mu\nu}$ are the right members in (2.1) and (2.4) resp.. $\varepsilon \operatorname{sgn} R^2$ is of course the same ε that occurs in (2.6). Substituting these values in (2.8), we get ⁽²⁾

$$(2.11) \quad d\theta^2 \equiv \gamma_{\alpha\beta}^e dx^\alpha dx^\beta = \varepsilon(x^5)^{-2} ((dx)^2 - \varepsilon(dx^5)^2). \quad [(dx)^2 \equiv g_{mn} dx^m dx^n]$$

$d\theta^2$ is thus expressed as the element of length in a certain five-dimensional Riemannian space ⁽²⁾ V_5 . Actually there are two V_5 's: V_5^+ , whose points are all the spheres lying in $Q^+(\varepsilon=+1)$ and V_5^- , whose points are all the spheres lying in $Q^-(\varepsilon=-1)$. Their metrics are $\gamma_{\alpha\beta}^+ = + (x^5)^{-2} g_{\alpha\beta}^+$ and $\gamma_{\alpha\beta}^- = - (x^5)^{-2} g_{\alpha\beta}^-$ resp. in these coordinates, where

$$(2.11') \quad g_{mn}^e = g_{mn}, \quad g_{5m}^e = 0, \quad g_{55}^e = -\varepsilon.$$

These metrics are infinite for $x^5=0$, so the null spheres are boundary points, limit spheres of non-null spheres which belong to neither V_5 .

It is easy to show ⁽⁹⁾ that the V_5 are of constant curvature $+1$. Hence we are using the device of studying angle-geometry by studying the metric geometry of the unit sphere about the origin ⁽⁹⁾.

We shall call the x^α *natural coordinates* for the V_5^e . They have direct geometrical meaning for the sphere (x^m =center, x^5 =radius), the null spheres are immediately recognizable in them ($x^5=0$), and the angle metric has an especially simple form in them. What now does a conformal sphere transformation look like in natural coordinates? The general form is easily worked out from (2.7) and (2.1). We give here the 15-parameter group M broken down, for the sake of the physical application, into subgroups.

⁽⁹⁾ Precisely: if R_6^e are the flat spaces with metrics $eg_{\mu\nu}$ in the cartesian coordinates Z^μ , then the V_5^e are the unit spheres Σ^e :

$$eg_{\mu\nu} Z^\mu Z^\nu = 1$$

in the R_6^e resp. via the imbedding

$$Z^0 = 1/x^5, \quad Z^m = x^m/x^5, \quad Z^5 = 1/2(x^5)^{-1}((x)^2 - \varepsilon(x^5)^2).$$

(cf. EISENHART: *Riemannian Geometry* (Princeton, 1926), p. 204. The constant curvature $+1$ of the V_5^e follows immediately from this.

$$(2.12) \quad \left\{ \begin{array}{ll} \text{a)} & \bar{x}^m = L^m_n x^n, \quad \bar{x}^5 = x^5 \quad [\text{proper Lorentz group, 6 parameter}] \\ \text{b)} & \bar{x}^m = x^m + a^m, \quad \bar{x}^5 = x^5 \quad [\text{space-time translations, 4 parameter}] \\ \text{c)} & \bar{x}^\alpha = \mu x^\alpha, \quad \mu > 0, \text{ const.} \quad [\text{uniform dilations, 1 parameter}] \\ \text{d)} & \bar{x}^1 = \Delta^{-1}(x^1 + \alpha[x]^2/2), \quad \bar{x}^i = \Delta^{-1}x^i \quad (i = 2, 3, 4), \quad \bar{x}^5 = \Delta^{-1}x^5 \\ & \quad [[x]^2 \equiv g_{mn}x^m x^n - \varepsilon(x^5)^2, \quad \Delta \equiv 1 + \alpha x^1 + \alpha^2[x]^2/4] \quad [1 \text{ parameter}] \\ \text{e-f)} & \text{formula d) with the permutations of the space indices (123)} \\ & \quad \text{and (132) resp.} \quad [2 \text{ parameter}] \\ \text{g)} & \bar{x}^j = D^{-1}x^j \quad (j = 1, 2, 3), \quad \bar{x}^4 = D^{-1}(x^4 + \beta[x]^2/2), \quad \bar{x}^5 = D^{-1}x^5 \\ & \quad [D \equiv 1 - \beta x^4 - \beta^2[x]^2/4] \quad [1 \text{ parameter}] \\ \text{h)} & \bar{x}^\alpha = -\frac{x^\alpha}{[x]^2} \quad [\text{fundamental inversion}]. \end{array} \right.$$

In d), e), f) and g) α, \dots , etc., and β are parameters. The inverses are given by $\alpha \rightarrow -\alpha$, etc., $\beta \rightarrow -\beta$. These are 1-parameter groups involving inversions, hence their non-linearity. Any transformation of M connectable to the group identity can be decomposed into a product of transformations a), ..., g); adjoining the fundamental inversion, we get the whole group. For instance, any inversion (inversion in any sphere) is the product of a translation, a dilation, and the fundamental inversion.

The basic fact about M for the Riemannian formalism is that it is the group of *motions* of the V_5^ε , the metric is form-invariant under M :

$$(2.13) \quad d\theta^2 = \varepsilon(x^5)^{-2}((dx)^2 - \varepsilon(dx^5)^2) = \varepsilon(\bar{x}^5)^{-2}((d\bar{x})^2 - \varepsilon(d\bar{x}^5)^2) \\ [(d\bar{x})^2 \equiv g_{mn}d\bar{x}^m d\bar{x}^n].$$

The proof is obvious for the subgroups a), b) and c); for d), ..., h) it will be omitted here ⁽¹⁰⁾. This completes the mathematical preliminaries.

2.3. Physical interpretation of the sphere space. — The metric (2.11) implies that we are confronted in nature with a five-dimensional physical continuum, i.e., that five independent numbers are needed for the complete specification of the physical «point». This statement may be argued pro and con on a priori grounds; the only meaningful criterion is the success or failure of the physical theory built upon this geometry. Accordingly, we make certain identifications without further justification, and remark their various physical consequences as they are developed.

⁽¹⁰⁾ These motions are the proper rotations about the origin in the spaces R_6^ε carrying the unit spheres Σ^ε into themselves, cf. footnote ⁽⁹⁾.

Say the x^ν have the physical dimension L — with this interpretation we will call our space *position space* (q -space). (By (2.11) $d\theta^2$ is dimensionless, as it should be.) We connect them with the physical variables — the directly measured quantities — of dimensions L , T , and M^{-1} as follows

$$(2.14) \quad x^1 = x, \text{ etc.}, \quad x^4 = ct, \quad x^5 = \frac{\hbar\omega}{c},$$

where c and \hbar ($=2\pi\hbar$) are light velocity and Planck's constant resp.; x, y, z, t are position and time relative to a Lorentz frame; the physical significance of ω , the *mass-gauge*, will be treated shortly. The fundamental angle form in terms of these variables is

$$(2.15) \quad d\theta^2 = \varepsilon \left(\frac{\hbar\omega}{c} \right)^{-2} \left(dr^2 - c^2 dt^2 - \varepsilon \frac{\hbar^2}{c^2} d\omega^2 \right), \quad [dr^2 = dx^2 + dy^2 + dz^2].$$

The fundamental inversion (2.12) h takes x^ν of any physical dimension into \bar{x}^ν of the inverse dimension. Therefore if we have assumed $\text{Dim } x^\nu = L$, we must also admit the interpretation $\text{Dim } x^\nu = L^{-1}$. We will call the x^ν , when interpreted with the dimension L^{-1} , k^α : (contravariant) *5-wave number* and the space with this interpretation, *wave number space* (k -space). Or, equally well, defining p^α : (contravariant) *5-momentum* of dimension MLT^{-1}

$$p^\alpha = \hbar k^\alpha,$$

we can call it *momentum space* (p -space). In this conjugate interpretation we introduce the physical variables of dimensions L^{-1} , T^{-1} , and M via

$$(2.16) \quad k^1 = k_x, \text{ etc.}, \quad k^4 = \nu/c, \quad k^5 = \frac{c}{\hbar} m.$$

Read: k_x , etc., and ν are wave number and frequency (radians time $^{-1}$) relative to a Lorentz frame, and m is rest mass. Or, for physical variables of dimensions MLT^{-1} , ML^2T^{-2} , M , via

$$(2.16)' \quad p^1 = p_x, \text{ etc.}, \quad p^4 = E/c, \quad p^5 = cm.$$

Read: p_x , etc., and E are momentum and energy relative to a Lorentz frame; m as before. It follows from these definitions that $p_x = \hbar k_x$, etc., $E = \hbar\nu$: if one set of physical variables is taken as primary, the other is defined by these relations. In terms of the physical variables of the wave number or

momentum space interpretation $d\theta^2$ takes the form

$$(2.17) \quad d\theta^2 = \varepsilon \left(\frac{cm}{\hbar} \right)^{-2} (dk^2 - c^{-2} dp^2 - \varepsilon c^2 / \hbar^2 dm^2), \quad [dk^2 \equiv dk_x^2 + dk_y^2 + dk_z^2]$$

$$(2.17)' \quad d\theta^2 = \varepsilon (cm)^{-2} (dp^2 - c^{-2} dE^2 - \varepsilon c^2 dm^2), \quad [dp^2 \equiv dp_x^2 + dp_y^2 + dp_z^2].$$

The above implies that in any theory built on sphere space, the physical fields are defined not just over position or wave-number space, but over both spaces. If we wish to consider position and momentum as the conjugate pair (as we shall generally do), substitute

$$(2.18) \quad p^\alpha = -\hbar x^\alpha / [x]^2, \quad x^\alpha = -\hbar p^\alpha / [p]^2$$

for (2.12)h). Because the transformations (2.18) are motions, an automatic reciprocity between q - and p -space results, having the aspects: 1) any equation of the theory in q -space gives *another* true equation in p -space on the substitution $x^\alpha \rightarrow p^\alpha$, or

$$(2.19) \quad x \rightarrow p_x, \text{ etc.}, \quad t \rightarrow E/c^2, \quad \omega \rightarrow c^2 m / \hbar,$$

and conversely; 2) any solution for the fields relative to a q -frame tensorially transformed under (2.18) gets new components representing the *same* solution relative to the associated p -frame, and conversely. Call the transformation (2.18) *Born conjugation* and the pair of properties (1) and (2) *Born reciprocity* after the foremost exponent of these ideas in modern physics. We remark that the points on the cones

$$(2.20) \quad [x]^2 = 0, \quad [p]^2 = 0,$$

play an exceptional role — their conjugate points $p^\alpha = \infty$ ($\alpha = 1, \dots, 5$), etc., coalesce and are called the infinite point. This automatic Born reciprocity is absent in theories based on special relativity because their group of motions, (2.12) a) and/or b), which leave unchanged the physical dimension, cannot carry one from one space to the conjugate space.

The 5-uple x^α will be interpreted as the labels necessary to specify completely a *test particle at an event*. Call this pair of things a *particle state* or *state* for short (« state » will also designate the 5-uple of numbers x^α or (\mathbf{r}, t, ω) , etc., labelling the state where no confusion can arise ⁽¹¹⁾). The test particle figures here only in its instantaneous aspect; one should not think of it as having any « identity » or « continuous existence » in time. E.g., it is meaningless to

⁽¹¹⁾ Cf. the corresponding usage of « event » in special relativity.

ask for the position of «the test particle» of the state (\mathbf{r}, t, ω) at some later time. The motion of test particles (free and under forces) is described by paths of particle states which are integrals of the motion equations (§ 3). Hence a test particle in this theory has *five* degrees of freedom as compared to the usual four. In the momentum picture these are \mathbf{p} , E , m : momentum, energy, and rest mass, which are thus assumed in general independent ⁽¹²⁾. In the position picture \mathbf{r} and t label its position relative to a Lorentz frame and ω , the mass-gauge, or $\hbar\omega/c$, the associated Compton wave length of this mass-gauge, is some measure of its finite size. We get a tentative idea of the model of the finite particle implied by the theory as follows. The state (\mathbf{r}, t, ω) corresponds to the sphere (hyperboloid as a real locus) of center \mathbf{r} , t and radius $\hbar\omega/c$

$$(2.21) \quad (\xi - \mathbf{r})^2 - c^2(\tau - t)^2 = \varepsilon (\hbar\omega/c)^2$$

in the space-time of coordinates (ξ, τ) ; indeed, this is its primary geometric meaning in this theory. This hyperboloid is the locus of all events influenceable ($\tau \geq t$) by our finite test particle at the event (\mathbf{r}, t) by signals propagating with light velocity — with the proviso that relative to the point ξ , it behaves like a disc of radius $\hbar\omega/c$ centered at \mathbf{r} perpendicular to $\xi - \mathbf{r}$ and capable of radiating signals only from its rim. Call $\hbar\omega/c$ the *size* of the particle. Note that by (2.18) under Born conjugation $\omega = 0 \rightarrow m = 0$ and $\omega \neq 0 \rightarrow m \neq 0$. In other words, test particles of finite and zero size have finite and zero mass resp. in the conjugate momentum picture, and conversely. For a null test particle (zero size, hence zero mass) the hyperboloid (2.21) degenerates into the light cone of the associated event.

We shall make the hypothesis that the meaning of these hyperboloids is that a test particle has an intrinsic non-localization in space-time varying directly with its size. Then it might be fruitful to identify the particle with this whole hyperboloid of events — evidently this depends critically on the observational significance of «particle». Similarly, in the momentum-energy variables $(\boldsymbol{\pi}, \eta)$ the hyperboloid

$$(2.21') \quad (\boldsymbol{\pi} - \mathbf{p})^2 - c^{-2}(\eta - E)^2 = \varepsilon (mc)^2$$

will mean an intrinsic non-localization of the test particle's momentum and energy which varies directly with its mass. A «Heisenberg conjugacy» ⁽¹³⁾ of 5-momentum and 5-position for particle states follows directly from the

⁽¹²⁾ For the free particle, the expected dependence occurs as a consequence of the motion equations (3.2).

⁽¹³⁾ W. HEISENBERG: *Die Physikalischen Prinzipien der Quantentheorie* (Leipzig, 1944), 4 Aufl., Kap. 2.

definition (2.18) of Born conjugation. For the product $[px] - \mathbf{p} \cdot \mathbf{r} - Et - \varepsilon \hbar \omega m$ satisfies

$$(2.22) \quad [px] = -\hbar.$$

If x^α and p^α are considered the 5-component quantities necessary to handle the size and mass covariantly, this says that the «5-size» and «5-mass» are related in a bilinear equation of uncertainty relation form. The action constant \hbar is a measure of the intrinsic correlation between «5-size» and «5-mass», i.e., between the localization in q - and p -space of the associated test particle.

A conceptual difference with former theories should be noted. Here the q -coordinates of a particle state *determine* the associated p -coordinates via (2.18), and conversely. The p^α are just another kind of coordinate, of different physical dimension from the x^α . The relation of the p 's to the velocity for a moving test particle comes out of the motion equations (§ 3).

Force fields are defined by means of their action on test particles. The field strengths at events unoccupied by particles not only do not come into question, but, strictly speaking, it is meaningless to ask for these values. This fundamental feature of the field concept is here automatically taken into account. For in this theory the fields will be defined on particle states, so that it will be impossible to give the value of a field at an event without specifying at the same time a test particle there on which it is to act. Whence the value of the field becomes the actual force on that test particle. The fact that the fields are functions of ω or m more complicated⁽¹⁴⁾ in general than a simple proportionality implies also an abandonment of the classical concept of the «field strength» where it sufficed to know the force on a test particle of unit source strength (charge, mass, etc.) to specify it for test particles of all strengths. This permitted the suppression of the particle source strengths from the domain of definition of the fields.

The question of the building of the *Möbius frames*, i.e., by what operations with physical meters (generic term for measuring device) we arrive at the numbers (\mathbf{r}, t, ω) or (\mathbf{p}, E, m) labelling a state is a deep one, meriting separate treatment, and cannot be properly gone into here. If we call the gauge-meter a *scale* for convenience, a *Möbius observer* for position space will be a Lorentz observer provided with a scale at each event to measure the sizes of test particles there. The exact constitution of a scale, which obviously depends on the observational significance of the hyperboloids (2.21), is not clear at the moment. We emphasize that only the coincidence of states has absolute significance for the class of Möbius observers, not the coincidence of events or test

⁽¹⁴⁾ Although in certain familiar cases (e.g., field of a resting gravitating particle) it reduces to the simple proportionality (cf. sequel).

particles sizes separately ⁽¹⁵⁾. The null test particles are special in that their zero size or zero mass remain zero on change of observer. It is probable, however, that light and the electron can be used in the definition *ab initio* of the Möbius frames by postulating that they propagate in them according to

$$(2.22) \quad \left\{ \begin{array}{l} \text{a) } dr^2 - c^2 dt^2 \equiv -c^2 d\tau^2 = 0, \quad d\omega = 0 \\ \text{b) } -c^2 d\tau^2 - \varepsilon \frac{\hbar^2}{c^2} d\omega^2 = 0, \end{array} \right. \quad [\tau \equiv \text{proper time}]$$

resp. in position space and

$$(2.23) \quad \left\{ \begin{array}{l} \text{a) } dk^2 - c^{-2} dv^2 \equiv -c^{-2} dv_0^2 = 0, \quad dm = 0 \\ \text{b) } -c^{-2} dv_0^2 - \varepsilon \frac{c^2 dm^2}{\hbar^2} = 0 \end{array} \right. \quad [v_0 \equiv \text{proper frequency}]$$

resp. in wave number space. With the aid of a length-meter (rod) and light one would first lay out the Lorentz frames as in special relativity (equations a); then the scales would be superimposed using the electron (equations b). Later results (§ 3 and the sequel) for free photon and electron motion are compatible with these assumptions. Here c and \hbar play the role of *conventional* constants — arbitrary but fixed numbers which serve to define and calibrate clocks and scales in terms of a given rod by *requiring* that light and electron propagation obey (2.22) a) and b) resp. for position space; correspondingly for wave number space. This description for constructing (properly set and calibrated) clocks and scales in terms of a given rod by using light and electrons can be said to constitute the «rigidity» of the Möbius observer.

The above interpretation of the angle metric then leads to the following enunciation. The quantities $d\tau$ (proper time) and $d\omega$ are separately non-invariant for the class of all Möbius observers. In the combination (2.15) however formed with the aid of the dimensional constants \hbar and c , they build the dimensionless invariant $d\theta^2$ of a sphere space M_3 . Correspondingly for dv_0 and dm in the conjugate space. Cf. obviously the analogous situation for length and time and the invariant $d\tau^2$ of the R_4 of special relativity.

2.4. *Physical interpretation of the group of motions.* — A physical interpretation of the mathematical transformations (2.12) means: given a Möbius observer M representing one system x^λ , an operationally meaningful prescription for recognizing, or building, the unique other Möbius observer \bar{M} representing the transformed system \bar{x}^λ . We recall the basic fact that because of the «rigidity» of the Möbius observer, it is not necessary to specify the behavior of all the elements making up the observer under the transformation. E.g., in

⁽¹⁵⁾ Cf. the analogous non-absoluteness of simultaneity.

(2.12) a) it is sufficient to give the (constant) velocity vector of one space point fixed in \bar{M} relative to M .

Since a Möbius observer is in particular a Lorentz observer, the proper Lorentz group a) and the space-time translations b) have their well known interpretations here. Their inclusion in the fundamental group makes any theory built on sphere space both isotropic and homogeneous in space-time. Under both groups ω is invariant, which means that test particle sizes are not renormalized. By (2.15) the cross-section X_1 of the space composed of all particle states with the same size $\hbar\omega/c$ behaves under these two groups like the special relativistic R_1 with the invariant length element $\hbar\omega d\theta/c$.

The motions c

$$\mathbf{r} \rightarrow \mu\mathbf{r}, \quad t \rightarrow \mu t, \quad \omega \rightarrow \mu\omega$$

are interpreted as uniform renormalizations (dilations) of the rods, clocks, and scales of a Möbius observer. By rigidity it is sufficient to prescribe that the rods dilate in the ratio μ^{-1} .

Physical interpretation of d): Let M and \bar{M} be Möbius observers initially ($t = \bar{t} = 0$) coincident, and N and \bar{N} resp. the space frames belonging to them. Then d) is interpreted as a translatory relative motion of N and \bar{N} such that \bar{O} , the origin of \bar{N} , performs the motion

$$(2.24) \quad x + (\alpha/2)(x^2 - c^2 t^2) = 0, \quad y = z = 0$$

in N . This is a uniform acceleration $a = \alpha c^2$ of \bar{O} along the x axis of N such that initially \bar{O} coincides with O , N 's origin, and is at rest with respect to it ⁽¹⁶⁾. Relativistic uniform acceleration is of course meant here (« Hyperbelbewegung »), defined shortly as ordinary uniform acceleration at every moment in an instantaneous rest frame. Then this physical interpretation of the mathematical transformation is a *law*; it makes experimentally verifiable predictions about the deformation of the material structures defining the Möbius observer on uniform acceleration. These deformations will be treated in detail below. The statement, «The velocity of light is constant, equal to c , for all Möbius observers», is another way of stating one aspect of this same law. Similarly for a statement about electron propagation and the constant \hbar , cf. (2.22) b). Note that this group of accelerative motions renormalizes the sizes $\hbar\omega/c$ of test particles non-uniformly depending both on the sizes and on the associated events. Another feature of the accelerative motions: test particles of different size at the same event for an observer correspond to different events as seen by an accelerated observer.

⁽¹⁶⁾ J. HAANTJES: *Proc. Ned. Akad. Wet.*, **43**, 1288 (1940); E. L. HILL: *Phys. Rev.*, **72**, 143 (1947).

The physical interpretation of the group g) is not known at present, though it must represent some sort of uniform relative acceleration of clocks. Again the size of test particles is non-uniformly renormalized, etc..

We know that the physical interpretation of Born conjugation (2.18) is the change from position observer to momentum observer (q -observer to p -observer for short) or vice-versa, hence its precise prescription must be an idealization of the change from q -measuring apparatus to p -measuring apparatus as it is actually performed in the laboratory. This difficult job will not be attempted here. Two general remarks will have to suffice. First: well known arguments⁽¹⁷⁾ on the nature of our measuring apparatus show that there is an ineradicable conjugate indeterminacy in our readings of particle position and momentum, due to the disturbance of one on measuring the other. This then means that in *any* consistent theory of particles which talks about their positions and momenta, this conjugate indeterminacy must be derivable mathematically from the axioms of the theory, if the theory claims to describe particles in the domain where these effects are not negligible. E.g., in quantum mechanics, whose mathematical framework is an operator ring on Hilbert space, the way in which the indeterminacy relations are derived from the axioms is well known. In the case of this theory, whose mathematical framework differs from that of quantum mechanics, these same physical arguments for the necessity of having a conjugate p - q indeterminacy in the theory then support some such conjugate non-localizability interpretation as we have made of eq. (2.22). Second: Born conjugation takes all the states with $[x]^2 > 0$ into unphysical images ($p^5 = mc < 0$), which must be interpreted as the p -unobservability, or unobservability of the momenta, of these states. We will say that the p -frame is *polarized* with respect to the cone $[x]^2 = 0$ which marks the boundary between the p -observable ($[x]^2 < 0$) and p -unobservable ($[x]^2 > 0$) states. This p -unobservability can be tentatively explained as follows. The associated p -frame cannot be regarded as instantaneously established throughout position space, rather it must be initiated at a definite time and place and built out from there with a finite velocity of extension. (E.g., if it consists of devices for sending and receiving signals, the velocity of extension cannot exceed the speed of the signals.) This explanation accords with general quantum mechanical views on the limitations of measuring apparatus, and is supported by the analysis of free particle motion under Born conjugation (3.2)⁽¹⁸⁾

Let C stand for Born conjugation. Then the motion T in the wave number

⁽¹⁷⁾ W. HEISENBERG: *op. cit.*, Chap. II and III.

⁽¹⁸⁾ Then the new q -frames defined by (2.12)d), e) and f), which take the cones $\Delta = 0$, etc., $D = 0$ into the infinite state (in position space) must evidently be regarded as polarized in the same sense with respect to these cones.

picture can be physically interpreted as the motion *OTC* in the position picture, which latter has been discussed above. Due to the perfect reciprocity between the two pictures, however, *T* should admit a direct interpretation without reference to the position picture ⁽¹⁹⁾.

The deformation of a small rod fixed in *M* at the state (\mathbf{r}, t, ω) as seen by \bar{M} , related to *M* by the accelerative motion (2.12) d), is obtained by computing $\partial\bar{x}/\partial x$ (parallel orientation) and $\partial\bar{y}/\partial y$ (transverse orientation, along *y*) and substituting for the x^α their values in terms of the \bar{x}^α . We get

$$(2.25) \quad \begin{cases} \frac{\partial\bar{x}}{\partial x} = \bar{\Delta} - (\alpha^2/2) \left(\bar{y}^2 + \bar{z}^2 - c^2 \bar{t}^2 - \varepsilon \frac{\hbar^2 \bar{\omega}^2}{c^2} \right), \\ \frac{\partial\bar{y}}{\partial y} = \bar{\Delta} - (\alpha^2/2) \bar{y}^2; \quad [\bar{\Delta} \equiv 1 - \alpha\bar{x} + (\alpha^2/4)[\bar{x}]^2]. \end{cases}$$

The similarly defined clock-period and mass-gauge (or test particle size) deformations at the state $(\bar{\mathbf{r}}, \bar{t}, \bar{\omega})$ are, resp.

$$(2.25)' \quad \frac{\partial\bar{t}}{\partial t} = \bar{\Delta} + (\alpha^2/2) c^2 \bar{t}^2, \quad \frac{\partial\bar{\omega}}{\partial \omega} = \bar{\Delta} + \varepsilon (\alpha^2/2) \frac{\hbar^2 \bar{\omega}^2}{c^2}.$$

Unlike the case of uniform relative velocity, the deformations depend on position in the space. In the range $(\alpha v^\beta)^2 \ll a\bar{v}$, ($\beta=1, \dots, 5$) the proportional deformations $\frac{\partial\bar{x}}{\partial x} - 1$, etc., are all the same and equal to

$$(2.26) \quad -a\bar{x}/c^2.$$

They are thus proportional both to the acceleration and the abscissa. A case for which these effects might be observable is the recession of the galaxies. The empirical law of red-shifts ⁽²⁰⁾ for the galaxies G_i ($i=1, 2, \dots$) at distances r_i from our galaxy \bar{G} is

$$\delta\lambda/\lambda = kr_i, \quad (> 0),$$

where $k \cong 5.7 \cdot 10^{-26} \text{ cm}^{-1}$. Now if the galaxies G_i are assumed to be fixed on the *x*-axes of Möbius frames $M_{(i)}$, initially coincident with frames $\bar{M}_{(i)}$ in each of which our galaxy \bar{G} is fixed at the space origin, all in the *same* uniform relative acceleration (magnitude $A > 0$) along the \bar{x} -axes of the corresponding

⁽¹⁹⁾ We mention in particular that test particle masses are invariant under translations and Lorentz transformations but are non-uniformly renormalized by the accelerative motions.

⁽²⁰⁾ E. HUBBLE: *The Observational Approach to Cosmology* (Oxford, 1937), p. 25.

$\bar{M}_{(i)}$, then by (2.26) the wave length λ of an atomic spectral line emitted from G_i will suffer the shift

$$\delta\lambda/\lambda = (A/c^2)r_i,$$

toward the red ($\delta\lambda/\lambda > 0$) as seen by \bar{G} . This agrees with the empirical law, and gives the small acceleration $A \cong 5.7 \cdot 10^{-5} \text{ cm s}^{-2}$.

From the exact expressions (2.25), (2.25)' it is seen that for a given acceleration a the distance \bar{d} from the origin for which the proportional deformation is of the order of unity is defined by $a\bar{d}/c^2 \cong 1$. It is interesting that this formula also defines the beginning of the wave zone of an accelerated particle in classical Maxwell theory, namely the distance \bar{d} from a charged particle moving with acceleration a at which the radiative begins to dominate the Coulomb field.

3. - Free Particles.

3.1. The geodesics. - The geodesics are the paths of minimum (or stationary) angle in the sphere space M_5 . A simple intuitive idea of them may be obtained by picturing our space as the surface of a ball as in footnote ⁽⁹⁾; they are then the « great circles ». In natural coordinates they come out to be (Appendix II)

$$(3.1) \quad (\text{null geodesic}) \quad \begin{aligned} x^m &= \kappa^m \kappa^{-2} (\sigma + \gamma)^{-1} + \delta^m, \\ x^5 &= \kappa^{-1} (\sigma + \gamma)^{-1} \end{aligned} \quad \left[\kappa \equiv \sqrt{|(\kappa)^2|} \right]$$

and

$$(3.2) \quad (\text{non-null geodesic}) \quad \begin{aligned} x^m &= \kappa^m \kappa^{-2} \operatorname{tg} (\theta + \gamma) + \delta^m, \\ x^5 &= \kappa^{-1} \sec (\theta + \gamma) \end{aligned}$$

where γ and δ^m are constants and $x^5 > 0$ requires $0 < \sigma + \gamma < \infty$, $-\pi/2 < \theta + \gamma < \pi/2$. The condition that x^5 be real imposes the condition on the κ^m

$$\operatorname{Sgn} (\kappa)^2 = \varepsilon.$$

3.2. The free particle paths. - Letting time be the running variable, and introducing new constants to facilitate the physical interpretation, we get the

paths in position space

$$x = v_x(t - t_0) + x_0, \text{ etc.}$$

$$(3.3) \quad (\text{null geodesic}) \quad \omega = \frac{c}{\hbar} |1 - v^2/c^2|^{\frac{1}{2}} c(t - t_0) \quad (t_0 < t < \infty)$$

and

$$(3.4) \quad (\text{non-null geodesic}) \quad \left\{ \begin{array}{l} x = v_x(t - t_0) + x_0, \text{ etc.} \\ \omega = \frac{c}{\hbar} |1 - v^2/c^2|^{\frac{1}{2}} \left[c^2(t - t_0)^2 + \left(\frac{\lambda_0}{1 - v^2/c^2} \right)^2 \right]^{\frac{1}{2}} \\ \quad (-\infty < t < \infty) \end{array} \right.$$

where we have set $\kappa^4 = \lambda_0^{-1}$, $\kappa^1 = v_x/c\lambda_0^{-1}$, etc., $v^2 = v_x^2 + v_y^2 + v_z^2$, $\delta^1 = x_0$, etc., $\delta^4 = ct_0$, and the sign condition on $(\kappa)^2$ becomes $\text{Sgn}(1 - v^2/c^2) = -\epsilon$. Note that the path (3.3) is independent of λ_0 , corresponding to its invariance under the dilation group (2.12) c).

The geodesics interpreted as paths in wave number or momentum space are given at once by making the substitution of Born reciprocity $x^\alpha \rightarrow k^\alpha$ or $x^\alpha \rightarrow p^\alpha$ in (3.1), (3.2). Equivalently, for momentum space say, we make the substitution (2.19) in (3.3), (3.4), rename the constants λ_0 , \mathbf{v} , \mathbf{r}_0 , and t_0 resp. \hbar/l_0 , \mathbf{u} , \mathbf{p}_0 , and E_0/c^2 . We get

$$(3.5) \quad \left\{ \begin{array}{l} (\text{null geodesic}) \quad \left\{ \begin{array}{l} p_x - p_{0x} = u_x \frac{(E - E_0)}{c^2}, \text{ etc.}, \\ m = |1 - u^2/c^2|^{\frac{1}{2}} \frac{(E - E_0)}{c^2}; \end{array} \right. \\ \\ (\text{non-null geodesic}) \quad \left\{ \begin{array}{l} p_x - p_{0x} = u_x \frac{(E - E_0)}{c^2}, \text{ etc.}, \\ m = |1 - u^2/c^2|^{\frac{1}{2}} \left\{ \left(\frac{E - E_0}{c^2} \right)^2 + \left(\frac{\hbar/l_0 c}{1 - u^2/c^2} \right)^2 \right\}^{\frac{1}{2}} \end{array} \right. \end{array} \right.$$

where the constants \mathbf{u} are subjected to the sign condition on the \mathbf{v} . (3.5) is more familiar in the form

$$(3.5)' \quad \left\{ \begin{array}{l} p_x - p_{0x} = \frac{m u_x}{|1 - u^2/c^2|^{\frac{1}{2}}}, \text{ etc.}, \quad E - E_0 = \frac{m c^2}{|1 - u^2/c^2|^{\frac{1}{2}}} \quad (u \neq c) \\ p_x - p_{0x} = \frac{(E - E_0)}{c} i_x, \text{ etc.}, \quad (i = \mathbf{u}/u), \quad m = 0 \quad (u = c) \end{array} \right.$$

in which m rather than E is the running variable for $u \neq c$.

We are thus led to interpret the geodesics as paths of free particles in uniform motion with constant velocity \mathbf{v} or \mathbf{u} ⁽²¹⁾. \mathbf{r} and $\hbar\omega/c$ are the position and size at time t of the free particle for a q -observer; alternatively \mathbf{p} and m are its momentum and rest mass at energy E for a p -observer ⁽²²⁾. Formula (3.5)' is a particularly strong theoretical support of the physical interpretation of § 2. And it has permitted us to normalize away a pure number factor in the fifth component of the metric (2.17)' undetermined on dimensional grounds alone.

The momenta of the free particles (3.3), (3.4) are calculated by Born conjugating these solutions. The details are given in App. III. Here we will treat only the case of the null geodesics. We get trajectories (3.5)' with the constants ⁽²³⁾

$$(3.7) \quad \mathbf{p}_0 = \frac{\hbar \mathbf{r}_0}{c^2 t_0^2 - r_0^2}, \quad \frac{E_0}{c} = \frac{\hbar c t_0}{c^2 t_0^2 - r_0^2}, \quad \mathbf{u} = \left(1 - \frac{2c t_0 c(t_0)_{\text{ret}}}{c^2 t_0^2 - r_0^2}\right)^{-1} \left(\mathbf{v} - \frac{2c^2(t_0)_{\text{ret}}}{c^2 t_0^2 - r_0^2} \mathbf{r}_0\right),$$

where

$$(3.8) \quad (t_0)_{\text{ret}} \equiv t_0 - \frac{\mathbf{v} \cdot \mathbf{r}_0}{c^2}.$$

Since the transformation gives m (or E) as a function of t , we can also give these their time-dependent form:

$$(3.9) \quad \mathbf{p} = \frac{m(\mathbf{v} + \mathbf{r}_0/(t - t_0))}{|1 - v^2/c^2|^{\frac{1}{2}}}, \quad E = \frac{mc^2}{|1 - v^2/c^2|^{\frac{1}{2}}} \left(\frac{t}{t - t_0}\right) \quad (v \neq c).$$

with

$$\frac{mc}{\hbar} = |1 - v^2/c^2|^{\frac{1}{2}} \left(2c(t_0)_{\text{ret}} + \frac{c^2 t_0^2 - r_0^2}{c(t - t_0)}\right)^{-1}$$

and

$$(3.9)' \quad \mathbf{p} = E/c^2 (\mathbf{v} + \mathbf{r}_0/(t - t_0)) \left(\frac{t - t_0}{t}\right), \quad m = 0 \quad (v = c)$$

with

$$E = \hbar \left(2(t_0)_{\text{ret}} + \frac{c^2 t_0^2 - r_0^2}{c^2(t - t_0)}\right)^{-1} \left(\frac{t}{t - t_0}\right).$$

⁽²¹⁾ The sign condition on the \mathbf{v} and \mathbf{u} seems to exclude $\varepsilon = +1$, as giving space-like motion to free particles. Moreover, $\varepsilon = +1$ make the spheres (2.21), (2.21)' representing a test particle related space-like to their centers.

⁽²²⁾ Incidentally, the problem of the « identity » of a particle through time disappears. We simply agree to call a 1-dimensional schar of particle states in which the position and size coordinates depend on the time coordinate as in (3.5) or (3.6) « a » free particle enduring in time.

⁽²³⁾ $u = c \longleftrightarrow v = c$; cf. App. III.

Asymptotically in time p and E go over into the expressions (3.5)' for constants $p_0 = E_0 = 0$, $u = v$ in terms of the (asymptotically) constant rest mass m_∞ and energy E_∞ resp. given by

$$(3.10) \quad \frac{m_\infty c}{\hbar} = \frac{|1 - v^2/c^2|^{\frac{1}{2}}}{2c(t_0)_{\text{ret}}}, \quad E_\infty = \hbar \nu_\infty \quad [\nu_\infty \equiv \frac{1}{2}(t_0)_{\text{ret}}^{-1}]$$

p , E , and m are thus (asymptotically) constant in time for the free particle, moreover, the p -velocity u is just the q -velocity v .

The following interpretation of the temporal behavior (3.9) and (3.9)' of the free particle momenta is a plausibility argument for the tentative explanation of the existence of p -unobservable states as due to their situation outside the domain of the gradually established p -frame (cf. 2.4). The key, we repeat, is to interpret unphysical values as the p -unobservability of the corresponding state. Now for the particles (3.3) $[x]^2 \leq 0$ asymptotically if and only if $(t_0)_{\text{ret}} \geq 0$. A particle with $(t_0)_{\text{ret}} < 0$ would thus be asymptotically p -unobservable, from which we conclude that it is completely outside the domain of the p -frame and the temporal behavior (3.9), (3.9)' without significance⁽²⁴⁾. A particle with $(t_0)_{\text{ret}} > 0$ (whose path states are thus eventually p -observable) may be called a p -observable particle, and its history analyzed thus: by (3.9), (3.9)' the interval (t_0, ∞) breaks into the two parts (t_0, t_{cr}) , (t_{cr}, ∞) , where $t_{\text{cr}} = t_0 + (r_0^2 - c^2 t_0^2)/2c^2(t_0)_{\text{ret}}$. E (or m) < 0 in the first interval, meaning that the p -frame has not yet «arrived at» the free particle. At the critical time $t = t_{\text{cr}}$, the moment of «arrival», the momenta are infinite. In the second interval E (or m) > 0 and decreases monotonely to the positive lower bound (3.10) at $t = \infty$. In this transient phase the momenta are observable and settling down to constant values as the perturbation due to the establishment of the p -frame attenuates. A certain spectrum of asymptotic masses or frequencies depending on $(t_0)_{\text{ret}}$ is obtained⁽²⁵⁾. These transient phases are expected to be very short under usual observational conditions. A fuller account of this will be published elsewhere.

By (3.3) the size ($v \neq c$) increases uniformly to infinity, hence these free particles would dislocalize or «disperse» naturally in time with the non-localization meaning of size. On the other hand, if it is p -observable, the mass decreases monotonely in time to a lower bound $m_\infty > 0$. That is, its localization in p -space increases up to a limit measured by m_∞ . For a free particle, then, the passage of time is an agent tending to dislocalize its position and localize its momentum.

⁽²⁴⁾ The tacit assumption here is that a particle can in time enter the domain of a p -frame, but once in, can never leave it.

⁽²⁵⁾ In the case of the non-null geodesics, this spectrum will depend also on λ_0 , i.e., on the initial sizes.

We now constate the remarkable fact that our free particles move with uniform velocity with respect to *all* Möbius observers. These include relatively accelerated observers (this will always mean in the precise sense of the prescription of 2'4). For in (a) of App. II, x^α referred to any Möbius frame. In Einstein relativity, on the other hand, if one of the Lorentz observers of 2'4 is assumed an inertial system, then the other observer, not moving with uniform velocity relative to the first, would be non-inertial, i.e., would feel a gravitational field. A free particle, by definition moving uniformly for the first observer, would perform non-uniform motion for the second, accelerated by this induced gravitational field. Let us say a test particle has the *Galilean property* under a group of changes of frame if whenever it moves uniformly in one frame, it moves uniformly in all frames connected with the first by a transformation of the group. Then we can characterize the situation shortly by saying that in this theory, free particles have the Galilean property under all uniform accelerations; in Einstein relativity, under only the subgroup of uniform velocities.

The explanation of this apparently paradoxical behavior of our free particles on an accelerative motion lies in the behavior of the fifth coordinate. A compensatory change of size takes place, just sufficient to transform uniform motion again into uniform motion (e.g., put (3.1) or (3.2) into (2.12) d)). Size, and this behavior of it, is obviously not to be predicated of macroscopic « particles » — complicated agglomerations of simpler elements — therefore we restrict our interpretation of the geodesics to free *elementary* particles, and the null geodesics, to photons and electrons for reasons which appear in the sequel. $v = c$ defines the photon, which implies by (3.3) and (3.5) that it is a null particle (zero rest mass and size). This is of course a Möbius invariant definition.

The above suggests a fundamental experiment of the Michelson-Morley type capable of choosing for physics between ordinary relativity and sphere space geometry.

Experiment: Observe a free photon or electron from two Lorentz frames relatively accelerated as prescribed in 2'4, one of which, say L , is an inertial system. Then this theory predicts a uniform motion relative to \bar{L} also. Einstein relativity predicts some non-uniform velocity in \bar{L} (the order of magnitude of deflection from uniform motion being that due to a gravitational field of strength $a = \alpha c^2$ in the \bar{x} direction) ⁽²⁶⁾. Note that the observation of uniform space-time motion in \bar{L} would suffice to reject Einstein relativity, quite apart from the behavior of the size whose observation depends on the

⁽²⁶⁾ A « conjugate » experiment in the momentum picture is immediately formulizable.

as yet problematical construction of the scales. The new uniform velocity predicted here is in general different from the old — the formulas are worked out in App. III. The particular path (3.3) with $\mathbf{r}_0 = \mathbf{t}_0 = 0$ however is invariant: $\bar{\mathbf{v}} = \mathbf{v}$, $\bar{\mathbf{r}}_0 = \mathbf{t}_0 = 0$.

Fine point: the prescription of the experiment assumes that we can recognize the force-free world (or force-free part thereof); equivalently, that we know what we mean by «a free particle» and «an inertial system». The difficulties of defining both of these in relativity without circularity, necessitating the introduction of elements logically extraneous to the theory like the «fixed stars», etc., are well known. Without further study we cannot say whether the same logical trouble exists in this theory. Therefore, faute de mieux, «free particle» and «Lorentz frame» for the purposes of the experiment are understood to mean what experimental physics is generally agreed to designate by those names.

One should not conclude from the above-predicted behavior of free particles that there is no «principle of equivalence» for sphere space theories. There exists such a principle here of course, stating that any change of frame ⁽²⁷⁾ *not one of the motions* (2.12) manifests itself as various induced physical forces, including gravitation (cf. the sequel). It differs from Einstein relativity however in having a wider group of motions, whence there exist changes of frame inducing a gravitational field there which induce no force fields in this theory.

In concluding this section, a caveat should be inserted. If the hyperboloids (2.21), (2.21)' really mean non-localized test particles, the observational significance of \mathbf{r} and t , «the position at a time of the particle» in the language of point particles used above, becomes unclear. Evidently an experiment designed to test whether free particles have the Galilean property under uniform acceleration *in the coordinates* \mathbf{r} , t has little chance of success if we do not know how to measure \mathbf{r} and t . Everything depends on the observational meaning of the hyperboloids. The photon, however, is perfectly localized ($\omega = m = 0$), hence it seems that at least for this particle \mathbf{r} and t may be given point particle meaning. In which case the proposed experiment goes through for light.

3.3. *Concluding general remarks.* — The behavior (Galilean property under uniform accelerations) predicted here in particular for free photon and electron, though strange from the viewpoint of macroscopic intuition, is really no odder than the relativistic constancy of light velocity. It suggests that elementary particles are even less like Newtonian billiard balls than we imagine today.

⁽²⁷⁾ Involving relative motion.

It is however at variance with the predictions of Einstein relativity, and therefore a new Michelson-Morley type experiment, this time with uniform relative accelerations, would be very welcome. A clear cut choice between this and the Lorentz geometry could be made, provided only that apparatus could be devised to raise the predicted effects into the observable range. Needless to say, these must be free particles — e.g., no strong electromagnetic fields to accelerate measuring devices could be allowed. In general one might expect that the observation of all elementary particles, free and under forces, under uniform relative acceleration of observers would yield interesting results.

Both classical and quantum electrodynamics suffer from infinities associated with point model particles; the former with divergent electromagnetic masses, etc., the latter with divergent additions to the «mechanical» mass due to the coupling of the matter field with the electromagnetic vacuum, etc. In an electrodynamics couched in this, rather than the Lorentz geometry, changes could be expected. For one thing, this geometry automatically requires finite particles. Even if these infinities subsisted, a re-appraisal of their significance would certainly be demanded. For elementary particle mass here is not an absolute. We found that free particle mass is (after a transient phase) constant in time (2'2), but in the presence of forces it will vary along the path. Moreover, test particle masses are renormalized non-uniformly by any accelerative change of observer. The masses of the particle states on the cone $\Delta = 0$ in (2.12) d) are in fact infinite for the new observer. But this infinity has no coordinate-free significance. These matters will be treated in the sequel.

APPENDIX I

We must evaluate

$$(1) \quad 1 - (d\theta)^2/2 = \cos d\theta = \varepsilon \frac{G_{\mu\nu}(X^\mu + dX^\mu)X^\nu}{|(X)| |(X + dX)|}$$

$$[\varepsilon \equiv \text{Sgn}(X)^2 = \text{Sgn}(X + dX)^2].$$

We have

$$|(X + dX)|^{-1} = |(X)|^{-1} \{1 + 2X_\mu dX^\mu + dX_\mu dX^\mu\}^{-\frac{1}{2}}$$

with $X_\mu \equiv S_{\mu\nu}X^\nu$, $dX_\mu \equiv S_{\mu\nu}dX^\nu$, $S_{\mu\nu}$ as in (2.8). If α is of first order smallness and $\beta \sim 0(\alpha^2)$, then

$$(1 + \alpha + \beta)^{-\frac{1}{2}} = 1 - \alpha/2 + (\frac{3}{8}\alpha^2 - \beta/2)$$

good to second order terms. Substituting $\alpha = 2X_\mu dX^\mu$, $\beta = dX_\mu dX^\mu$ in this, we get the factor $(1 - X_\mu dX^\mu + \frac{3}{2}(X_\mu dX^\mu)^2 - \frac{1}{2}dX_\mu dX^\mu)$ in (1). Multiplying out, first order terms cancel, and we get

$$1 - \frac{1}{2} (S_{\mu\nu} - X_\mu X_\nu) dX^\mu dX^\nu$$

for the right member, from which (2.8) follows.

APPENDIX II

The geodesics are the integral curves of

$$(1) \quad d^2x^\alpha/d\theta^2 + \left\{ \begin{matrix} \alpha \\ \beta\gamma \end{matrix} \right\} (dx^\beta/d\theta)(dx^\gamma/d\theta) = 0$$

where for the null geodesics ($d\theta = 0$ along the curve), $\theta \rightarrow \sigma$, σ any running parameter. In natural coordinates the Christoffel symbols are

$$\left\{ \begin{matrix} p \\ q5 \end{matrix} \right\} = -(1/x^5) \delta_q^p, \quad \left\{ \begin{matrix} 5 \\ pq \end{matrix} \right\} = -(\varepsilon/x^5) g_{pq}, \quad \left\{ \begin{matrix} 5 \\ 55 \end{matrix} \right\} = -1/x^5, \quad \text{other} \quad \left\{ \begin{matrix} \alpha \\ \beta\gamma \end{matrix} \right\} = 0.$$

Putting these in (1) we get

$$\begin{aligned} d^2x^m/d\theta^2 - 2(d \log x^5/d\theta)(dx^m/d\theta) &= 0, \\ d^2x^5/d\theta^2 - (1/x^5)(dx^5/d\theta)^2 - (\varepsilon/x^5)(dx/d\theta)^2 &= 0, \\ [(dx/d\theta)^2 &\equiv g_{mn}(dx^m/d\theta)(dx^n/d\theta)], \end{aligned}$$

$\theta \rightarrow \sigma$ for the null geodesics. This has the immediate first integral

$$(3) \quad dx^m/d\theta = \kappa^m (x^5)^2 \quad [\kappa^m \text{ constants}].$$

From (2.11)

$$(dx^5/d\theta)^2 = -(x^5)^2 + \varepsilon(dx/d\theta)^2$$

and in the null case $\theta \rightarrow \sigma$ and the $-(x^5)^2$ term on the right is absent. Putting $(dx/d\theta)^2 = (\kappa)^2 (x^5)^4$, $(\kappa)^2 \equiv g_{mn} \kappa^m \kappa^n$, from (3) into this, it is easily integrable. Then this solutions for x^5 is put into (3) and the integration performed. We get the solutions (3.1).

APPENDIX III

In computing the change of constants in (3.1) resulting from any motion (2.12), the typical identity to be satisfied is

$$(1) \quad \bar{A}(\sigma + \gamma)^{-1} + \bar{B} = \frac{A^\alpha(\sigma + \gamma)^{-1} + B^\alpha}{C(\sigma + \gamma)^{-1} + D}.$$

We want the new (barred) constants in terms of the old. The fact that the quadratic terms cancel out of the denominator on the right is the characteristic property of the paths (3.1) which makes such an identity possible. Cross-multiplying, etc., and equating coefficients of σ^2 , σ , and 1, we get

$$(2) \quad \begin{cases} D\bar{B}^\alpha = B^\alpha, \\ D\bar{B}^\alpha(\gamma + \bar{\gamma}) + C\bar{B}^\alpha + D\bar{A}^\alpha = B^\alpha(\gamma + \bar{\gamma}) + A^\alpha, \\ D\bar{B}^\alpha\gamma\bar{\gamma} + D\bar{A}^\alpha\gamma + C\bar{B}^\alpha\bar{\gamma} + \bar{A}^\alpha C = A^\alpha\bar{\gamma} + B^\alpha\gamma\bar{\gamma}. \end{cases}$$

These have the solutions

$$(3) \quad \bar{B}^\alpha = B^\alpha/D, \quad \bar{A}^\alpha = \bar{D}^1(A^\alpha - CB^\alpha/D), \quad \bar{\gamma} = \gamma + C/D \quad [D \neq 0]$$

and, if $B^\alpha = 0$, $C \neq 0$

$$(4) \quad \bar{B}^\alpha = A^\alpha/C, \quad \bar{A}^\alpha = 0, \quad \bar{\gamma} = \text{anything} \quad [D = 0].$$

In all other cases the transformed path is indeterminate. For Born conjugation, our constants are (cf. (3.1) and (2.18))

$$\begin{aligned} \bar{A}^m &= \bar{\kappa}^m \bar{\kappa}^{-2}, & \bar{A}^5 &= \bar{\kappa}^{-1}, & \bar{B}^m &= \bar{\delta}^m, & \bar{B}^5 &= 0, \\ A^m &= -\hbar \kappa^m \kappa^{-2}, & A^5 &= -\hbar \kappa^{-1}, & B^m &= -\hbar \delta^m, & B^5 &= 0, \\ C &= 2(\kappa \delta) \kappa^{-2} [(\kappa \delta) \equiv g_{mn} \kappa^m \delta^n], & D &= (\delta)^2, \end{aligned}$$

where these are linked with the « physical » constants in p - and q -space via

$$\begin{aligned} \bar{\kappa} &= (\mathbf{u}/c)(l_0/\hbar), & \bar{\kappa}^4 &= l_0/\hbar, & \bar{\kappa} &= (l_0/\hbar) |1 - u^2/c^2|^{\frac{1}{2}}, & \bar{\delta} &= \mathbf{p}_0, & \bar{\delta}^4 &= E_0/c, \\ \kappa &= (\mathbf{v}/c)(1/\lambda_0), & \kappa^4 &= 1/\lambda_0, & \kappa &= (1/\lambda_0) |1 - v^2/c^2|^{\frac{1}{2}}, & \delta &= \mathbf{r}_0, & \delta^4 &= ct_0. \end{aligned}$$

Then the application (3) gives (3.7) as well as

$$l_0 = \frac{2t_0 \mathbf{v} \cdot \mathbf{r}_0 - (c^2 t_0^2 + r_0^2)}{\lambda_0}, \quad \bar{\gamma} = \gamma + \left(\frac{1}{1 - v^2/c^2} \right) \frac{2c\lambda_0(t_0)_{\text{ret}}}{c^2 t_0^2 - r_0^2},$$

$$\bar{\beta} = \beta \left(1 - \frac{2ct_0 c(t_0)_{\text{ret}}}{c^2 t_0^2 - r_0^2} \right)^{-1}, \quad \beta = |1 - v^2/c^2|^{\frac{1}{2}}, \quad \bar{\beta} = |1 - u^2/c^2|^{\frac{1}{2}}.$$

The explicit formulae for the other interesting motions, the accelerative ones, are now easily obtainable.

RIASSUNTO (*)

Nel presente lavoro si esaminano le conseguenze matematiche derivanti dal basare una teoria di campo (classica o quantistica) sulla geometria conforme. Lo spazio in questione è quello di tutte le sfere in R_4 (spazio lineare quadridimensionale di segnatura $(+++ -)$) invariante fondamentale, l'angolo d'intersezione di due sfere. Nelle premesse matematiche (§ 1) si sviluppa un opportuno formalismo non omogeneo, che permette di trattare la sfera come un punto in uno spazio Riemanniano a 5 dimensioni di curvatura unitaria costante il cui elemento di lunghezza è l'angolo infinitesimo tra due sfere adiacenti. Il gruppo conforme (trasformazioni di Lorentz proprie, traslazioni, dilatazioni uniformi, e inversioni nelle sfere) è il gruppo di moti a 15 parametri (trasformazioni conservanti la metrica) di questo spazio. Nel § 2 le sfere si interpretano come particelle di prova finite (non localizzate). I campi fisici sono così definiti su particelle di prova anzichè (per esempio, nello spazio di posizione) soltanto sugli eventi occupati dalle particelle di prova. Le sfere possono distinguersi o con la 5-posizione (posizione e dimensione nello spazio-tempo della particella di prova) in un sistema q , o col 5-momento (4-momento e massa a riposo della particella di prova) in un sistema p . Esiste un moto che trasforma lo spazio q nello spazio p e inversamente (in altre parole gli osservatori in q e in p sono equivalenti), in virtù del quale, si dimostra, ogni teoria conforme presenta automaticamente una *reciprocità di Born* tra lo spazio p e lo spazio q . La 5-posizione e il 5-momento soddisfano una equazione del tipo della relazione di indeterminazione; cioè, le non localizzazioni negli spazi q e p stanno in relazione inversa con l' \hbar di Planck che misura la correlazione intrinseca. Tutti gli altri moti si possono formare da sottogruppi che portano gli spazi q e p in se stessi. Questi si interpretano sistematicamente come cambiamenti del sistema di riferimento. Quelli che coinvolgono moti relativi rappresentano accelerazioni relative *uniformi* di osservatori di Lorentz (gruppo di Lorentz \longleftrightarrow accelerazioni zero). La massa e le dimensioni delle particelle di prova sono invarianti nel gruppo di Lorentz ma non uniformemente rinormalizzate

(*) Traduzione a cura della Redazione.

dai moti accelerati. Nel § 3 si dimostra che le geodetiche dello spazio delle sfere (equazioni di moto delle particelle di prova (elementari)) descrivono moti uniformi nel caso presente (in assenza di forze). Le particelle di prova tendono a delocalizzarsi nello spazio q al crescere del tempo e nello spazio p al crescere dell'energia. La costanza nel tempo dei 5-momenti, la loro interdipendenza data dalla dinamica della relatività speciale seguono da queste equazioni di moto. Si dimostra che le particelle elementari libere mantengono in tutti i moti, in particolare in quelli accelerati, uno stato di velocità uniforme. Ciò è in contraddizione con la relatività ordinaria e suggerisce un'esperienza atta in linea di principio a fare per la Fisica una scelta fra la geometria conforme e la geometria di Lorentz.

The Wave Function of Photons and their Configurational Equation.

W. KRÓLIKOWSKI

Institute of Theoretical Physics, University of Warsaw (Poland)

(ricevuto il 4 Settembre 1954)

Summary. — In the first part of this paper the configurational wave functions of photons are discussed for both the Tamm-Dancoff and the Bethe-Salpeter types as well as for the more general type given by Günther. In the second part the configurational equation corresponding to the Bethe-Salpeter equation is derived for photons. All results obtained in this paper are applicable, *mutatis mutandis*, to mesons.

1. — Covariant Wave Function of Photons.

We denote by α the complete set of commuting observables describing the state of a free photon. Let a_α be the annihilation operator of the photon in the state $|\alpha\rangle$. Let us assume that the operators of the set α commute with the energy of the free photon \hat{H} . Then we may describe the electromagnetic field in the interaction picture using the operator

$$(1) \quad \varphi_\mu(x) = \sum_\alpha a_\alpha \varphi_{\mu\alpha}(x),$$

where $\varphi_{\mu\alpha}(x) = \varphi_{\mu\alpha}(\mathbf{x}) \exp[-iE_\alpha t/\hbar]$, $\varphi_{\mu\alpha}(\mathbf{x}) = \langle \mathbf{x} \mu | \alpha \rangle$, E_α is the energy of the photon in the state $|\alpha\rangle$, and $\mu=1, 2, 3, 4$ is the vector index. Functions $\varphi_{\mu\alpha}(\mathbf{x})$ describe the states $|\alpha\rangle$ in the Schrödinger representation of the photon.

Let $\Psi[\sigma]$ be the state vector in the interaction picture of the physical system consisting of the electromagnetic and electron fields. We denote by x_1, \dots, x_N the 4-positions of N photons placed on a space-like hypersurface σ , and by μ_1, \dots, μ_N the vector indices of these photons. The $|\mathbf{x} \mu\rangle = \exp[i\hat{H}_0 t/\hbar] |\mathbf{x} \mu\rangle$ are eigenvectors of the position operators \mathbf{x} of photons in the interaction picture. In the representation given by the base $|\mathbf{x}_1 \mu_1 \dots \mathbf{x}_N \mu_N\rangle$, where

$N=0, 1, 2, \dots$ (for $N=0$ we have the state of the vacuum of free photon. $|0\rangle$), the components of the state vector $\Psi[\sigma]$ have the well known form:

$$(2) \quad \Psi_{\mu_1 \dots \mu_N}(x_1 \dots x_N)[\sigma] = \langle x_1 \mu_1 \dots x_N \mu_N | \Psi[\sigma] \rangle = \\ = \frac{1}{\sqrt{N!}} \langle 0 | \varphi_{\mu_1}(x_1) \dots \varphi_{\mu_N}(x_N) \Psi[\sigma] \rangle.$$

Functions (2) are the wave functions of photons. They are also probability amplitudes with regard to photons and furthermore abstract state vectors with regard to the electron field.

Obviously, it is more convenient to describe the electromagnetic field by means of its 4-potential $A_\mu(x)$ then by means of $\varphi_\mu(x)$. Therefore we will base the definition of the wave functions on the operators $\varphi_\mu(x)$. Then these functions will not give the probability amplitudes. They will, however, serve to calculate the scalar products of states, but by means of another formula than the conventional one.

Assuming

$$(3) \quad \varphi_{\mu\alpha}(x) = \frac{1}{\sqrt{V}} e_\mu \exp[ik_\nu x_\nu], \quad \text{where} \quad e_\mu^2 = 1, \quad k_\mu^2 = 0,$$

we have

$$A_\mu(x) = A_\mu^+(x) + A_\mu^-(x),$$

where

$$(4) \quad A_\mu^+(x) = \sum_\alpha \left(\frac{\hbar c}{2k} \right)^{\frac{1}{2}} a_\alpha \varphi_{\mu\alpha}(x) = \pm A_\mu^{+*}(x).$$

Here « + » is proper for $\mu=1, 2, 3$, « - » for $\mu=4$ ($A_4=i\varphi(x)$). On the strength of (1), (3) and (4) we have for any operator Ω independent of x :

$$\int d_3x \varphi_\mu^*(x) \Omega \varphi_\mu(x) = \int d_3x A_\mu^{+*}(x) \Omega \left(-\frac{2}{\hbar c} \frac{\partial}{\partial x_4} \right) A_\mu^+(x),$$

(we use the notation where $x_4=ix_0=ict$, $k_4=ik_0$ while $k_0=|\mathbf{k}|=k$). The above formula may be transcribed in the covariant form:

$$(5) \quad \int_\sigma d_3\sigma \varphi_\mu^*(x) \Omega \varphi_\mu(x) = \int_\sigma d_3\sigma_\nu A_\mu^{+*}(x) \Omega \frac{2}{\hbar c} d_\nu A_\mu^+(x),$$

where

$$d_\nu = -i\partial/\partial x_\nu \quad (d_3\sigma_4 = -i d_3x = -i dx_1 dx_2 dx_3).$$

Using (2) and (5) we may represent the scalar product of two arbitrary states as follows:

$$\begin{aligned}
 (6) \quad \langle \Psi^{(1)} \Psi^{(2)} \rangle &= \sum_N \int_{\sigma} d_3 \sigma_1 \dots d_3 \sigma_N \langle \Psi_{\mu_1 \dots \mu_N}^{(1)}(x_1 \dots x_N) [\sigma] \Psi_{\mu_1 \dots \mu_N}^{(2)}(x_1 \dots x_N) [\sigma] \rangle = \\
 &= \sum_N \int_{\sigma} d_3 \sigma_{v_1} \dots d_3 \sigma_{v_N} \langle F_{\mu_1 \dots \mu_N}^{(1)}(x_1 \dots x_N) [\sigma] \left(\frac{2}{\hbar c} \right)^N d_{v_1} \dots d_{v_N} F_{\mu_1 \dots \mu_N}^{(2)}(x_1 \dots x_N) \rangle
 \end{aligned}$$

($x_i = (x_{\mu_i})$) ($i = 1, \dots, N$), where we have introduced the notation:

$$(7) \quad F_{\mu_1 \dots \mu_N}(x_1 \dots x_N) [\sigma] = \frac{1}{\sqrt{N!}} \langle 0 | A_{\mu_1}^+(x_1) \dots A_{\mu_N}^+(x_N) \Psi[\sigma] \rangle.$$

Standard bra and standard ket appearing on the right side of (6) relate to the electron field.

We observe, that the functions (7) are not the probability amplitudes for finding photons at points x_1, \dots, x_N on σ , in which they differ from (2). However, on the basis of (6) they may serve to calculate the scalar products of states and thus may be considered as wave functions of photons. They are more convenient to use than functions introduced for photons by LANDAU and PEIERLS ⁽¹⁾.

In further considerations we shall use instead of the Schrödinger representation the mixed representation introduced by GÜNTHER ⁽²⁾ in the case of electrons. In this representation a certain fixed number N of photons will be described configurationally, while the remaining photons will be described by means of occupation numbers. The mixed representation is defined — when N is fixed — by the base $|N_1 N_2 \dots, x_1 \mu_1 \dots x_N \mu_N\rangle$. In this representation the components of the state vector $\Psi[\sigma]$ have the form:

$$\begin{aligned}
 \Psi_{\mu_1 \dots \mu_N}(N_1 N_2 \dots, x_1 \dots x_N) [\sigma] &= \langle N_1 N_2 \dots, x_1 \mu_1 \dots x_N \mu_N | \Psi[\sigma] \rangle = \\
 &= \langle N_1 N_2 \dots | \psi_{\mu_1 \dots \mu_N}(x_1 \dots x_N) [\sigma] \rangle,
 \end{aligned}$$

where the following notation is introduced:

$$(8) \quad \psi_{\mu_1 \dots \mu_N}(x_1 \dots x_N) [\sigma] = \frac{1}{\sqrt{N!}} \varphi_{\mu_1}(x_1) \dots \varphi_{\mu_N}(x_N) \Psi[\sigma].$$

In view of the completeness of the system $|N_1 N_2 \dots\rangle$ the vector (8) is the wave function of the N photons. It is furthermore the abstract state vector

(1) L. LANDAU and R. PEIERLS: *Zeits. Phys.*, **62**, 188 (1930).

(2) M. GÜNTHER: *Phys. Rev.*, **94**, 1347 (1954).

with regard to the electron field as well as to the «non-configurational» photons.

Performing an analogous transition to the transition from (2) to (7) we introduce instead of (8) the following wave function:

$$(9) \quad f_{\mu_1 \dots \mu_N}(x_1 \dots x_N)[\sigma] = \frac{1}{\sqrt{N!}} A_{\mu_1}^+(x_1) \dots A_{\mu_N}^+(x_N) \Psi[\sigma].$$

Now, the rule for the calculation of scalar products for any states with N «configurational» photons is given in the formula

$$(10) \quad \langle \Psi^{(1)} \Psi^{(2)} \rangle = \int \prod_{\sigma} d_3 \sigma_{r_1} \dots d_3 \sigma_{r_N} \langle f_{\mu_1 \dots \mu_N}^{(1)}(x_1 \dots x_N)[\sigma] \left(\frac{2}{\hbar c} \right)^N d_{r_1} \dots d_{r_N} f_{\mu_1 \dots \mu_N}^{(2)}(x_1 \dots x_N) \rangle.$$

Here the standard bra and standard ket on the right side pertain equally to the electron field and to the «non-configurational» photons.

The component of the vector (9) corresponding to the vacuum of free electrons and photons $|V_0\rangle$ is the covariant wave function of the Tamm-Dancoff type for the system consisting of N photons only (cf. (3)).

In passing to the Heisenberg picture we drop the functional dependence on σ from the vector (9):

$$(11) \quad f_{\mu_1 \dots \mu_N}(x_1 \dots x_N) = U^{-1}[\sigma, -\infty] f_{\mu_1 \dots \mu_N}(x_1 \dots x_N)[\sigma] = \\ = \frac{1}{\sqrt{N!}} A_H^{\mu_1}(x_1) \dots A_H^{\mu_N}(x_N) \Psi[-\infty],$$

where we use the label H for operators in the Heisenberg picture.

In formula (11) points x_1, \dots, x_N lie on the space-like hypersurface σ . We can therefore transcribe (11) as follows:

$$(12) \quad f_{\mu_1 \dots \mu_N}(x_1 \dots x_N) = T(A_H^{\mu_1}(x_1) \dots A_H^{\mu_N}(x_N)) \Psi[-\infty],$$

where symbol $T(\dots)$ is a chronological product as defined by Wick (4).

We adopt the formula (12) as the definition in the Heisenberg picture of the wave function of the N photons for any relative position of points x_1, \dots, x_N (cfr. (2)).

The component of the vector (12) corresponding to the true vacuum of electrons and photons $|V\rangle$ (i.e. the vacuum of the interacting particles) is

(3) M. CINI: *Nuovo Cimento*, **10**, 526 (1953).

(4) G. C. WICK: *Phys. Rev.*, **80**, 269 (1950).

the covariant wave function of the Bethe-Salpeter type for the system consisting of N photons only (cf. ⁽⁵⁾). It has the form (cf. ⁽⁵⁾)

$$(13) \quad f_{\mu_1 \dots \mu_N}(V, x_1 \dots x_N) = \langle V | f_{\mu_1 \dots \mu_N}(x_1 \dots x_N) \rangle = \\ = \langle V_0 | \sum_{n=0}^{\infty} \frac{1}{n!} \left(-\frac{i}{\hbar c} \right)^n \int_{-\infty}^{+\infty} dx'_1 \dots dx'_n T(\mathcal{H}(x'_1) \dots \mathcal{H}(x'_n) A_{\mu_1}^+(x_1) \dots A_{\mu_N}^+(x_N)) \Psi[-\infty],$$

where $|V_0\rangle$ is the vacuum of free electrons and photons, and

$$\mathcal{H}(x) = -\frac{1}{c} j_{\mu}(x) A_{\mu}(x), \quad j_{\mu}(x) = iec : \bar{\psi} \gamma_{\mu} \psi(x) :, \quad ((\gamma_{\mu}) = (-i\beta\alpha, \beta)).$$

2. - Configurational Covariant Equation of Photons.

The last relation in formula (13) presents the construction of the wave function of the system of N photons made of matrix elements corresponding with the Feynman diagrams (irreducible as well as reducible). It is well known that this construction may be re-expressed by the integral equation in the kernel of which appear terms corresponding to irreducible diagrams exclusively. In this way we get the Bethe-Salpeter equation for photons (cf. ⁽⁶⁾).

Calculating the right side of formula (13) by Wick's method we find that the terms giving the interaction between two photons appear for the first time in the fourth order of the coupling constant. They are terms corresponding to the diagrams shown on Fig. 1.

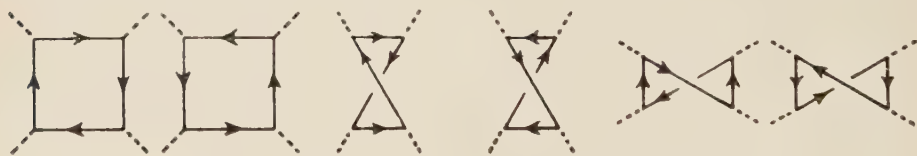


Fig. 1.

If we consider only these irreducible diagrams, we obtain the following integral equation describing the stable states of the system of photons:

$$(14) \quad f_{\mu_1 \mu_2}(V, x_1 x_2) = f_{\mu_1 \mu_2}^0(V, x_1 x_2) + \int_{-\infty}^{+\infty} dx'_1 \dots dx'_4 D_+^{\text{ret}}(x_1 - x'_1) D_+^{\text{ret}}(x_2 - x'_2) \cdot \\ \cdot G_{\mu_1 \dots \mu_4}(x'_1 \dots x'_4) f_{\mu_3 \mu_4}(V, x'_3 x'_4),$$

⁽⁵⁾ M. GELL-MANN and F. LOW: *Phys. Rev.*, **84**, 350 (1951).

⁽⁶⁾ E. E. SALPETER and H. A. BETHE: *Phys. Rev.*, **84**, 1233 (1951).

where

$$f_{\mu_1\mu_2}^0(V, x_1x_2) = \langle V_0 | A_{\mu_1}^+(x_1) A_{\mu_2}^+(x_2) \Psi[-\infty] \rangle$$

is the wave function of two free photons, and

$$(15) \quad G_{\mu_1 \dots \mu_4}(x_1 \dots x_4) = - \left(\frac{e^2}{\hbar c} \right)^2 \text{tr} [2 \gamma_{\mu_1} S_+(x_1 - x_2) \gamma_{\mu_2} S_+(x_2 - x_3) \gamma_{\mu_3} S_+(x_3 - x_4) \cdot \\ \cdot \gamma_{\mu_4} S_+(x_4 - x_1) + \gamma_{\mu_1} S_+(x_1 - x_3) \gamma_{\mu_2} S_+(x_3 - x_2) \gamma_{\mu_3} S_+(x_2 - x_4) \gamma_{\mu_4} S_+(x_4 - x_1)]$$

Moreover, we use in formula (14) the following notations:

$$D_+^{\text{ret}}(x - x') = \begin{cases} D_+(x - x') & t > t', \\ 0 & t < t', \end{cases}$$

$$S_{+\alpha\beta}(x - x') = \psi_+^\alpha(x) \bar{\psi}_\beta^+(x') = \frac{1}{2} S_{F\alpha\beta}(x - x'),$$

$$\hbar c \delta_{\mu\nu} D_+(x - x') = A_\mu^+(x) A_\nu^+(x') = \frac{1}{2} \hbar c \delta_{\mu\nu} D_F(x - x').$$

The integral equation (14) can be reduced to the following integro-differential equations (which are obviously richer in solutions than the former one):

$$\left\{ \begin{aligned} \square_1 f_{\mu_1\mu_2}(V, x_1x_2) &= i \int_{-\infty}^{+\infty} dx'_2 dx'_3 dx'_4 D_+^{\text{ret}}(x_2 - x'_2) G_{\mu_1 \dots \mu_4}(x_1 x'_2 x'_3 x'_4) f_{\mu_3\mu_4}(V, x'_3 x'_4), \\ \square_2 f_{\mu_1\mu_2}(V, x_1x_2) &= i \int_{-\infty}^{+\infty} dx'_1 dx'_3 dx'_4 D_+^{\text{ret}}(x_1 - x'_1) G_{\mu_1 \dots \mu_4}(x'_1 x_2 x'_3 x'_4) f_{\mu_3\mu_4}(V, x'_3 x'_4), \end{aligned} \right.$$

or

$$\square_1 \square_2 f_{\mu_1\mu_2}(V, x_1x_2) = - \int_{-\infty}^{+\infty} dx'_3 dx'_4 G_{\mu_1 \dots \mu_4}(x_1 x_2 x'_3 x'_4) f_{\mu_3\mu_4}(V, x'_3 x'_4).$$

The configurational equation given above may be used to describe the scattering processes of photons by photons as well as to investigate the bound states of photons. In the last case we omit in the equation (14) the free term $f_{\mu_1\mu_2}^0(V, x_1x_2)$ ⁽⁶⁾.

All results obtained in this paper are applicable, *mutatis mutandis*, to mesons.

The author is indebted to Dr. M. GÜNTHER for his suggestions and valuable discussion.

A more detailed paper concerning the same problem will be published in *Acta Physica Polonica*.

RIASSUNTO (*)

Nella prima parte del presente lavoro si discutono le funzioni d'onda di configurazione sia per i tipi di Tamm-Dancoff e di Bethe-Salpeter sia per il tipo più generale dato da GÜNTHER. Nella seconda parte si deriva per i fotoni l'equazione di configurazione corrispondente all'equazione di Bethe-Salpeter. Tutti i risultati ottenuti nel presente lavoro si applicano, *mutatis mutandis*, ai mesoni.

(*) Traduzione a cura della Redazione.

Interactions des électrons avec la matière.

CH. A. D'ANDLAU

Laboratoire de Physique de l'École Polytechnique - Paris

(ricevuto il 15 Settembre 1954)

Résumé. — Une expérience faite au niveau de la mer, avec une chambre de Wilson contenant un seul écran, placée dans un champ magnétique, a permis d'étudier les interactions des électrons avec la matière. Cette expérience permet de connaître l'énergie de l'électron incident et le nombre et l'énergie des électrons de la gerbe produite dans l'écran. Les résultats expérimentaux sont comparés avec les résultats de la théorie des gerbes dans le cas des approximations *A* et *B*, et avec les résultats obtenus par la méthode de Monte-Carlo.

1. — Méthode expérimentale.

Une chambre de Wilson thermostatisée, de dimensions $50 \times 22 \times 12$ cm est placée dans un champ magnétique de 5100 gauss, dont les variations n'excèdent pas 2%.

Un écran de plomb est disposé dans la chambre à 30 cm de la partie supérieure. Trois séries d'expériences ont été faites en faisant varier à chaque fois l'épaisseur de l'écran. Les épaisseurs choisies sont 1, 2,08 et 3,48 longueurs de radiation (soient 1,44, 3 et 5 longueurs de gerbe).

La chambre de Wilson est déclenchée par quatre bancs de compteurs, *A*, *B*, *C*, *D* de dimensions 12×20 cm, mis en coïncidences. *A* et *D* sont juste au-dessus de la chambre; *A*, *B*, et *C* sont dans un même plan horizontal et sont séparés par une distance de 20 cm; les bancs *B* et *C* sont protégés latéralement par 5 cm de plomb et sont recouverts de 5 mm de plomb. Afin de ne pas favoriser les déclenchements par des gerbes contenant des électrons énergiques il n'y a pas de bancs de compteurs sous la chambre.

Avant de pénétrer dans la chambre les électrons incidents traversent une épaisseur équivalente de 2 mm de plomb.

La courbure des trajectoires est mesurée au moyen de calibres; le moment des électrons a pu être mesuré jusqu'à une valeur de 2,5 GeV/c.

Dans chaque série d'expériences correspondant à une épaisseur déterminée de l'écran de plomb, 500 phénomènes ont été analysés.

2. - Groupement des énergies des électrons incidents.

Les résultats théoriques sont relatifs à des gerbes produites par des électrons d'énergie E_0 bien déterminée; comme les électrons du rayonnement cosmique ont des énergies variant de quelques MeV à plusieurs GeV, on a groupé les énergies des électrons en plusieurs intervalles. A l'intérieur de chaque intervalle on a choisi une valeur moyenne de l'énergie E_0 , soit \bar{E}_0 , et l'on a supposé que tous les électrons compris dans l'intervalle $E_0 - \Delta E_0$ et $E_0 + \Delta E_0$ avaient la même énergie E_0 .

Ce mode de groupement a l'avantage de rendre négligeables les erreurs sur la mesure de l'énergie, c'est-à-dire sur la mesure de la courbure et sur la mesure du champ magnétique ainsi que les erreurs dues à l'inclinaison de l'électron par rapport à l'écran.

Comme certains résultats théoriques font intervenir le terme $\ln E_0/\varepsilon_0$ (ε_0 , énergie critique dans le plomb, est prise égale à 7,6 MeV), le mode de groupement utilisé est tel que si E_1 et E_2 sont les valeurs extrêmes des énergies de l'intervalle, l'on ait:

$$\ln (E_2/E_1) = 0,5.$$

Le tableau I donne les valeurs moyennes des différents intervalles et la valeur correspondante de E_0 en MeV.

TABLEAU I.

$\ln E_0/\varepsilon_0$	2,12	2,62	3,12	3,62	4,12	4,62	5,12	5,62	6,12
\bar{E}_0 MeV	63	104	170	280	460	770	1 250	2 100	> 3 000

3. - Nombre moyen de particules sous l'écran en fonction de l'énergie de l'électron incident à épaisseur traversée constante.

La fig. 1 donne à une même échelle les valeurs de \bar{N}_s (nombre moyen de particules sous l'écran) relatives aux trois séries d'expériences; les erreurs statistiques sont du même ordre de grandeur dans les trois séries d'expériences; elles n'ont été figurées que sur une des courbes.

Toutes ces courbes passent par l'origine bien qu'il n'y ait aucun point expérimental qui permette de le prouver. L'origine correspond en effet à: $N_s = 0$ pour $\ln E_0/\varepsilon_0 \rightarrow 0$, soit $E_0 = \varepsilon_0$.

Pour la courbe tracée pour $t = 1$ longueur de radiation (et à fortiori pour les autres), si l'on néglige les fluctuations dans la perte d'énergie par collision, d'après la définition même de l'énergie critique ε_0 , tout électron d'énergie $E_0 = \varepsilon_0$ doit en effet être absorbé dans un écran d'une longueur de radiation.

3.1. Comparaison avec les résultats théoriques. — Les résultats précédents ont été comparés avec les résultats théoriques d'ARLEY⁽¹⁾, p. 159]. Une correction a été faite pour la valeur de l'énergie critique prise par cet auteur ($\varepsilon_0 = 10$ MeV).

Pour les résultats relatifs à $t = 1,44$ longueurs de gerbe, les points sur la courbe théorique ont été déterminés par interpolation graphique des valeurs théoriques relatives à $t = 0,8, 1, 2$ et 3 longueurs de gerbe. Les résultats des deux autres séries d'expériences (écrans d'épaisseurs égales à 3 et 5 longueurs de gerbe) et les résultats théoriques sont directement comparables. Pour chaque épaisseur d'écran on a trois points sur la courbe théorique (valeurs données par ARLEY: $\ln E_0/\varepsilon_0 = 2, 4, 6$). Cette détermination par trois points est suffisante pour que l'on ait l'allure général des courbes théoriques.

Dans le cas où $t = 1,44$ longueurs de gerbe l'accord entre les résultats théoriques et expérimentaux est satisfaisant, mais il semble dû à certaines approximations faites par ARLEY pour trouver un « modèle » permettant de calculer le développement des gerbes. Les résultats théoriques pour $t = 3$ et 5 longueurs de gerbe semblent difficiles à concilier avec les résultats expérimentaux.

Donc pour les épaisseurs d'écran inférieures à 1 longueur de radiation on doit trouver un nombre de secondaries supérieur à celui donné dans la théorie

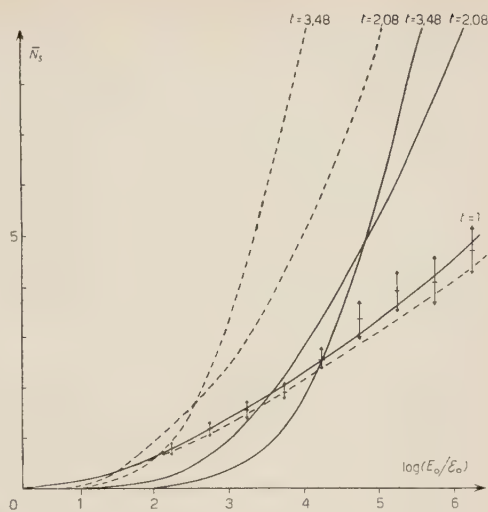


Fig. 1. — Nombre moyen \bar{N}_s de particules dans une gerbe produite, dans un écran de plomb d'épaisseur t , par un électron d'énergie E_0 : t : en longueurs de radiation; E_0 : en MeV; ε_0 : énergie critique dans le plomb (7,6 MeV).

—— Résultats expérimentaux.
 - - - - - Résultats théoriques (ARLEY).

⁽¹⁾ N. ARLEY: *Stochastic Processes and their application to the Theory of Cosmic Radiation*.

d'Arley, tandis que pour des épaisseurs dépassant 1 longueur de radiation, à cause des approximations faites dans la théorie, la valeur de \bar{N}_s donnée par ARLEY dépasse celle trouvée expérimentalement.

Pour $t = 1$ longueur de radiation, il y a une coïncidence fortuite entre les résultats théoriques et expérimentaux. La théorie d'Arley ne semble utilisable que lorsque l'épaisseur de l'écran est de l'ordre de 1 longueur de radiation.

Dans les courbes expérimentales, il y a des fluctuations dues au petit nombre de mesures, surtout aux grandes énergies, mais dans l'ensemble, les points expérimentaux montrent une variation continue du nombre moyen de particules sous l'écran avec $\ln E_0/\varepsilon_0$.

Or pour la courbe relative à $t = 3,48$ longueurs de radiation, dans l'intervalle d'énergie $49 < E_0 < 81$ MeV, sur 66 électrons incidents tous ont été arrêtés dans l'écran de plomb sauf un seul de 74 MeV qui a donné sous l'écran une particule de 8 MeV, ce qui donne $\bar{N}_s = 0,01$; dans les mêmes conditions la courbe théorique montre que l'on devrait avoir $\bar{N}_s = 0,75$, cette valeur semble inconciliable avec la valeur trouvée expérimentalement.

Comme on l'a déjà fait remarquer [(2), § 5, 15] la théorie des gerbes n'est pas valable dans les éléments lourds, (l'approximation de Born n'est plus correcte) surtout aux énergies inférieures à 100 MeV.

La différence des valeurs de N_s trouvées théoriquement et expérimentalement est due aux approximations qu'il a été nécessaire de faire dans la théorie des gerbes dans le cas de l'approximation B (*).

En effet la perte d'énergie par collision, si elle est plus faible à une énergie supérieure à 10 MeV (dans le plomb) que la perte d'énergie par radiation, n'est pas complètement négligeable.

L'effet du scattering, important aux basses énergies, diminue le nombre de particules que l'on peut voir sous l'écran; il faut donc tenir compte de l'étalement latéral des gerbes.

On peut considérer que parmi les électrons de 10 à 20 MeV qui ont encore une longueur de radiation à parcourir, au moins un tiers des électrons ne sort pas de l'écran, la distance parcourue par des électrons de faible énergie dans l'écran de plomb étant beaucoup plus grande que l'épaisseur de l'écran elle-même.

Enfin pour les seuls phénomènes intervenant dans la théorie des gerbes

(2) B. Rossi: *High Energy Particles* (New York).

(*) Les principales approximations de la théorie des gerbes, dans le cas de l'approximation A consistent à négliger la perte d'énergie par collision et à ne considérer les phénomènes de perte d'énergie par radiation et de production de paire que dans le cas limite d'effet d'écran total. Dans l'approximation B , au contraire, on tient compte de la perte d'énergie par collision et on la suppose constante par longueur de radiation (cf. B. Rossi: *High Energy Particles*, § 5, 2, page 223).

(perte d'énergie par radiation et production de paire), la perte d'énergie fractionnelle par radiation et la probabilité totale de production de paire par longueur de radiation, diminuent avec l'énergie de la particule incidente. Ainsi, alors que la probabilité totale de production de paire a une valeur limite $\mu_0=0,773$, valeur limite atteinte à une énergie supérieure à 10^4 MeV elle n'a plus que la valeur 0,4 pour une énergie de 30 MeV.

Les photons dont les énergies sont comprises entre 50 et 10 MeV ont donc une probabilité beaucoup plus faible de se matérialiser dans une épaisseur de matière donnée ⁽³⁾. Au point de vue expérimental de tels photons sortent de l'écran sans se matérialiser et l'on trouve dans une gerbe moins de particules sous l'écran que ne l'indique la théorie.

Indépendamment de la non validité des approximations faites dans la théorie des gerbes dans les éléments lourds et aux basses énergies, ARLEY a fait d'autres approximations concernant le mode de développement d'une gerbe ⁽¹⁾.

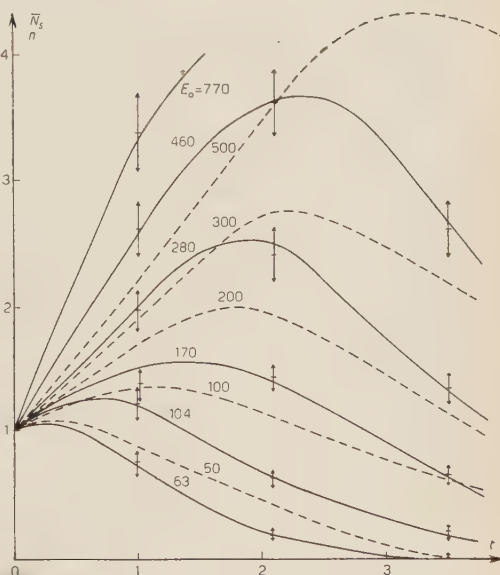
4. - Nombre moyen de particules sous l'écran en fonction de l'épaisseur traversée.

Des résultats précédents on peut déduire le nombre moyen de particules sous l'écran en fonction de l'épaisseur traversée, les énergies des électrons incidents étant toujours groupées de la même façon.

La fig. 2. donne la valeur de N_s , pour plusieurs valeurs de E_0 (énergie de l'électron incident). Pour chaque courbe, on a trois points expérimentaux, correspon-

Fig. 2. - Nombre moyen N_s de particules dans une gerbe, en fonction de l'épaisseur de plomb traversée t (en longueurs de radiation), pour plusieurs valeurs de l'énergie de la particule initiale E_0 (en MeV).

— Résultats expérimentaux.
 - - - - - Méthode de Monte-Carlo.



⁽³⁾ K. GREISEN: *Phys. Rev.*, **75**, 1071 (1949).

dant aux trois épaisseurs d'écran choisies. plus un point défini par $\bar{N}_s \approx 1$ pour $t \rightarrow 0$.

On sait d'autre part que:

$$\bar{N}_s = 0, \quad \text{pour } t \gg t_M.$$

t_M , valeur de l'abscisse du maximum, dépend de la valeur de l'énergie du primaire.

Les courbes ont été tracées pour des valeurs de l'énergie de l'électron incident ne dépassant pas 770 MeV (ce qui correspond à: $\ln E_0/\varepsilon_0 = 4,62$). Pour des valeurs plus grandes de l'énergie, les erreurs statistiques ne permettent plus de tracer les courbes avec une précision suffisante, d'autant plus que la valeur maximum du nombre moyen de particules sous l'écran correspond à une épaisseur d'écran supérieure à l'épaisseur la plus grande qui a été choisie.

4.1. Comparaison avec les résultats théoriques ^(4,5). — La surface comprise sous chaque courbe: $\bar{N}_s = f(t)$ doit être égale à E_0/ε_0 .

En effet, l'énergie initiale de la particule est finalement dissipée sous forme de perte d'énergie par collision, c'est-à-dire que:

$$E_0 = \int_0^{\infty} N(E_0, 0, t) \frac{dE'}{dt} dt,$$

où: dE'/dt est la perte d'énergie par collision, par longueur de radiation.

La surface sous chacune des courbes est $S = \int_0^{\infty} N(E_0, 0, t) dt$. Si l'on suppose que: $dE'/dt = \varepsilon_0 = \text{const.}$ l'on voit que $S = E_0/\varepsilon_0$.

Les courbes théoriques déterminées par SNYDER ⁽⁵⁾ limitent des surfaces dont les aires sont égales à E_0/ε_0 à 10 % près.

La surface sous chacune des courbes expérimentales est beaucoup plus petite que E_0/ε_0 où $\varepsilon_0 = 7,6$ MeV.

Une intégration graphique permet de voir qu'aux erreurs de tracé près, la surface S sous chaque courbe est égale à E_0/ε_1 avec: $\varepsilon_1 \neq \varepsilon_0$.

Le tableau II donne les valeurs de l'intégration graphique S ainsi que les valeurs du rapport $\varepsilon_1 = E_0/S$.

TABLEAU II.

E_0 MeV	63	104	170	280	460
S	1,32	2,70	8,6	8,75	13,5
ε_1	47,5	38,5	37,5	32,5	34,5

⁽⁴⁾ B. ROSSI et K. GREISEN: *Rev. of Mod. Phys.*, **13**, 240 (1941).

⁽⁵⁾ H. S. SNYDER: *Phys. Rev.*, **76**, 1563 (1949).

La moyenne arithmétique des cinq valeurs de ε_1 , ainsi obtenue est: $\varepsilon_1 = 37,5$ MeV.

Les résultats, et la façon régulière dont les courbes dépendent de E_0/ε_0 , montrent qu'il ne peut y avoir de fluctuations importantes dans les résultats expérimentaux. Il y a donc une différence systématique entre les résultats théoriques (cas de l'approximation B) et expérimentaux.

Il faut remarquer que les approximations faites dans la théorie et notamment le fait de négliger le scattering, ne peuvent conduire la théorie qu'à trouver dans une gerbe un nombre de particules supérieur au nombre réel, tandis qu'expérimentalement toute erreur dans le dénombrement des particules sous l'écran (électrons difficiles à compter dans le corps d'une gerbe, électrons sortant de l'écran assez loin des autres particules de la gerbe et non comptés dans les mesures) ne peut conduire qu'à trouver une valeur trop faible pour le nombre des particules sous l'écran. Néanmoins la différence des résultats théoriques et expérimentaux est trop grande pour qu'elle puisse être uniquement attribuée à une erreur systématique inhérente à la méthode expérimentale employée.

Il faut donc penser que la différence est due, en partie, tant aux approximations faites dans la théorie des gerbes qu'au « modèle » choisi pour déterminer le développement des gerbes.

Les résultats théoriques dans le cas de l'approximation B ne sont donc pas conciliables avec les résultats expérimentaux.

4.2. Comparaison avec les résultats de la méthode de Monte Carlo ⁽⁶⁾. — Les résultats expérimentaux sont en assez bon accord avec les résultats de la méthode de Monte Carlo, si le nombre de particules « n » considéré dans cette méthode, est seulement le nombre de particules contenues dans le corps de la gerbe et faisant un angle de moins de 30° avec la direction de l'axe de la gerbe.

Mais, dans cette méthode, le nombre total de particules dans la gerbe, compte tenu de la correction pour la diffusion multiple, est supérieur au nombre de particules sous l'écran trouvé expérimentalement.

A. M. SHAPIRO ⁽⁷⁾ a fait une expérience à la chambre de Wilson avec des électrons de 200 MeV produits artificiellement; le nombre de particules de gerbe qu'il a trouvé est inférieur à celui calculé par la méthode de Monte Carlo. Ces résultats expérimentaux sont donc en bon accord avec les résultats de la présente expérience.

Sur la fig. 2 on a tracé les courbes $n = f(t)$ relatives à la méthode de Monte Carlo. L'ordonnée « n » est le nombre de particules sous l'écran, faisant un angle de moins de 30° avec l'axe de la gerbe.

⁽⁶⁾ R. R. WILSON: *Phys. Rev.*, **86**, 261 (1952).

⁽⁷⁾ A. M. SHAPIRO: *Phys. Rev.*, **82**, 307 (1951).

5. — Nombre maximum de secondaires.

C'est la valeur du maximum de chaque courbe donnant le nombre moyen de particules sous l'écran en fonction de l'épaisseur traversée, pour un électron incident d'énergie donnée.

La détermination de N_M ne peut se faire que graphiquement et n'a été faite que sur les courbes de la fig. 2.

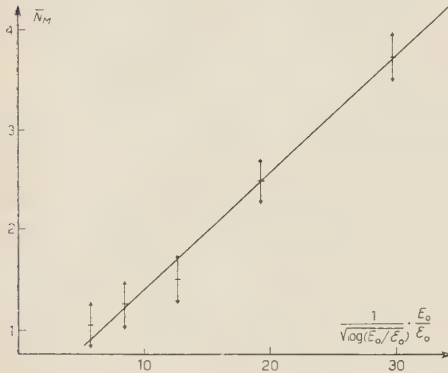


Fig. 3. — Nombre maximum de particules d'une gerbe produite par un électron d'énergie E_0 (en MeV). E_c énergie critique dans le plomb (7,6 MeV).

Ces courbes présentent un maximum assez aplati, aussi (sauf pour la courbe relative à $E_0 = 770$ MeV), l'erreur graphique ne dépasse pas $\pm 0,25 N_s$.

Les résultats sont représentés sur la fig. 3.

Afin de pouvoir comparer ces résultats avec les résultats théoriques, on a porté en abscisse :

$$\frac{1}{\sqrt{\ln(E_0/E_c)}} \frac{E_0}{E_c}.$$

Par les points déterminés expérimentalement on peut faire passer une droite, ce qui vérifie qualitativement la théorie des gerbes.

La droite déterminée par la théorie des gerbes a un coefficient angulaire plus grand que la droite expérimentale.

6. — Nombre moyen de particules sous l'écran $\bar{N}_s(E)$, d'énergie supérieure à une valeur E .

La détermination de $\bar{N}_s(E)$ permet de comparer les résultats expérimentaux et ceux obtenus par la théorie dans le cas de l'approximation A.

La valeur de $\bar{N}_s(E)$ est donnée pour plusieurs valeurs de E_0/E dans l'article de B. ROSSI et K. GREISEN [(4), § 30)].

Mais les valeurs données du rapport E_0/E sont beaucoup trop grandes pour être comparées avec les résultats expérimentaux, si l'on veut prendre pour E une énergie nettement supérieure à l'énergie critique.

Comme le nombre de mesures pour les électrons de grande énergie ($E_0 \sim 1$ GeV) est faible, pour que les erreurs statistiques soient les plus faibles possibles,

la courbe:

$$\overline{N}_s(E) = f(t) \quad \text{à } E_0/E \text{ constant}$$

n'a été tracée que dans 3 cas.

Le tableau III donne les valeurs des intervalles choisis, les valeurs moyennes E_0 et les valeurs du rapport E_0/E pour les trois courbes qui ont été tracées sur la fig. 4.

TABLEAU III.

	E_0 MeV	E MeV	E_0/E
$220 < E_0 < 360$	280	48	10
$360 < E_0 < 600$	480	48	10
$360 < E_0 < 600$	480	24	20

Les deux courbes relatives à $E_0/E = 10$ devraient être superposées, car théoriquement pour une valeur donnée de E_0/E , $\overline{N}_s(E)$ ne dépend pas de E_0 , mais seulement de l'épaisseur traversée et de E_0/E .

La distance verticale qui sépare les points de ces deux courbes relatives à une même valeur de E_0/E est partout inférieure à l'erreur statistique, aussi l'on peut considérer que l'accord avec la théorie est satisfaisant.

Les valeurs théoriques de $\overline{N}_s(E)$ peuvent être calculées à partir de plusieurs fonctions dont les valeurs numériques sont données dans l'article de B. ROSSI et K. GREISEN [(4), § 30].

Le calcul de $\overline{N}_s(E)$ a été fait pour $E_0/E = 10$ et 20, pour deux valeurs du paramètre s ($s = 1,2$ et $s = 1,4$) auxquelles correspondent les deux valeurs de t : $t = 2$ et $t = 2,9$ longueurs de radiation

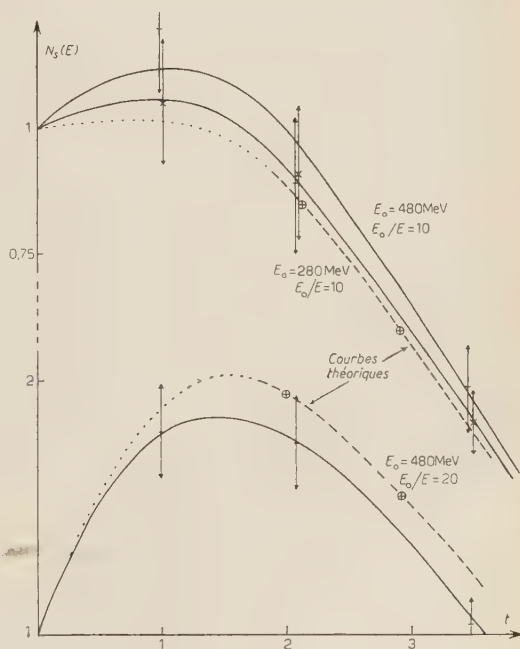


Fig. 4. — Nombre moyen $\overline{N}_s(E)$ de particules d'énergie $\geq E$ dans une gerbe, en fonction de l'épaisseur t de plomb traversée. t : en longueurs de radiation. E_0 : énergie de la particule initiale, en MeV. E : énergie des particules sous l'écran de plomb.

(pour des valeurs inférieures à $t = 2$ on ne peut plus calculer $\overline{N}_s(E)$ par cette méthode).

Les courbes théoriques ainsi obtenues ont été tracées sur la fig. 4. Pour $t < 2$ la courbe est extrapolée jusqu'au point $\overline{N}_s(E) = 1$ pour $t = 0$.

Il n'y a aucun désaccord entre les résultats expérimentaux et théoriques et la théorie des gerbes dans le cas de l'approximation *A* semble être vérifiée quantitativement, si dans le rapport E_0/E , on prend pour E une valeur trois ou quatre fois supérieure à l'énergie critique (soit 30 MeV dans une expérience faite avec un écran de plomb).

7. — Conclusion.

Cette expérience montre qu'il existe un désaccord très net entre les résultats expérimentaux et les résultats théoriques dans le cas de l'approximation *B*. Dans le cas de l'approximation *A* les résultats théoriques et expérimentaux semblent être en assez bon accord quand l'énergie des particules sous l'écran est plus grande que l'énergie critique. Enfin la méthode de Monte Carlo donne des résultats comparables avec les résultats de la présente expérience.

Ce travail a été fait sous la direction de Monsieur LEPRINCE-RINGUET; nous lui demandons de trouver ici l'expression de notre reconnaissance.

Nos remerciements vont également à MM. B. GREGORY, W. E. HAZEN, A. LAGARRIGUE et C. PEYROU pour l'aide qu'ils nous ont apportée dans l'interprétation des résultats.

RIASSUNTO (*)

Un'esperienza eseguita al livello del mare, con una camera di Wilson contenente un solo schermo, posta in un campo magnetico, ha permesso di studiare le interazioni degli elettroni con la materia. Questa esperienza permette di conoscere l'energia dell'elettrone incidente e il numero e l'energia degli elettroni dello sciame prodotto nello schermo. I risultati sperimentali si confrontano coi risultati della teoria degli sciami per le approssimazioni *A* e *B*, e coi risultati ottenuti col metodo di Monte Carlo.

(*) Traduzione a cura della Redazione.

Estimation statistique de l'exposant du spectre d'énergie du rayonnement cosmique primaire.

T. F. HOANG, L. JAUNEAU, J. JOUVIN et C. MABBOUX

Laboratoire de Physique de l'École Polytechnique - Paris

(ricevuto il 15 Settembre 1954)

Summary. — The object of the present article is to use a statistical method on the basis of the maximum likelihood to estimate the exponent s of the power law E^{-s} representing the integral energy spectrum of the primary cosmic radiation. The method has been applied successively to the primary protons observed from jets recorded in photographic emulsions by present authors and to the heavy primaries with $Z \geq 6$ published by KAPLON *et al.*. Both results are consistent with the value of s not exceeding much unity. Errors due to statistical fluctuations are large, a detailed discussion of which has been given.

Dans l'étude du rayonnement cosmique primaire, il est habituel de représenter le spectre d'énergie des particules primaires par une loi de puissance de la forme:

$$N(> E) \sim 1/E^s.$$

L'exposant s déduit des résultats expérimentaux varie de 1,1 à 1,8 ⁽¹⁾. Le domaine d'énergie envisagé s'étend jusqu'à une dizaine de GeV pour les protons primaires et à une cinquantaine de GeV par nucléon dans le cas des noyaux lourds primaires ⁽²⁾. La technique de mesures limite le domaine d'étude des énergies des primaires. Nous avons remarqué ⁽³⁾ qu'il est possible d'aborder le spectre des protons primaires d'énergie supérieure à 20 GeV par les « jets » que l'on observe dans les émulsions photographiques.

⁽¹⁾ H. V. NEHER: *Progress in Cosmic Ray Physics* (Amsterdam, 1951), vol. I.

⁽²⁾ B. PETERS: *Progress in Cosmic Ray Physics* (Amsterdam, 1951), vol. I.

⁽³⁾ T. F. HOANG: *Journ. Phys.*, **5**, 337 (1954).

D'autre part, les phénomènes qui se rattachent directement au rayonnement cosmique primaire de très grande énergie étant assez rares, les résultats expérimentaux dont on dispose pour fixer la forme du spectre primaire sont, en général, limités à un petit nombre. Le problème se pose alors de déterminer la valeur la mieux adaptée de l'exposant s du spectre dans un large domaine d'énergie. Nous avons choisi pour cette estimation la méthode dite du maximum de vraisemblance. Dans l'hypothèse d'un spectre d'énergie de la forme

$$\text{Prob}(E > x) = a/x^s,$$

la loi de fréquence s'écrit :

$$(1) \quad \frac{sE_0^s}{x^{s+1}} dx \quad \text{ou} \quad s \exp [-(\log x - \log E_0)] d(\log x) ;$$

x appartient à l'intervalle $(E_0, +\infty)$, E_0 étant la limite inférieure du domaine de validité du spectre d'énergie envisagé. On peut prendre pour E_0 la valeur de la coupure due au champ magnétique terrestre à la latitude géomagnétique 52° N, soit environ 2 GeV. Les conditions expérimentales (observation des « jets ») sont, d'autre part, telles que les énergies mesurées soient comprises dans un domaine (E_{\min}, E_{\max}) .

Soient N le nombre total de particules primaires d'énergie supérieure à E_0 produisant une interaction dans le bloc d'émulsion utilisé, et n le nombre de primaires dont les énergies ont effectivement été mesurées dans le domaine considéré (E_{\min}, E_{\max}) .

Si l'on considère que la section efficace d'interaction ne varie pas dans le domaine $(E_0, +\infty)$, c'est-à-dire que le critère de choix utilisé n'introduit pas une déformation du spectre primaire, on peut écrire la loi de probabilité de l'ensemble des n résultats expérimentaux :

$$L = \frac{N!}{(N-n)!} s^n q^{N-n} \exp \left[-s \sum (\log E_i - \log E_0) \right] \prod_{i=1}^n d(\log E_i), \quad (*)$$

avec :

$$\begin{aligned} q &= 1 - p = 1 - \int_{E_{\min}}^{E_{\max}} \frac{s \exp [s \log E_0]}{x^{s+1}} dx = \\ &= 1 - \exp [-s (\log E_{\max} - \log E_0)] + \exp [-s (\log E_{\min} - \log E_0)]. \end{aligned}$$

(*) Le calcul est analogue à celui de la vie moyenne d'un atome radioactif. Voir, par exemple, FORTET: *Calcul de Probabilité* (C.N.R.S., 1950, Paris), p. 305 et suivantes.

L'équation du maximum de vraisemblance conduit, pour l'estimation s , à :

$$(2) \quad \frac{1}{s} = \frac{\sum (\log E_i - \log E_0)}{n} - \frac{N - n}{n} \frac{q'(s)}{q(s)}.$$

Le nombre N est inconnu, mais on sait que n/p est une variable aléatoire, d'espérance N et de variance Nq/p (BERNOULLI).

Donc, si les mesures étaient effectuées dans tout l'intervalle $(E_0, +\infty)$, l'estimation de $1/s$ serait donnée par :

$$\frac{1}{s_0} = \frac{1}{n} \sum (\log E_i - \log E_0),$$

avec, d'après (1) :

$$\text{var} \left(\frac{1}{s_0} \right) = \frac{1}{ns^2} \quad \text{soit :} \quad \sigma \left(\frac{1}{s_0} \right) / \frac{1}{s} = \frac{1}{\sqrt{n}}.$$

Lorsque les mesures auront été effectuées seulement dans l'intervalle (E_{\min}, E_{\max}) , $1/s$ sera donné par la formule (2) dans laquelle on remplacera le nombre inconnu N par n/p . Remarquant que : $((N - n)/n)(q'/q)$ se réduit alors à $-p'/p$, on obtient :

$$\frac{1}{s_1} = \frac{1}{n} \sum (\log E_i - \log E_0) - \frac{\log \frac{E_m}{E_0} - \left(\frac{E_m}{E_M} \right)^s \log \frac{E_M}{E_0}}{1 - \left(\frac{E_m}{E_M} \right)^s}.$$

On a commis une erreur supplémentaire en remplaçant N par n/p , variable aléatoire de variance : $Nq/p \approx nq/p^2$. D'où, en négligeant les termes : $(E_M/E_m)^s$ et $(E_M/E_0)^s$:

$$\text{var} \left(\frac{1}{s_1} \right) = \frac{1}{n} \left[\frac{1}{s^2} + f(s) \right], \quad f(s) = s^2 \left[\log \frac{E_m}{E_0} \right]^2 \frac{1}{1 - (E_0/E_m)^s},$$

soit :

$$f(s) = \frac{y}{y-1} [\log y]^2 \quad \text{avec :} \quad y = \left(\frac{E_m}{E_0} \right)^s.$$

L'expression de $1/s_1$ peut encore s'écrire :

$$\frac{1}{s_1} = \frac{1}{n} \sum \log E_i - \log E_m + \frac{\log E_M/E_m}{(E_M/E_m)^s - 1}.$$

Dans le cas où $E_M \ll E_m$, la fraction du second membre agit comme un terme correctif dans lequel on peut remplacer s par la valeur approchée s'_1 :

$$\frac{1}{s'_1} = \frac{1}{n} \sum \log E_i - \log E_m.$$

Appliquons d'abord la méthode au cas des protons d'énergie supérieure à 20 GeV. Nous utilisons les résultats expérimentaux de HOANG sur des jets ayant chacun moins de quatre branches noires ou grises: $n_h \leq 4$ et plus de de cinq branches au minimum d'ionisation: $n_s \geq 5$. Ces jets ont été repérés dans un dépouillement systématique d'émulsions exposées à 30 km d'altitude. Une analyse complète de l'ensemble des résultats ⁽³⁾ montre que les jets produits par des primaires de charge unité sont en grande majorité dus aux protons primaires. La distribution des énergies des primaires estimées d'après la répartition angulaire des secondaires de jets est résumée dans le tableau suivant.

TABLEAU I. — *Energie des protons primaires déduite des jets.*

Energie des Primaires en GeV	20	30	40	50	60	70	80	90	100	180	260	300	700	900
Nombre de cas	10	5	2	3	3	1	1	1	2	1	1	1	1	1

D'où nous déduisons:

$$s'_1 = 1,05,$$

et en prenant pour E_M la plus grande valeur observée:

$$s_1 = 0,98,$$

$$\frac{1}{s_1} = 0,45, \quad \text{d'où} \quad s_1 = 0,98^{+0,77}_{-0,30}.$$

Si au lieu de prendre $E_m = 20$ GeV, nous nous limitons aux primaires d'énergie supérieure à 50 GeV, nous trouvons dans ce cas: $s'_1 = 1,12$, qui est en accord avec la valeur précédente dans la limite des erreurs expérimentales.

Comme autre application de la méthode d'approche ainsi exposée, nous nous proposons d'examiner le spectre d'énergie des noyaux lourds primaires, d'après les résultats publiés par KAPLON *et al.* ⁽⁴⁾. Ces auteurs ont étudié les effets obus à balles des noyaux lourd primaires de Z compris entre 6 et 26,

⁽⁴⁾ M. F. KAPLON, B. PETERS, H. L. REYNOLDS et D. M. RITSON: *Phys. Rev.*, **85**, 295 (1951).

SUBSCRIPTIONS TO "IL NUOVO CIMENTO"
AND MEMBERSHIP FEES FOR 1955

Subscription rates to IL NUOVO CIMENTO and SUPPLEMENTO:

<i>For Italy</i>	{	normal subscription	6.000 lire
		sponsoring subscription	25.000 lire at least
<i>For foreign countries</i>			6.500 lire

Membership fees:

<i>For Italy</i>	{	individual members	5.000 lire
		organizations	10.000 lire
		sponsoring members	25.000 lire at least
<i>For foreign countries</i>			5.500 lire

To members of the Società Italiana di Fisica IL NUOVO CIMENTO and the SUPPLEMENTO are sent free of charge.

Membership fees and subscription rates are to be paid to the Publisher - Nicola Zanichelli - Bologna, Via Irnerio 34, directly or through a bookseller.

Members and subscribers are kindly requested to see timely to the payment for 1955 in order to avoid suspension of the regular dispatch of the review.

(voltare)

ABBONAMENTI A "IL NUOVO CIMENTO" E QUOTE SOCIALI PER IL 1955

Prezzi di abbonamento al NUOVO CIMENTO e relativo SUPPLEMENTO:

<i>Per l'Italia</i>	{	abbonamento ordinario	L. 6.000	
		abbonamento sostenitore	» 25.000	almeno
<i>Per l'estero</i>	-	abbonamento ordinario	» 6.500	

Quote sociali:

<i>Per l'Italia</i>	{	socio individuale	L. 5.000	
		socio collettivo	» 10.000	
		socio sostenitore	» 25.000	almeno
<i>Per l'estero</i>	-	socio individuale	» 5.500	

Ai soci della Società Italiana di Fisica IL NUOVO CIMENTO e il SUPPLEMENTO sono inviati gratuitamente.

Le somme per l'abbonamento e le quote di associazione vanno pagate (queste direttamente, quelle o direttamente o per mezzo di un libraio) all'Editore Nicola Zanichelli, - Bologna, Via Irnerio, 34 (C/c postale 8/36).

Per evitare la sospensione dell'invio del Giornale si pregano i soci e gli abbonati di provvedere con sollecitudine ai pagamenti per il 1955.

(turn, please)

subissant des collisions avec les noyaux des atomes de l'émulsion. Pour estimer l'énergie par nucléon du primaire, ils utilisent à la fois la méthode basée sur l'ouverture du cône des particules α provenant de la désintégration du primaire par suite de la collision qu'il a subie dans son passage à travers l'émulsion, et celle du scattering mesuré sur les secondaires. Les résultats des deux méthodes, selon ces auteurs, donnent la même distribution aux erreurs expérimentales près.

Prenons les résultats relatifs à la première méthode, nous obtenons d'après la fig. 6 de leur article la distribution suivante:

TABLEAU II. — *Noyaux Lourds Primaires de $Z \geq 6$ (d'après KAPLON et al.).*

Énergie: GeV par nucléon	Nombre de cas	Énergie: GeV par nucléon	Nombre de cas
2	6	8.5	2
2.5	4	11	1
3	8	11.5	2
3,5	7	12	2
4	10	12.5	1
4,5	3	13	1
5	3	15	1
5.5	1	16	1
6	2	18	1
6.5	1	20	1
7	3	23	1
7.5	1	38	1
8	3	44	1

De là, nous déduisons les valeurs suivantes de l'exposant s en prenant successivement pour limite inférieure du spectre: $E_m = 2, 2,5$ et 5 GeV. Nous prenons ici: $E_0 = 0,4$ GeV, correspondant à la latitude géomagnétique 55° N de l'exposition.

TABLEAU III.

Limite inférieure de l'énergie	n	Première approximation s'_1	Seconde approximation s_1
2 GeV	68	1,02	0,85 \pm 0,29 — 0,11
2.5 GeV	62	1,08	0,94 \pm 0,34 — 0,20
5 GeV	58	1,08	0,95 \pm 0,31 — 0,29

Les valeurs ainsi obtenues pour l'exposant s sont compatibles avec la valeur donnée par les auteurs, et également avec la valeur que nous avons obtenue

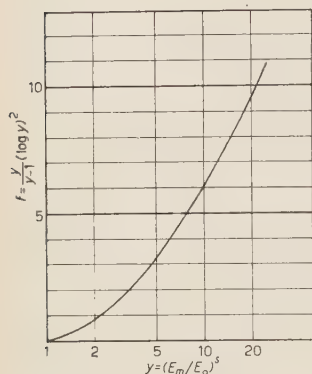


Fig. 1.

pour le spectre d'énergie des protons primaires. Les erreurs sont d'ailleurs grandes par suite, d'une part du petit nombre de mesures disponibles, et d'autre part de la limite inférieure E_m de l'énergie des primaires considérés, les variances sur $1/s$ étant respectivement $1/ns^2$ et $(1/n)f(s)$. La fonction f dépend de $(E_m/E_0)^s$: ses variations sont représentées sur la figure ci-contre.

Enfin il faut remarquer que l'écart-type sur s que donne la méthode du maximum de vraisemblance n'est qu'une limite inférieure. Un calcul plus rigoureux doit tenir compte de la déformation du spectre due aux erreurs expérimentales, plus particulièrement aux basses énergies. Mais cette correction ne nous paraît pas nécessaire pour la présente étude puisqu'en prenant des valeurs différentes de la limite inférieure E_m du spectre nous avons trouvé des valeurs cohérentes pour l'exposant s du spectre.

Nous tenons à exprimer à Monsieur le Professeur LEPRINCE-RINGUET nos remerciements pour l'intérêt continu qu'il a manifesté pour ce travail. Les auteurs de cet article ont bénéficié d'une allocation du Centre National de la Recherche Scientifique, Paris.

Note ajoutée à la correction: Le problème de l'estimation statistique de l'exposant s à partir des résultats fournis par des jets a été envisagé également par ENGLER et HABER SCHAIM: *Phys. Rev.*, **95**, 1700 (1954).

RIASSUNTO (*)

Oggetto del presente lavoro è l'impiego di un metodo statistico basato sulla teoria della massima verosimiglianza (« maximum likelihood ») per la stima dell'esponente s della legge esponenziale E^s che rappresenta lo spettro integrale d'energia della radiazione cosmica primaria. Il metodo è stato applicato successivamente ai protoni primari da noi osservati nei jets registrati in emulsioni fotografiche, e ai primari pesanti con $Z \geq 6$ pubblicati da KAPLON *et al.*. Le due serie di risultati indicano un valore di s non molto maggiore dell'unità. Gli errori dovuti alle fluttuazioni statistiche sono elevati, e se ne dà una discussione dettagliata.

(*) Traduzione a cura della Redazione.

Spettrometro beta ad alto potere di collezione.

G. BOLLA, S. TERRANI e L. ZAPPA

Istituto di Fisica Sperimentale del Politecnico - Milano

(ricevuto il 16 Settembre 1954).

Riassunto. — Viene descritto uno spettrometro beta ad immagine intermedia del tipo Slätis-Siegbahn. Si danno i risultati delle prove di focalizzazione ed alcuni esempi di spettri ottenuti.

1. — Introduzione.

È noto che l'aberrazione cromatica di un sistema ottico-elettronico viene utilizzata per separare elettroni di diversa velocità negli spettrometri beta a lente. I primi tentativi di realizzare strumenti a lente magnetica separatori di velocità sono dovuti a KAPITZA ⁽¹⁾, TRICKER ⁽²⁾, KLEMPERER ⁽³⁾. In generale le proprietà delle lenti magnetiche sono state studiate da DEUTSCH, ELLIOT e EVANS ⁽⁴⁾, COSSLETT ⁽⁵⁾, SIEGBAHN ⁽⁶⁾, DUMOND ⁽⁷⁾, PERSICO ⁽⁸⁾, VERSTER ⁽⁹⁾.

I pregi di uno spettrometro a lente vengono comunemente definiti assegnando di volta in volta grandezze adimensionali (coefficienti di merito ⁽¹⁰⁾) dipendenti dal potere risolutivo e dal potere di collezione. La limitazione più

⁽¹⁾ P. KAPITZA: *Proc. Camb. Phil. Soc.*, **22**, 3 (1924).

⁽²⁾ R. A. TRICKER: *Proc. Camb. Phil. Soc.*, **22**, 454 (1924).

⁽³⁾ O. KLEMPERER: *Phil. Mag.*, **20**, 45 (1935).

⁽⁴⁾ M. DEUTSCH, L. G. ELLIOT e R. D. EVANS: *Rev. Sci. Instr.*, **15**, 178 (1944).

⁽⁵⁾ V. E. COSSLETT: *Journ. Sci. Instr.*, **17**, 259 (1940); *Proc. Phys. Soc.*, **52**, 511 (1940).

⁽⁶⁾ K. SIEGBAHN: *Ark. Mat. Astr. Fys.*, A **30**, n. 1 (1943).

⁽⁷⁾ J. W. DUMOND: *Rev. Sci. Instr.*, **20**, 160, 616 (1949).

⁽⁸⁾ E. PERSICO: *Rev. Sci. Instr.*, **20**, 191 (1949).

⁽⁹⁾ N. F. VERSTER: *Appl. Sci. Research*, B **1**, 363 (1950).

⁽¹⁰⁾ E. PERSICO e C. GEOFFRION: *Rev. Sci. Instr.*, **21**, 945 (1950).

importante al coefficiente di merito di uno strumento è posta dalla aberrazione di sfericità presente in ogni lente elettronica. È noto infatti che la lunghezza focale di una lente dipende dall'angolo di apertura del fascio elettronico. Si deve a SIEGBAHN ⁽¹¹⁾ l'osservazione che l'aberrazione di sfericità può essere corretta, almeno in parte, utilizzando un campo in cui $\partial H_z / \partial r < 0$ (H_z è il campo lungo l'asse della lente). Tale condizione implica che il campo lungo l'asse abbia un minimo tra la sorgente ed il rivelatore.

Durante la costruzione di uno spettrometro corretto per l'aberrazione di sfericità SLÄTIS e SIEGBAHN ⁽¹²⁾ scoprirono un nuovo ed efficace tipo di focalizzazione. Venne infatti notato che, variando opportunamente il campo lungo l'asse, era possibile ottenere una prima immagine anulare nel piano mediano dello strumento ed una seconda immagine puntiforme sull'asse dello strumento in corrispondenza del rivelatore. Questo tipo nuovo di focalizzazione, ad «immagine intermedia», permette di utilizzare fasci elettronici di grande apertura con conseguente aumento del potere di collezione.

Una teoria dello spettrometro ad immagine intermedia è stata trattata, per un caso molto semplice di due lenti magnetiche sottili disposte simmetricamente rispetto al centro dello strumento, da BOTHE ⁽¹³⁾. RICHARDSON ⁽¹⁴⁾ ha discusso

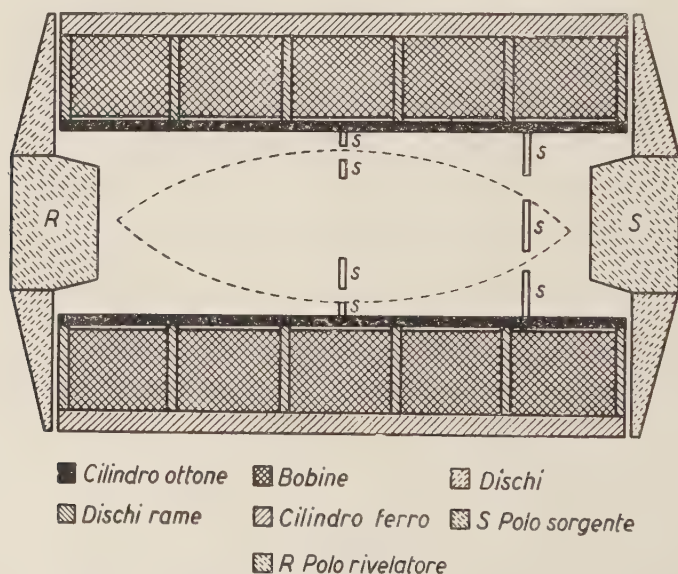


Fig. 1. - Schema generale dello spettrometro.

⁽¹¹⁾ K. SIEGBAHN: *Phil. Mag.*, **37**, 162 (1946).

⁽¹²⁾ H. SLÄTIS e K. SIEGBAHN: *Ark. Fys.*, **1**, 339 (1949).

⁽¹³⁾ W. BOTHE: *Naturwiss.*, **37**, 41 (1950).

⁽¹⁴⁾ H. O. W. RICHARDSON: *Proc. Phys. Soc.*, A **64**, 163 (1951).

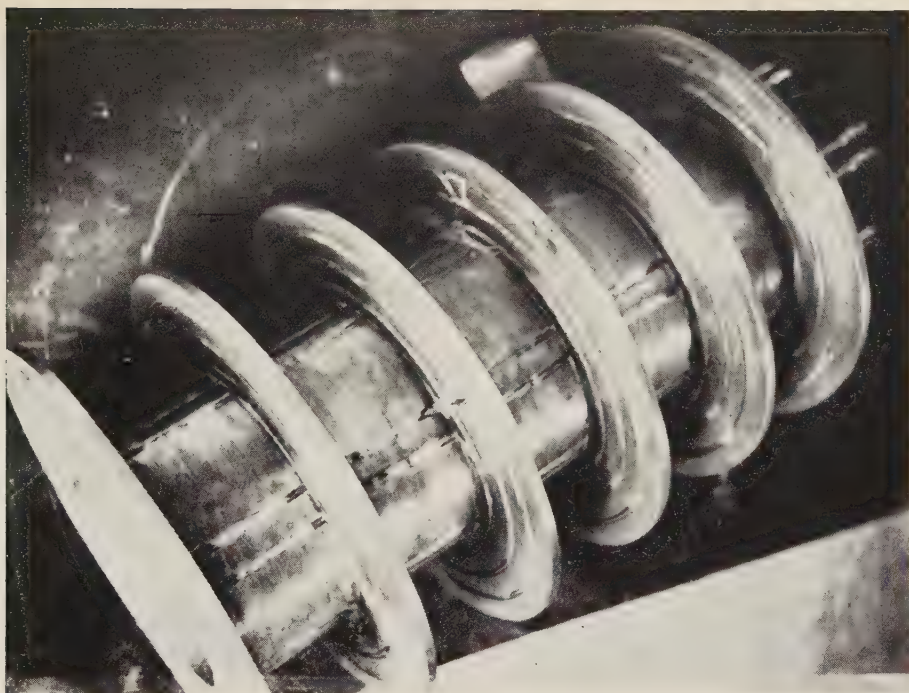


Fig. 2. - La camera con le sedi degli avvolgimenti e le condutture per il raffreddamento.

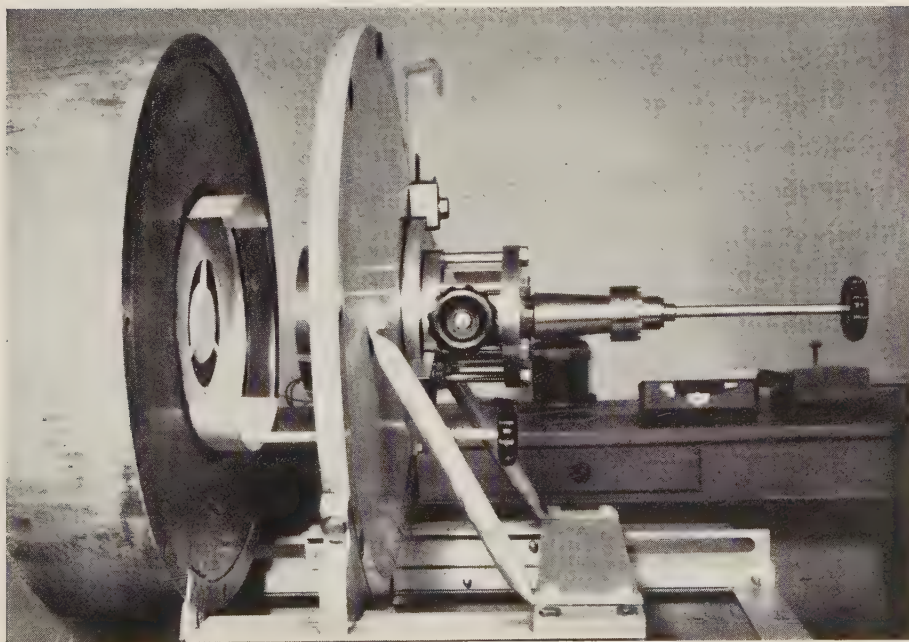


Fig. 3. Il disco col polo portasorgente montato.

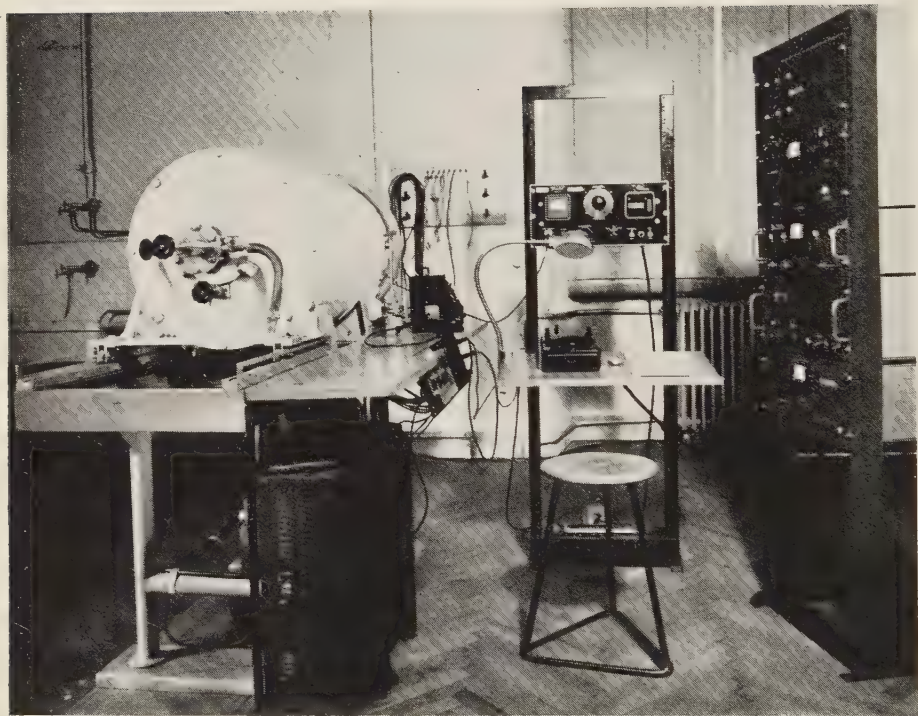


Fig. 4. — Veduta complessiva dello spettrometro con l'apparecchiatura per la stabilizzazione della corrente e la rivelazione.

il problema della focalizzazione intermedia per un campo magnetico realizzato tra due espansioni polari a sezione iperbolica.

Si descrivono brevemente nel presente lavoro le caratteristiche dello spettrometro ad immagine intermedia realizzato in questo Istituto, rimandando per un'esauriente discussione del principio di funzionamento al lavoro di SLÄTIS e SIEGBAHN (¹²).

2. - Descrizione dello spettrometro.

a) *Schema generale dello spettrometro.* - In fig. 1 è riportato lo schema generale dello spettrometro. Sono visibili le traiettorie elettroniche proiettate su un piano meridiano.

b) *La camera a vuoto ed il magnete.* - La camera a vuoto è costituita da un cilindro di ottone (fig. 2) ($230 \times 700 \times 10$ mm) su cui sono saldati ad uguali intervalli 6 dischi di rame (diametro 490 mm) che recano in opportune scanalature le condutture di rame costituenti il sistema di refrigerazione. L'andata e il ritorno di tali condutture corrono sulla superficie esterna del cilindro resa uniforme per mezzo di pezzi di rame opportunamente calandratati.

Fra i dischi di rame sono contenute cinque bobine. Le due estreme consistono di 2100 spire e le tre centrali di 640 spire di rame (2 mm di diametro, smaltato e ricoperto di un doppio strato di cotone).

Il nucleo di ferro è costituito da un cilindro ($700 \times 560 \times 25$ mm) chiuso da due dischi che recano i poli opportunamente sagomati. I dischi si appoggiano alla camera a tenuta di vuoto (fig. 3). Le singole parti, costruite in ferro Armeo, a lavorazione avvenuta sono state sottoposte al processo termico di ricottura presso l'Istituto di Ricerche e Controlli della Soc. Falk.

Uno dei poli (fig. 3) porta la sorgente ed è corredato da un dispositivo che permette la sostituzione del preparato durante le misure, senza immissione d'aria nello spettrometro. L'altro polo porta il rivelatore e i raccordi dei misuratori di vuoto.

Nella camera sono disposti due schermi che determinano con la loro posizione la luminosità ed il potere risolutivo (cfr. paragrafo seguente); la posizione del primo schermo che costituisce la pupilla d'ingresso è regolabile dall'esterno (fig. 3). Il secondo schermo, disposto nel piano mediano dello strumento, sostiene un blocco di piombo per assorbire le radiazioni emesse dalla sorgente nella direzione dell'asse dello strumento.

Lo spettrometro è vuotato con una pompa a diffusione Leybold della velocità di 35 l/s a 10^{-3} mm di Hg, preceduta da una rotativa Leybold della velocità di 5 m³/h a pressione atmosferica. Il vuoto è misurato con una coppia

termoelettrica fino a 10^{-3} mm di Hg e con un vacuometro di Penning al di sotto di tale pressione. Nelle condizioni di funzionamento la pressione all'interno dello spettrometro è inferiore a 10^{-5} mm di Hg.

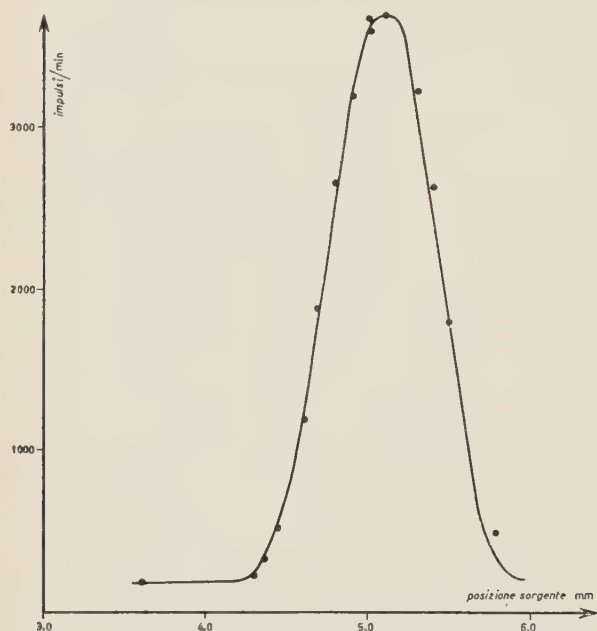


Fig. 5. - Distribuzione delle intensità della riga F del ThB in funzione del rapporto delle correnti.

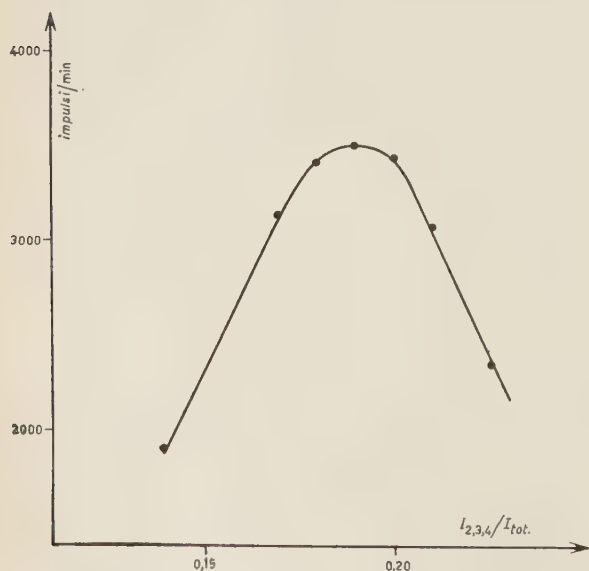


Fig. 6. - Distribuzione delle intensità della riga F del ThB in funzione della posizione della sorgente.

c) *Il rivelatore.* - Il rivelatore è costituito da un contatore di Geiger Müller completamente metallico, del tipo convenzionale, con una finestra laterale di nylon di 10 mm di diametro e dello spessore equivalente a $0,1 \text{ mg/cm}^2$. Viene riempito con una miscela di argon e metano alla pressione di 10 cm di Hg.

d) *L'alimentazione del magnete.* - La corrente per le bobine viene fornita da un gruppo motore-dinamo (Marelli) in grado di erogare una potenza massima di 4,5 kW ad una tensione di 350 V. La corrente viene mantenuta ad un valore costante (± 1 per mille) per mezzo di uno stabilizzatore a controreazione costruito presso la ditta SELO di Milano.

La veduta complessiva dello spettrometro con la apparecchiatura per la stabilizzazione della corrente e la rivelazione, è data in fig. 4.

3. - Focalizzazione.

L'influenza del rapporto delle correnti nelle diverse

Fig. 7. — Variazione del potere risolutivo in funzione della posizione del 2° schermo.

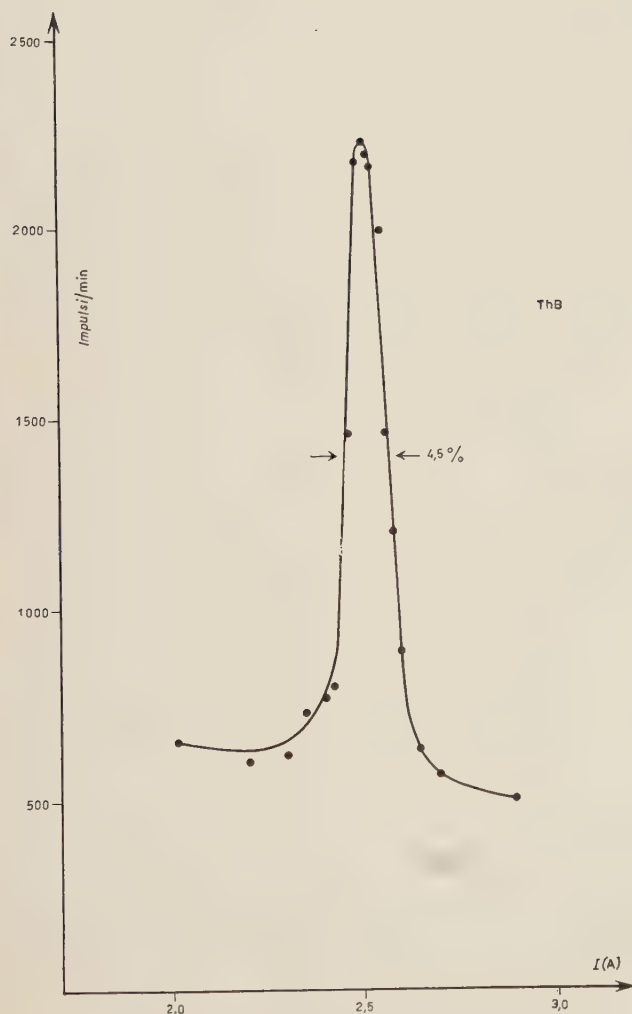
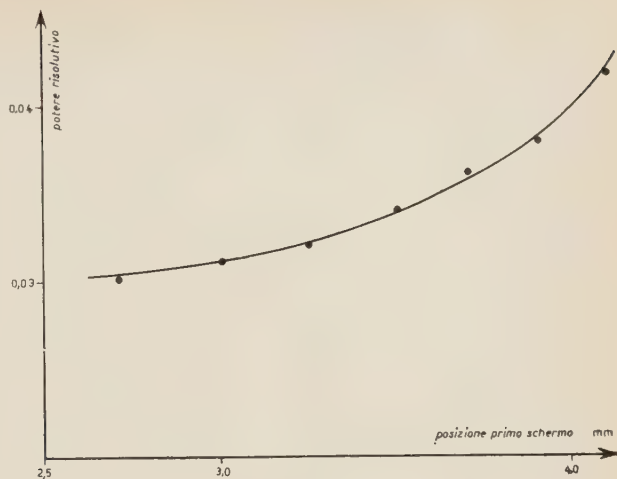


Fig. 8. — La riga F del ThB presa con basso potere risolutivo.

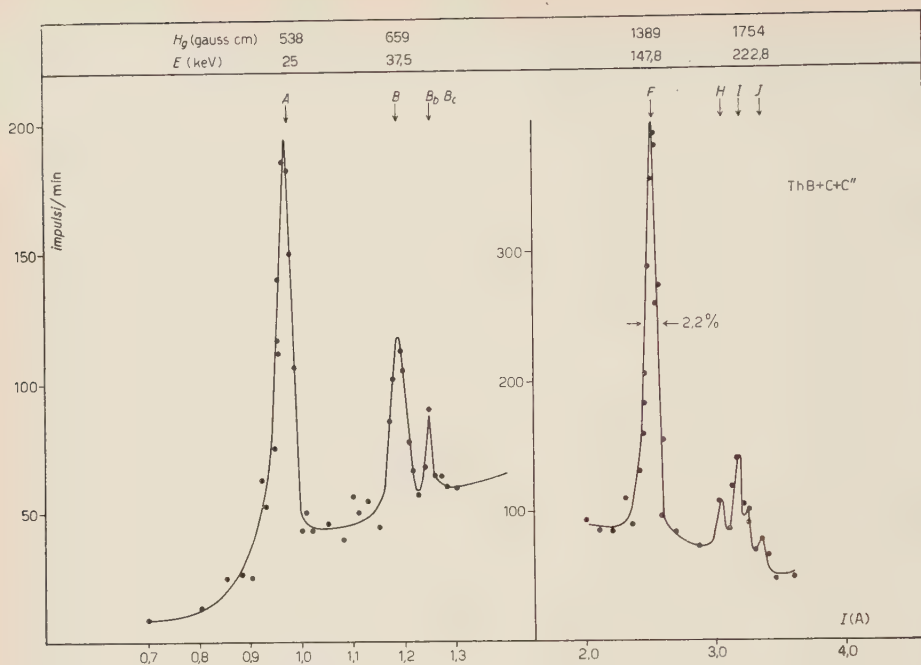
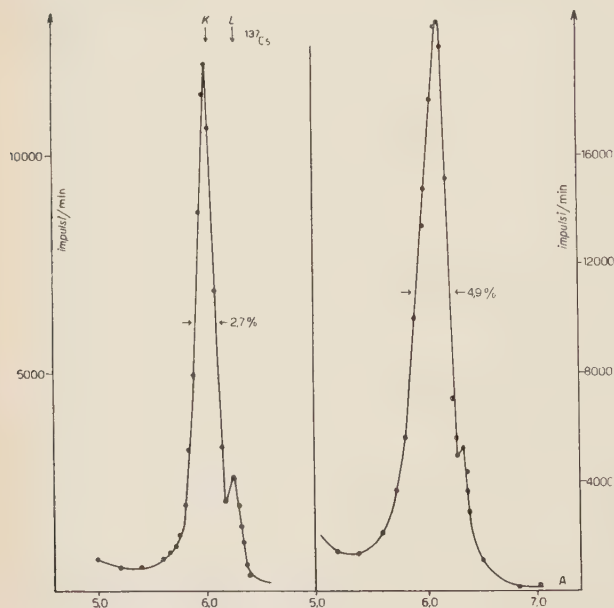


Fig. 9. - Lo spettro del ThB+C+C'' preso con alto potere risolutivo.

bobine, delle posizioni della sorgente e degli schermi e delle aperture degli schermi stessi sulla focalizzazione è stata studiata accuratamente usando come sorgente un preparato di ThB + C + C''.



a) *Rapporto delle correnti.* - La fig. 5 mostra la distribuzione delle intensità della riga F del ThB in funzione del rapporto $I_{2,3,4}/I_{tot}$ ($I_{2,3,4}$ rappresenta la corrente nelle tre bobine centrali in serie, I_{tot} la corrente totale) per un dato schermo cen-

Fig. 10. - Le righe di conversione interna K ed L del ¹³⁷Cs prese con basso ed alto potere risolutivo.

trale ed una data posizione della sorgente. A parità di potere risolutivo il massimo potere di collezione è stato ottenuto con $I_{2,3,4}/I_{\text{tot}}=0,185$.

b) *Posizione della sorgente.* — Date le proprietà simmetriche del tipo di focalizzazione, una variazione di qualche millimetro nella posizione della sorgente determina una sensibile variazione del potere di collezione dello spettrometro. In fig. 6 sono riportate le intensità della riga F del ThB in funzione delle posizioni della sorgente mantenendo inalterate le posizioni degli schermi.

c) *Posizione 1° schermo.* — Un avanzamento di questo schermo permette l'ingresso nello spettrometro di traiettorie elettroniche

che si svolgono sempre più vicino all'asse dello strumento e che risentono quindi meno dell'errore di sfericità. D'altra parte l'avanzamento determina una riduzione dell'angolo solido del fascio elettronico e quindi una diminuzione del potere di collezione.

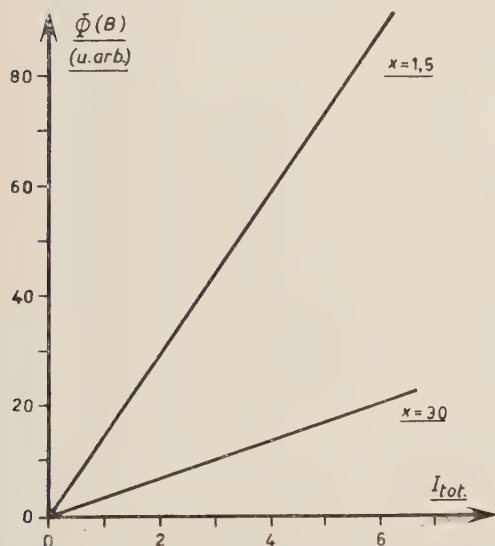


Fig. 12. — Relazione corrente-campo sul polo ed al centro dello spettrometro.

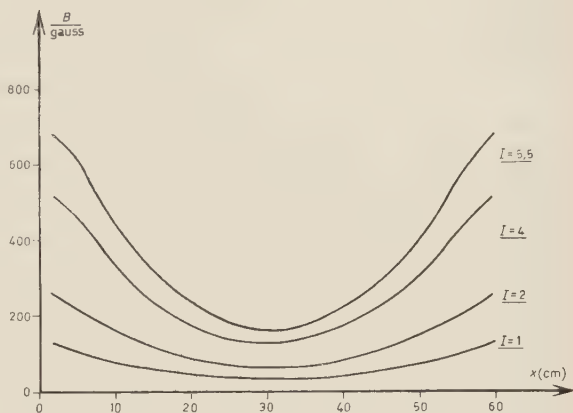


Fig. 11. Andamento del campo lungo l'asse dello strumento.

La posizione migliore è stata ricercata per tentativi. L'effetto è illustrato in fig. 7.

d) *Apertura 2° schermo.* — Gli effetti prodotti dalla variazione di apertura del 2° schermo sono visibili nelle figg. 8, 9, 10 sugli spettri del ThB + C + C' e del ^{137}Cs . Con un'apertura di 8,5 mm e con un diametro della sorgente pari a 5 mm la risoluzione ottenuta è del 5% circa; il potere di collezione risulta in tali condizioni dell'8%. Gli spettri al 2% e 3% sono stati ottenuti con un'apertura del 2° schermo di 2 mm e un diametro della sorgente pari a 2 e 3 mm rispettivamente.

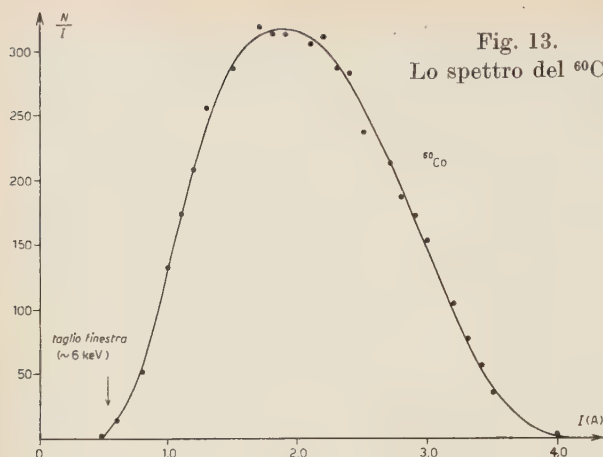


Fig. 13.
Lo spettro del ^{60}Co .

4. - Misura del campo magnetico e calibrazione dello spettrometro.

Il campo magnetico è stato misurato lungo l'asse dello strumento con un flussometro. I risultati ottenuti con un rapporto di correnti pari a $I_{2,3,4}/I_{\text{tot}} = 0,185$ sono riportati in fig. 11. La fig. 12 mostra la dipendenza del campo dalla corrente in diversi punti dell'asse. Dato il tipo di ferro usato, l'andamento è perfettamente lineare. Si ottiene quindi per la relazione corrente-momento degli elettroni focalizzati:

$$H_Q = kI, \quad k = \text{cost.}$$

La costante k è stata determinata usando le righe F ed I del $\text{ThB} + \text{C} + \text{C}''$ e i picchi di conversione interna K ed L del γ a 661.7 keV del ^{137}Cs . Per una data posizione della sorgente e per un dato rapporto delle correnti si è ottenuto: $k = 554,1$.

In fig. 13 è riportato lo spettro β^- del ^{60}Co . Il diagramma di Fermi-Kurie di questo spettro è mostrato in fig. 14. La

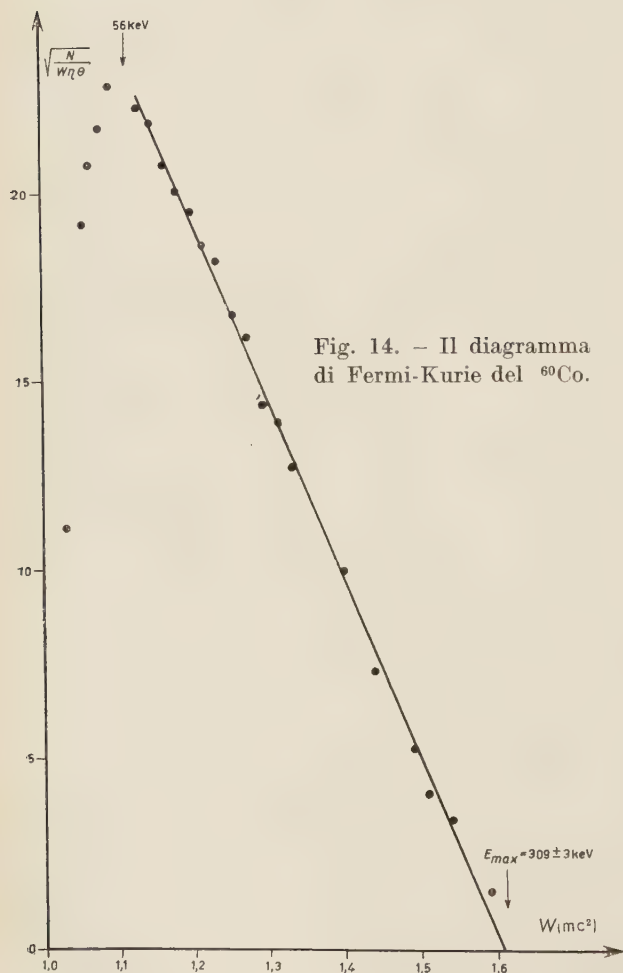


Fig. 14. - Il diagramma di Fermi-Kurie del ^{60}Co .

energia massima ottenuta è:

$$E_0 = 309 \pm 3 \text{ keV}.$$

L'andamento è lineare fino a circa 56 keV dove cominciano a manifestarsi gli effetti dell'autoassorbimento del preparato e del backscattering.

Ringraziamo i professori H. SLÄTIS e K. SIEGBAHN, presso i quali uno di noi (L. ZAPPA) ha lavorato dall'Agosto al Dicembre 1951 ed ha potuto prendere visione dei disegni dello spettrometro a immagine intermedia; le Acciaierie e Ferriere Falk e in particolare il dott. M. SIGNORA, direttore del Centro Ricerche e Controlli e il dott. F. BALDI; l'ing. P. GOBBATO, delle Officine Motori Marini G. Carraro di Milano che ha curato con particolare interesse la parte meccanica del magnete; l'Istituto Nazionale di Fisica Nucleare e la Direzione del Politecnico, le cui sovvenzioni hanno reso possibile la realizzazione dello strumento.

SUMMARY

An intermediate image type Slätis-Siegbahn beta-spectrometer is described. Focusing experiments and some spectra are reported.

Optics in Terms of Observable Quantities.

E. WOLF

Department of Astronomy, The University, Manchester, England

(ricevuto il 26 Settembre 1954)

Summary — Space-time correlation functions are defined which express the correlation between components of the electromagnetic field vectors in stationary fields. These functions form sets of 3×3 matrices, the individual elements of which obey the wave equation. Unlike the field vectors which are not measurable at the high frequencies encountered in Optics our correlation functions may be determined with the help of standard optical instruments. The results enable a unified treatment of theories of partial coherence and partial polarization to be obtained, and suggest a formulation of a wide branch of Optics in terms of observable quantities only.

In all Optical experiments the only quantities which are observable are the averages of certain quadratic functions of the field components. It is therefore tempting to try to formulate the laws of Optical fields directly in terms of such quantities rather than in terms of the unmeasurable field vectors as has been customary in the past.

It was as early as 1852 that STOKES ⁽¹⁾ showed that a nearly monochromatic (plane) light wave may be characterized at each point by four parameters which now bear his name (*). If

$$(1) \quad E_x = a_1(\mathbf{x}, t) \cos \{2\pi\nu_0 t - \alpha_1(\mathbf{x}, t)\}, \quad E_y = a_2(\mathbf{x}, t) \cos \{2\pi\nu_0 t - \alpha_2(\mathbf{x}, t)\},$$

⁽¹⁾ G. G. STOKES: *Trans. Camb. Phil. Soc.*, **9**, 399 (1852). Also his *Mathematical and Physical Papers* (Cambridge, 1901), vol. III, p. 233.

(*) Very good accounts of the Stoke's parameters may be found in CHANDRA-SEKHAR ⁽²⁾ and WALKER ⁽³⁾.

are the components of the electric vector of such a wave in two mutually orthogonal directions at right angles to the direction of propagation, the Stokes parameters are defined by

$$(2) \quad \begin{cases} P = \langle a_1^2 + a_2^2 \rangle, & Q = \langle a_1^2 - a_2^2 \rangle, \\ U = \langle 2a_1 a_2 \cos(\alpha_1 - \alpha_2) \rangle, & V = \langle 2a_1 a_2 \sin(\alpha_1 - \alpha_2) \rangle, \end{cases}$$

the brackets $\langle \dots \rangle$ denoting time average. Then the intensity $I(\psi, \varepsilon)$ associated with vibrations in the direction which makes an angle ψ with the x -direction, when retardation ε is introduced between the two components, is given by (see CHANDRASEKHAR ⁽²⁾, p. 29)

$$(3) \quad I(\psi, \varepsilon) = \frac{1}{2}[P + Q \cos 2\psi + (U \cos \varepsilon - V \sin \varepsilon) \sin 2\psi].$$

By measuring I for different values of ψ and ε , the four parameters may be determined.

Let us now introduce in place of E_x and E_y , the associated complex vectors

$$(4) \quad \hat{E}_x = a_1(\mathbf{x}, t) \exp \{i[2\pi\nu_0 t - \alpha_1(\mathbf{x}, t)]\}, \quad \hat{E}_y = a_2(\mathbf{x}, t) \exp \{i[2\pi\nu_0 t - \alpha_2(\mathbf{x}, t)]\}.$$

Next we construct the four functions

$$(5) \quad \mathfrak{E}_{ij} = \langle \hat{E}_i(\mathbf{x}, t) \hat{E}_j^*(\mathbf{x}, t) \rangle,$$

where i and j can each take on the value x or y and asterisk denotes the complex conjugate. The knowledge of these four quantities is equivalent to the knowledge of the four Stokes parameters; in fact the Stokes parameters are simple linear combinations of the \mathfrak{E}_{ij} 's. If (3) is expressed in terms of these quantities, one finds after a simple calculation that

$$(6) \quad I(\psi, \varepsilon) = I_x(\psi) + I_y(\psi) + 2\sqrt{I_x(\psi)I_y(\psi)}|\gamma_{xy}|\cos[\arg \gamma_{xy} + \varepsilon],$$

where

$$(7) \quad I_x(\psi) = \mathfrak{E}_{xx} \cos^2 \psi, \quad I_y(\psi) = \mathfrak{E}_{yy} \sin^2 \psi,$$

and

$$(8) \quad \gamma_{xy} = \frac{\mathfrak{E}_{xy}}{\sqrt{\mathfrak{E}_{xx}}\sqrt{\mathfrak{E}_{yy}}};$$

⁽²⁾ S. CHANDRASEKHAR: *Radiative Transfer* (Oxford, 1950).

⁽³⁾ M. J. WALKER: *Amer. Journ. Phys.*, **22**, 170 (1954).

and the well-known inequality $P^2 \geq Q^2 + U^2 + V^2$ becomes simply $|\gamma_{\alpha\alpha}| \leq 1$. Equation (6) is formally identical with the *generalized interference law* derived in recent years in the theory of partially coherent scalar fields (ZERNIKE ⁽⁴⁾, HOPKINS ⁽⁵⁾, WOLF ⁽⁶⁾). In the special case when $\gamma = 0$, (6) reduces to the usual law for the combination of completely incoherent fields; when $|\gamma| = 1$ it reduces to the ordinary interference law for fields which are perfectly coherent. Partially coherent and partially polarized fields are characterized by the intermediate values of $|\gamma|$.

Now the Stokes parameters (or the 2 by 2 matrix whose elements are defined by (5)) give the intensity and express the correlation between the components of \mathbf{E} at the *same* point in space and at the *same* instant of time. Moreover they are defined only for a plane wave whose effective frequency range is sufficiently narrow. In order to characterize a general stationary field (*), we introduce, by analogy with the scalar case (see WOLF ⁽⁷⁾), correlation functions between field components at different points in space and at different instants of time.

Let

$$(9) \quad E_i(\mathbf{x}, t) = \int_0^\infty a_{vi}(\mathbf{x}) \cos \{2\pi\nu t - \alpha_{vi}(\mathbf{x})\} d\nu, \quad (i = x, y \text{ or } z)$$

be the Fourier representation of a typical field component over the time interval $-T \leq t \leq T$, \mathbf{E} being formally assumed to be zero outside this range, and define the functions

$$(10) \quad \hat{E}_i(\mathbf{x}, t) = \int_0^\infty a_{vi}(\mathbf{x}) \exp \{i[2\pi\nu t - \alpha_{vi}(\mathbf{x})]\} d\nu.$$

We now introduce a 3×3 correlation matrix \mathcal{E} whose elements are

$$(11) \quad \mathcal{E}_{ij}(\mathbf{x}_1, \mathbf{x}_2, \tau) = \langle \hat{E}_i(\mathbf{x}_1, t + \tau) \hat{E}_j^*(\mathbf{x}_2, t) \rangle.$$

Similar considerations to those employed in connection with scalar fields of

⁽⁴⁾ F. ZERNIKE: *Physica*, **5**, 785 (1938).

⁽⁵⁾ H. H. HOPKINS: *Proc. Roy. Soc.*, A **208**, 263 (1951).

⁽⁶⁾ E. WOLF: *Proc. Roy. Soc.*, A **225**, 96 (1954).

(*) By a stationary field we mean here a field of which all *observable* properties are constant in time. This includes as a special case the usual case of high frequency periodic time-dependence; or the field constituted by the steady flux of polychromatic radiation through an optical system. But it excludes fields for which the time average over a macroscopic time interval of the flux of radiation depends on time.

⁽⁷⁾ E. WOLF: *Proc. Roy. Soc.*, in press.

arbitrary frequency range and with vector fields characterized by the Stokes parameters indicate, that the expressions for the electric energy density appropriate to various experimental conditions are simple functions of the elements of the \mathcal{E} -matrix; and moreover that all these elements may be determined from experiments by means of standard optical instruments.

Since the electric vector satisfies the wave equation, it can readily be shown that each element of the \mathcal{E} -matrix satisfies two equations.

$$(12) \quad \begin{cases} \nabla_1^2 \mathcal{E}_{ij} = \frac{1}{c^2} \frac{\partial^2 \mathcal{E}_{ij}}{\partial \tau^2}, \\ \nabla_2^2 \mathcal{E}_{ij} = \frac{1}{c^2} \frac{\partial^2 \mathcal{E}_{ij}}{\partial \tau^2}, \end{cases}$$

where ∇_1^2 and ∇_2^2 are the Laplacian operators with respect to the coordinates of \mathbf{x}_1 and \mathbf{x}_2 , and c is the velocity of light in the vacuum. Thus not only the unmesurable field vectors, but also the *observable correlation functions* here introduced *obey rigorous propagation laws*. This result should prove particularly useful in connection with scattering problems.

In addition to the \mathcal{E} -matrix, one can introduce similar matrices involving components of the other field vectors (\mathbf{H} , \mathbf{D} and \mathbf{B}) and also matrices involving mixed pairs like E_i and H_j . On account of Maxwell's equations, these matrices are related by a set of first order partial differential equations with respect to the variables \mathbf{x}_1 , \mathbf{x}_2 , and τ . In the analysis of all optical experiments $c\tau$ will play the part of an optical path difference. The actual time, like the frequency has been eliminated.

Unlike the \mathcal{E} -matrix, the \mathcal{H} matrix is not likely to be of any interest in Optics, since no radiation detectors appear to be available at Optical wavelengths which would respond to the magnetic rather than the electric field. It may, however, prove useful in connection with applications to other types of partially coherent radiation, e.g. in Radio Astronomy. The matrix containing the mixed pairs should prove useful in experiments where the (averaged) flux of energy rather than the energy density is measured.

The matrices here introduced may be expected to play a role in Electromagnetic field theory which is somewhat analogous to that which the Density matrix of von NEUMAN⁽⁸⁾ plays in Quantum Mechanics. An analogy between the Stokes parameters and the Density Matrix has been noted previously (PERRIN⁽⁹⁾, FALKOFF and MACDONALD⁽¹⁰⁾; see also FANO⁽¹¹⁾). It is, how-

⁽⁸⁾ J. V. NEUMANN: *Gött. Nachr.*, 245 (1927).

⁽⁹⁾ F. PERRIN, *Journ. Chem. Phys.*, 10, 415 (1942).

⁽¹⁰⁾ D. L. FALKOFF and J. E. MACDONALD: *Journ. Opt. Soc. Amer.*, 41, 861 (1951).

⁽¹¹⁾ U. FANO: *Phys. Rev.*, 93, 121 (1954).

ever, evident that only by considering more general correlation functions, such as those here introduced, does one obtain an adequate tool for the study of propagation problems in a general stationary electromagnetic field.

A fuller discussion of the subject matter of this note will be published at a later date.

This work was carried out during the tenure of an Imperial Chemical Industries Research Fellowship and was also supported by a grant from the Carnegie Trust for the Universities of Scotland, both of which are gratefully acknowledged.

RIASSUNTO (*)

Si definiscono funzioni di correlazione spazio-tempo che esprimono la correlazione fra componenti dei vettori del campo elettromagnetico in campi stazionari. Queste funzioni formano gruppi di 3×3 matrici i cui elementi individuali soddisfano all'equazione d'onda. A differenza dei vettori di campo che, alle alte frequenze che intervengono in Ottica, non sono misurabili, le nostre funzioni di correlazione possono essere determinate con l'ausilio degli ordinari apparecchi ottici. I risultati consentono un trattamento unificato delle teorie della coerenza parziale e della polarizzazione parziale e suggeriscono una formulazione di un ampio settore dell'Ottica in termini di sole grandezze osservabili.

(*) *Traduzione a cura della Redazione.*

Tracce di rinculo in stelle di disintegrazione nucleare generate da protoni di energia definita (50, 100, 150, 250 e 450 MeV).

M. GRILLI e B. VITALE

Istituto di Fisica dell'Università - Padova
Istituto Nazionale di Fisica Nucleare - Sezione di Padova

P. E. HODGSON

University College - London

M. LADU (*)

Istituto di Fisica dell'Università - Cagliari

(ricevuto l'11 Ottobre 1954)

Riassunto. — Sono presentati i risultati di misure effettuate sulle tracce di rinculo presenti in stelle di disintegrazione nucleare prodotte in emulsione fotografica da protoni di 50, 100, 150, 250 e 450 MeV; essi sono inoltre confrontati con quelli previsti mediante una analisi statistica (tipo « Montecarlo » ⁽¹⁾), per protoni primari di 400 MeV. Nei limiti degli errori sperimentali il modello precedentemente proposto (v. ⁽¹⁾) per la formazione del rinculo rende conto della maggior parte dei risultati sperimentali, o non risulta contraddittorio con essi.

Introduzione.

In un lavoro precedente (GRILLI *et al.* ⁽¹⁾) sono stati dati i risultati di una analisi sistematica delle tracce di rinculo presenti nelle stelle di disintegrazione nucleare, prodotte dalla radiazione cosmica in emulsioni nucleari esposte a quota di montagna. Le stelle studiate erano suddivise, in base al numero ed all'energia dei rami, in tre categorie corrispondenti ad una energia media dei primari di, rispettivamente, 250, 400 e 700 MeV. I risultati ottenuti per

(*) Attualmente presso l'Istituto Nazionale di Fisica Nucleare, Sezione di Milano.

⁽¹⁾ M. GRILLI e B. VITALE: *Nuovo Cimento*, **10**, 1047 (1953).

la seconda categoria erano poi confrontati con quelli di una analisi statistica (tipo « Montecarlo ») basata su disintegrazioni generate da primari di 400 MeV.

Si era giunti così ad alcune interessanti conclusioni sul meccanismo di formazione del rinculo, sul legame del rinculo con i processi che si sovrappongono durante una disintegrazione nucleare e sull'intervento di altri fenomeni (quali l'evaporazione locale) necessari per spiegare alcune caratteristiche delle distribuzioni sperimentali. Il campione sperimentale era però per vari motivi insoddisfacente: erano ignote la natura e la direzione dei primari, e l'attribuzione di una stella ad una delle tre categorie energetiche era resa dubbia dalle larghe fluttuazioni presenti, a parità di energia del primario, nel numero di rami ionizzanti.

Abbiamo quindi ritenuto utile perfezionare il campione sperimentale, analizzando stelle prodotte da primari ionizzanti di energia ben definita; abbiamo usato a questo scopo protoni accelerati in ciclotrone fino a energie di 50, 100, 150, 250 e 450 MeV. I risultati ottenuti verranno discussi nei sei paragrafi seguenti:

- 1) Condizioni sperimentali.
- 2) Distribuzione angolare dei rinculi.
- 3) Distribuzione in lunghezza dei rinculi.
- 4) Angoli tra rami e rinculi.
- 5) Angoli tra rami e primario, in stelle con rinculo e senza rinculo.
- 6) Discussione e conclusioni.

1. - Condizioni sperimentali.

Le emulsioni usate, le condizioni di esposizione al fascio di protoni ed il tipo di sviluppo al quale esse sono state sottoposte sono riassunti nella tab. I.

Le lastre della III e V cat. sono state sottosviluppate perchè fosse in esse possibile la discriminazione tra protoni e particelle α , discriminazione questa già possibile nelle C2 della I e II cat.

1.1. Simboli e notazioni usati. - Nel seguito useremo i seguenti simboli e notazioni con il significato qui indicato:

- ϑ = proiezione sul piano dell'emulsione dell'angolo tra un ramo ed il primario di una stella;
- ϑ_r = proiezione dell'angolo tra rinculo e primario;
- $(\vartheta - \vartheta_r)$ = proiezione dell'angolo tra ramo e rinculo;
- L = lunghezza del rinculo sul piano dell'emulsione;

TABELLA I.

Categoria	Emulsione	Energia primari	Angolo incl. primari-emulsione	Sviluppo	Note
I - 50 MeV	Ilford C2 200 μ	45 ± 4 MeV 68 ± 4 MeV	3°	normale	(¹)
II - 100 MeV	Ilford C2 200 μ	94 ± 4 MeV 122 ± 4 MeV	3°	normale	(¹)
III - 150 MeV	Ilford G5 600 μ	147 ± 6 MeV	10°	sottosvil. a 11°	(¹)
IV - 250 MeV	Ilford G5 300 μ	240 ± 10 MeV	10°	normale	(²)
V - 450 MeV	Ilford G5 600 μ	450 ± 30 MeV	10°	sottosvil. a 11°	(³)

(1) Esposizione dovuta alla cortesia del Dott. D. M. SKYRME.
 (2) Esposizione dovuta alla cortesia del Prof. R. E. MARSHAK.
 (3) Esposizione dovuta alla cortesia del Prof. M. SCHEIN.

ramo nero N : con ionizzazione corrispondente a quella di un protone di $En \leq 20$ MeV;

ramo grigio G : con ionizzazione corrispondente a quella di un protone di $En > 20$ MeV;

$$R = \frac{\text{rinculi in avanti}}{\text{rinculi indietro}} = \frac{\text{stelle con } 0^\circ \leq \vartheta_r \leq 90^\circ}{\text{stelle con } 90^\circ < \vartheta_r \leq 180^\circ};$$

$$B = \frac{\text{rami con } 0^\circ \leq \vartheta \leq 90^\circ}{\text{rami con } 90^\circ < \vartheta \leq 180^\circ};$$

$$C = \frac{\text{rami con } 90^\circ < (\vartheta - \vartheta_r) \leq 180^\circ}{\text{rami con } 0^\circ \leq (\vartheta - \vartheta_r) < 90^\circ}.$$

1.2. *Statistica raccolta.* - Abbiamo definito come «rinculo» ogni traccia con $1 \leq L \leq 5 \mu$ (per le ragioni che giustificano questa definizione, e per le precauzioni prese nei casi dubbi, v. (¹)).

Raccolte separatamente le distribuzioni che interessavano per ogni energia del primario, l'assenza di ogni sensibile differenza tra i risultati ottenuti per 45 e 68 MeV e per 94 e 122 MeV ci ha indotto a raggrupparli in due sole categorie (I e II cat.) alle quali abbiamo attribuito una energia media di 50 e 100 MeV; questo ci ha permesso di aumentare la statistica per le prime categorie, diminuendo gli errori statistici sulle relative distribuzioni.

Si è tentato di eliminare dalla statistica raccolta il contributo dovuto alle disintegrazioni in nuclei leggeri dell'emulsione, identificando queste ultime mediante il criterio delle particelle α di bassa energia, già sviluppato da uno di noi (HODGSON ⁽²⁾). Il comportamento delle α e dei protoni nelle stelle così selezionate è stato analizzato, e sarà oggetto di un successivo lavoro; esso è, sotto molti aspetti, in buon accordo con l'attribuzione di queste disintegrazioni a nuclei leggeri. Anche il comportamento dei « rinculi » in queste stelle risulta nettamente diverso da quello corrispondente dei « rinculi » nelle stelle attribuite a nuclei pesanti ed è in genere coerente con una interpretazione di queste tracce corte come α e protoni molto lenti prodotti nella disintegrazione di un nucleo leggero, o come frammenti nucleari leggeri, piuttosto che come veri e propri nuclei di rinculo.

Il numero di stelle in nucleo pesante raccolte e studiate per le varie energie del primario è dato in tabella II:

TABELLA II.

Energia	50	100	150	250	450
Numero di stelle . . .	89	111	143	171	201

L'analisi che segue si riferisce solo alle stelle in nuclei pesanti.

2. - Distribuzione angolare dei rinculi.

In tabella III è dato il valore del rapporto R per le differenti categorie (gli errori indicati, qui e nel seguito, sono gli errori quadratici medi); in fig. 1 è riportata la distribuzione di R al variare dell'energia del primario; in fig. 2 è riportata la $f(\vartheta_r)$ per stelle di 450 MeV, e la corrispondente distribuzione prevista dal Montecarlo.

TABELLA III.

Energia	50	100	150	250	450
$R =$	$8,1 \pm 2,8$	$6,7 \pm 1,9$	$3,4 \pm 0,7$	$2,7 \pm 0,5$	$2,5 \pm 0,4$

L'unico valore sperimentale già noto (SEED ⁽³⁾) è $R = 6,3$ per stelle gene-

⁽²⁾ P. E. HODGSON: *Phil. Mag.*, **45**, 190 (1954).

⁽³⁾ R. G. SEED: *Phys. Rev.*, **87**, 182 (1952).

rate da protoni di 100 MeV; il punto corrispondente è indicato in fig. 1 e si accorda molto bene con i nostri dati.

Il disaccordo tra i dati sperimentali e le previsioni del Montecarlo è sensibile: non è infatti presente il massimo previsto sui 60° - 80° , e l'anisotropia trovata per i rinculi è nettamente inferiore a quella prevista (il MC infatti dà: $R = 8,5 \pm 3,5$). È questo, come vedremo, l'unico punto di sostanziale differenza tra i risultati del MC e i dati sperimentali per stelle della V categoria; non crediamo, quindi, che esso possa, da solo, inficiare il modello proposto per la formazione del rinculo, ma piuttosto che esso possa essere attribuito alla non validità di qualcuna delle ipotesi utilizzate durante il MC, ipotesi che risulta determinante nella definizione della direzione del rinculo ma non interviene in modo sensibile nelle altre distribuzioni raccolte (lunghezza dei rinculi, angoli rami-rinculi, ecc.). Ad esempio, è probabile che si sia sopravvalutato il valore del rapporto n_{ev}/p_{ev} (infatti le stelle del MC mostrano un difetto di rami ionizzanti rispetto a quelle generate da primari di 450 MeV); e poichè i neutroni evaporativi, di energia media molto minore di quella dei protoni, riescono più difficilmente a modificare la direzione dell'impulso ceduto dai rami di emissione diretta (diretto in genere in avanti), è evidente che una tale sopravvalutazione porta di preferenza a rinculi più collimati in avanti.

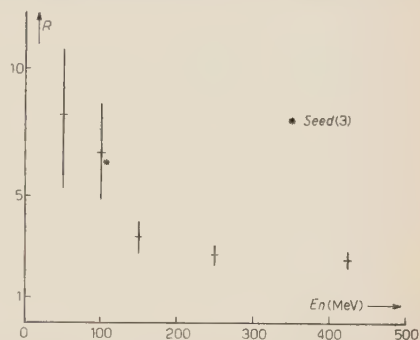


Fig. 1. - Variazione di R al variare dell'energia del primario.

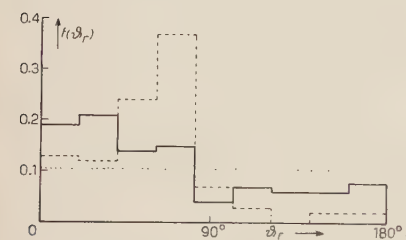


Fig. 2. - Distribuzione angolare dei rinculi rispetto al primario. — Risultati sperimentali per le stelle della V categoria: ---- risultati del Montecarlo (primari di 400 MeV).

a causa del maggior numero di rami presenti, in genere, nel semipiano in avanti. Infatti, se ciò fosse, la perdita dovrebbe interessare soprattutto i rinculi molto corti, e quindi la lunghezza media dei rinculi in avanti ed indietro dovrebbe essere diversa, con un valore più alto per i rinculi in avanti. I dati sperimentali, al contrario, non mettono in evidenza alcun fenomeno di questo tipo.

Il decrescere di R all'aumentare dell'energia è coerente con il modello proposto: all'aumentare del numero di rami la parte di essi maggiormente colli-

mata, i grigi, cede un impulso sempre minore al nucleo (v. formula (5) in ⁽¹⁾); i rami che contribuiscono di più alla formazione del rinculo, i neri di emissione diretta ed i grigi di più bassa energia, sono sempre più sparpagliati: in definitiva la direzione dell'impulso totale ceduto al nucleo è sempre meno collegata alla direzione del primario.

3. - Distribuzione in lunghezza dei rinculi.

In tabella IV è dato il valore della lunghezza media dei rinculi, \bar{L} , per le differenti categorie; in fig. 3 è riportata la distribuzione di \bar{L} al variare dell'energia del primario.

TABELLA IV.

Energia	50	100	150	250	450
$\bar{L} =$	1,9 μ	1,9 μ	2,1 μ	2,6 μ	2,8 μ

Il valore di \bar{L} previsto dal Montecarlo era di 2,8 μ : l'accordo con l' \bar{L} della V categoria è, come si vede, ottimo, ma non è eccessivamente significativo. Infatti lo spettro in \bar{L} previsto dal MC ha un andamento differente da quello sperimentale: nel primo vi è un netto predominio di rinculi molto corti (tra 1 e 2 μ), nel secondo il massimo è tra 2 e 3 μ , e non è molto pronunciato. Un simile disaccordo è chiaramente collegato ad una perdita preferenziale di rinculi molto piccoli ed è pienamente giustificabile dal punto di vista sperimentale; esso però rende un poco casuale l'accordo ritrovato per \bar{L} .

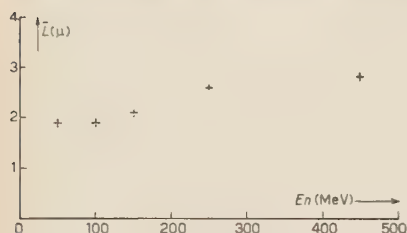


Fig. 3. - Variazione di \bar{L} al variare dell'energia del primario.

rende un poco casuale l'accordo ritrovato per \bar{L} .

L'aumentare di \bar{L} al crescere dell'energia è, per le stesse ragioni esposte nel par. precedente, coerente con il modello proposto: l'aumento del numero di rami, nel mentre rende più isotropo l'impulso totale ceduto al nucleo, lo rende anche sempre più grande.

4. - Angoli tra rami e primario, in stelle con e senza rinculo visibile.

In tab. V è dato il valore del rapporto B per le differenti categorie e per i rami neri N e grigi G , separatamente per le stelle con e senza rinculo visibile e per tutte le stelle; in fig. 4 è riportata la distribuzione di B per i N al variare dell'energia del primario.

TABELLA V.

Energia	50	100	150	450
Rami neri:				
Stelle c.r. . .	$1,3 \pm 0,2$	$1,2 \pm 0,1$	$1,5 \pm 0,2$	$1,2 \pm 0,1$
Stelle s.r. . .	$3,2 \pm 0,6$	$2,6 \pm 0,4$	$1,9 \pm 0,2$	$1,6 \pm 0,2$
Tutte le stelle	$1,8 \pm 0,2$	$1,6 \pm 0,1$	$1,7 \pm 0,1$	$1,4 \pm 0,1$
Rami grigi:				
Stelle c.r. . .	—	—	$4,3 \pm 1,4$	$3,2 \pm 0,6$
Stelle s.r. . .	—	—	$11,5 \pm 4,4$	$5,7 \pm 1,1$
Tutte le stelle	—	—	$6,7 \pm 1,4$	$3,8 \pm 0,4$

(Le lastre esposte a protoni di 250 MeV, Ilford G5 sviluppate normalmente, si sono dimostrate disadatte ad una buona discriminazione tra N e G , avendo fissato a 20 MeV il taglio tra le due categorie di rami: in questo paragrafo e nel successivo non sarà tenuto conto, quindi, dei risultati ottenuti per la IV categoria).

La fig. 4 mostra chiaramente che: *a*) al crescere dell'energia del primario la anisotropia dei rami neri diminuisce; *b*) nelle stelle con rinculo visibile l'anisotropia è molto piccola e nettamente minore di quella presentata, per la stessa energia del primario, dalle stelle senza rinculo visibile.

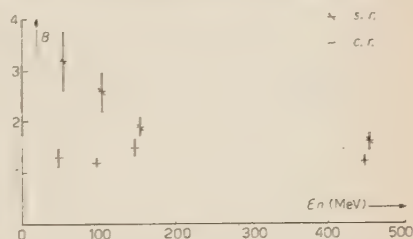


Fig. 4. - Variazione di B al variare dell'energia del primario, per stelle con rinculo (c.r.) e senza rinculo (s.r.).

Il primo fenomeno, già ritrovato in stelle generate dalla radiazione cosmica, è facilmente spiegabile mediante una analisi del sovrapporsi dell'emissione diretta e della evaporazione in una disintegrazione nucleare (BELLIBONI *et al.* ⁽⁴⁾): i rami neri di emissione diretta presenti nelle stelle di debole energia sono generati durante le prime collisioni della cascata nucleonica e risultano quindi notevolmente collimati in avanti; al crescere dell'energia del primario è sempre più probabile che i rami di bassa energia di emissione diretta rappresentino termini degli ultimi stadi della cascata ed abbiano quindi una più debole correlazione con la direzione di moto del primario.

Il secondo fenomeno era stato già previsto dal Montecarlo ⁽¹⁾ e ci aveva

⁽⁴⁾ G. BELLIBONI e B. VITALE: *Nuovo Cimento*, **11**, 372 (1954).

portato a formulare l'ipotesi che la formazione di un rinculo visibile fosse dovuta in modo determinante a fluttuazioni nella distribuzione angolare dei rami, piuttosto che in quella energetica, nel senso che un più largo sparpagliamento dei rami uscenti dalla disintegrazione favorisse la cessione di impulso al nucleo in quantità sufficiente perchè il rinculo risultasse osservabile. La conferma sperimentale ora ritrovata a varie energie del primario è un dato a favore della validità del modello proposto per la formazione del rinculo.

Può essere interessante osservare che, nelle stelle con rinculo visibile, l'anisotropia dei neri e dei grigi dipende anche dalla direzione del rinculo: per le stelle della V categoria (450 MeV) si ottiene infatti:

	rami neri	rami grigi
rinculo in avanti:	$B = 0,8 \pm 0,1$	$2,5 \pm 0,4$
rinculo indietro:	$B = 4,3 \pm 1,0$	$6,1 \pm 1,9$

5. - Angoli tra rami e rinculi.

In tabella VI è dato il valore del rapporto C per le differenti categorie e per i rami neri N e grigi G separatamente per le stelle con rinculo in avanti e indietro e per tutte le stelle; in figg. 5 e 6 sono riportate le distribuzioni $f(\theta - \theta_r)$ per i N ed i G della V categoria e le corrispondenti distribuzioni previste dal Montecarlo

TABELLA VI. - Rapporto C .

Energia	50	100	150	450
Rami neri:				
Rinculo in avanti	$1,9 \pm 0,3$	$2,2 \pm 0,3$	$1,6 \pm 0,2$	$2,1 \pm 0,3$
Rinculo indietro	—	$3,6 \pm 1,4$	$5,3 \pm 1,6$	$4,3 \pm 0,9$
Tutte le stelle	$2,0 \pm 0,3$	$2,5 \pm 0,3$	$2,1 \pm 0,3$	$2,5 \pm 0,4$
Rami grigi:				
Rinculo in avanti	—	—	$0,7 \pm 0,3$	$0,9 \pm 0,1$
Rinculo indietro	—	—	$2,3 \pm 0,6$	$7,3 \pm 2,4$
Tutte le stelle	—	—	$1,0 \pm 0,3$	$1,6 \pm 0,2$

I dati precedenti e le figg. 5 e 6 mostrano chiaramente che: *a*) il rapporto C non varia in modo sensibile al crescere dell'energia del primario ; *b*) esso è sensibilmente più alto nelle stelle con rinculo indietro rispetto a quelle con

rinculo in avanti; *c*) l'accordo tra Montecarlo e dati sperimentali è ottimo per i rami di bassa energia (il Montecarlo dà: $C = 2,2 \pm 0,5$), abbastanza buono per i *G*, almeno per quanto riguarda il valore di *C* (per i *G* il Monte-

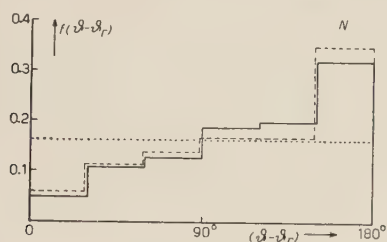


Fig. 5. - Distribuzione angolare in $(\vartheta - \vartheta_r)$. — risultati sperimentali per i rami *N* delle stelle della V categoria; - - - - risultati del Montecarlo (primari di 400 MeV).

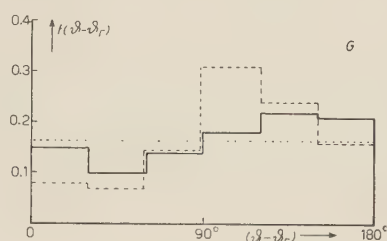


Fig. 6. - Distribuzione angolare in $(\vartheta - \vartheta_r)$. — risultati sperimentali per i rami *G* delle stelle della V categoria; - - - - risultati del Montecarlo (primari di 400 MeV).

carlo dà: $C = 2,4 \pm 0,4$); la distribuzione in $(\vartheta - \vartheta_r)$ prevista è, invece, diversa da quella sperimentale, presentando un netto massimo sui 90° - 150° che non si ritrova sperimentalmente.

6. - Discussione e conclusioni.

I dati precedenti si prestano ad alcune considerazioni sia sul confronto possibile con le previsioni statistiche già ottenute con il Montecarlo per la V categoria, sia sulle variazioni osservate con l'energia del primario per i vari parametri analizzati. Il confronto è, in generale, positivo: l'impulso medio ceduto al nucleo dall'emissione diretta e dall'evaporazione, la dipendenza della anisotropia angolare dalla presenza di rinculo visibile, i valori assunti dal rapporto *C* e la loro dipendenza dalla direzione del rinculo mostrano un buon accordo con le previsioni statistiche; l'unico netto disaccordo è stato osservato nelle distribuzioni angolari dei rinculi, per i quali l'analisi statistica prevedeva una maggiore collimazione nella direzione del primario. Le probabili ragioni di questo disaccordo sono state già discusse nel § 2.

Il modello proposto in ⁽¹⁾ per la formazione del rinculo, oltre a portare a conseguenze particolari per le disintegrazioni prodotte da primari di 450 MeV, permetteva alcune previsioni sull'andamento di alcuni dei parametri più caratteristici del fenomeno (*R*, \bar{L} , *B*) al variare dell'energia del primario. Come si è visto nei §§ precedenti, anche in questo caso l'accordo tra le previsioni dedotte dal modello e i dati sperimentali è, in genere, buono. La costanza del rapporto *C* con l'energia del primario, invece, non ci sembra possa essere direttamente dedotta dal modello proposto.

Quest'ultimo, quindi, almeno nei limiti degli errori sperimentali, è in condizione di spiegare la maggior parte dei dati sperimentali relativi alla presenza di tracce di rinculo nelle stelle di disintegrazione nucleare, o non risulta contraddittorio con essi.

Desideriamo ringraziare i proff. N. DALLAPORTA e G. PUPPI per l'interesse dimostrato verso il nostro lavoro; i proff. G. FRONGIA e A. ROSTAGNI per aver reso possibile la nostra collaborazione. Uno di noi (P.E.H.) desidera ringraziare il D.S.I.R. per una « Senior Research Award ».

Siamo grati al Sig. D. NARCISO per il valido aiuto datoci durante il presente lavoro.

SUMMARY

The results of measurements on the recoil tracks from nuclear disintegrations produced by protons accelerated to 50, 100, 150, 250 and 450 MeV, are presented and compared with those predicted for primary protons of 400 MeV by a statistical analysis by the Montecarlo method. The paper is divided into six parts: 1) Experimental details. 2) Angular distribution of the recoil tracks. Table III gives the variation of the ratio R of forward to backward recoils with respect to the direction of the primary as a function of the energy of the primary, and shows that it decreases with increasing energy. The value obtained for stars of 450 MeV is considerably less than that predicted by the Montecarlo calculations, and possible reasons for this are discussed. 3) Range distribution of the recoil tracks. Table IV gives the variation of the mean range of the recoils with the energy of the primary and shows that it increases with increasing energy. The experimental value of the mean range for the disintegrations produced by protons of 450 MeV is in good accord with the Montecarlo calculations and the variation of the mean range with primary energy is qualitatively accounted for by the model proposed for the formation of recoils. 4) The angles between the secondary tracks and the primary in stars with and without recoil. Table V gives the value of the ratio B of forward to backward tracks with respect to the primary as a function of the energy of the primary. The observed anisotropy decreases with increasing energy, and is significantly less for stars with recoils than for stars without recoils. Both these effects are accounted for by a model of the disintegration process which considers the superposition of the tracks due to the direct emission and the evaporation stages. The second of these effects also shows that the formation of the recoil can be attributed to fluctuations in the angular distribution of the emitted particles. 5) The angles between the secondary tracks and the recoil. Table VI gives the variation of the ratio C of backward to forward tracks with respect to the recoil. It does not vary significantly with the energy of the primary and it is much higher for stars with recoil in the backward direction than for those with recoil in the forward direction. The agreement with the Montecarlo calculations is good for the low energy tracks and is qualitatively correct for the grey tracks. 6) Discussion and conclusions. This paper leads to the conclusion that, within experimental error, the model proposed previously ⁽¹⁾ for the formation of recoils accounts for most of the experimental data on the tracks of recoils from nuclear disintegrations, and that no results are in essential disagreement with it.

Further Considerations on Nuclear Polarization by Means of Electron Resonance Saturation.

P. BROVETTO and G. CINI

Istituto Nazionale di Fisica Nucleare - Sezione di Torino

(ricevuto il 12 Ottobre 1954)

Summary. — In this paper we discuss the main experimental features in order to use the Overhauser effect as a technique to obtain high nuclear polarization.

It is well known that in paramagnetic substances, in which an interaction of the type $S.I$ between the electronic and nuclear spins exists, a nuclear polarization effect is to be expected under the condition of electron resonance saturation. This polarization is given by ⁽¹⁾:

$$(1) \quad P = \frac{2I + 1}{2I} \coth (2I + 1) \frac{s\beta}{kT} H_0 - \frac{1}{2I} \coth \frac{s\beta}{kT} H_0$$

where:

$$(2) \quad s = 1 - \frac{M_z}{M_0}$$

is the saturation parameter. M_z which appears in formula (2) is the component of the resultant magnetic moment per unit volume along the direction of the external magnetic field H_0 , while the substance is irradiated with an alternating transverse magnetic field H_ω of frequency $\omega = 2\beta H_0/\hbar$. M_0 is the equilibrium value which will be reached by M_z when H_ω is turned off.

⁽¹⁾ P. BROVETTO and G. CINI: *Nuovo Cimento*, **11**, 618 (1954). P. BROVETTO and S. FERRONI: *Nuovo Cimento*, **12** 90 (1954).

Eqs. (1) in the case $s \cong 1$, is valid for any paramagnetic substance in which $S = \frac{1}{2}$. In the expression for P we have neglected the nuclear magnetic moment against β . Further on we have assumed that the electronic spin system is a perfect system; this condition is realized e.g. in the hydrated gadolinium sulphate as it is proved by the agreement of the experimental values of the susceptibility with the theoretical values calculated by the Brillouin formula. In any case this condition may be obtained by means of dilution of the paramagnetic ions.

It is interesting to calculate, in view of polarization experiments, the intensity of the alternating field and the power absorbed by the substance, when the resonance is near saturation, as a function of the susceptibility χ_0 , of the longitudinal and transversal relaxation times τ_l and τ_t and of the field H_0 . For this purpose we shall use the following equation for the variation of the polarization vector \mathbf{M} :

$$(3) \quad \dot{\mathbf{M}} - \gamma(\mathbf{M} \times \mathbf{H}) + \frac{M_x}{\tau_t} \mathbf{i} + \frac{M_y}{\tau_t} \mathbf{j} + \frac{M_z - M_0}{\tau_l} \mathbf{k} = 0,$$

where γ is the gyromagnetic ratio. The resultant external field is:

$$(4) \quad \mathbf{H} = 2H_\omega \cos \omega t \mathbf{i} + H_0 \mathbf{k}.$$

The steady-state solution of eqs. (3) and (4) for $H_\omega \ll H_0$ are given by:

$$(5) \quad \begin{cases} M_x = \frac{M_0 \tau_t}{1 + \gamma^2 H_\omega^2 \tau_l \tau_t} \gamma H_\omega \sin \omega t, \\ M_y = \frac{M_0 \tau_t}{1 + \gamma^2 H_\omega^2 \tau_l \tau_t} \gamma H_\omega \cos \omega t, \\ M_z = \frac{M_0}{1 + \gamma^2 H_\omega^2 \tau_l \tau_t} \end{cases}$$

From eqs. (2) and (5) we obtain:

$$(6) \quad H_\omega = \frac{1}{\gamma \sqrt{\tau_l \tau_t}} \left(\frac{s}{1-s} \right)^{\frac{1}{2}}.$$

In fig. 1 H_ω is plotted against $\sqrt{\tau_l \tau_t}$ for different values of s .

The same result has been obtained by OVERHAUSER ⁽²⁾ by means of per-

(2) A. W. OVERHAUSER: *Phys. Rev.*, **92**, 411 (1953).

turbation theory, under the hypothesis that the absorption line is Lorentzian in shape. The power absorbed per unit volume from the alternating field is

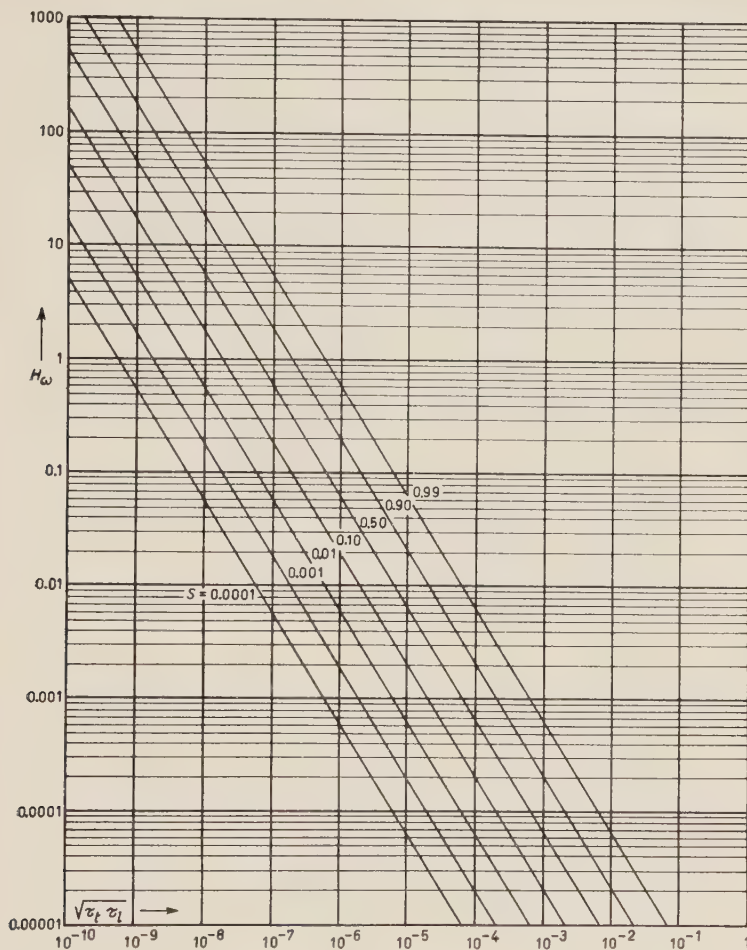


Fig. 1. — Values of H_ω plotted against $\sqrt{\tau_t \tau_l}$ for different values of s .

given by the following equation:

$$(7) \quad W = \frac{\omega}{2\pi} \int_0^{2\pi/\omega} M_x H_x dt.$$

Remembering eqs. (5), (6) we have:

$$W = s \frac{\chi_0}{\tau_l} H_0^2.$$

In Fig. 2 W is plotted versus the specific susceptibility χ_0 for different values of τ_i and H_0 . Since at temperature below 1 °K the relaxation times are very

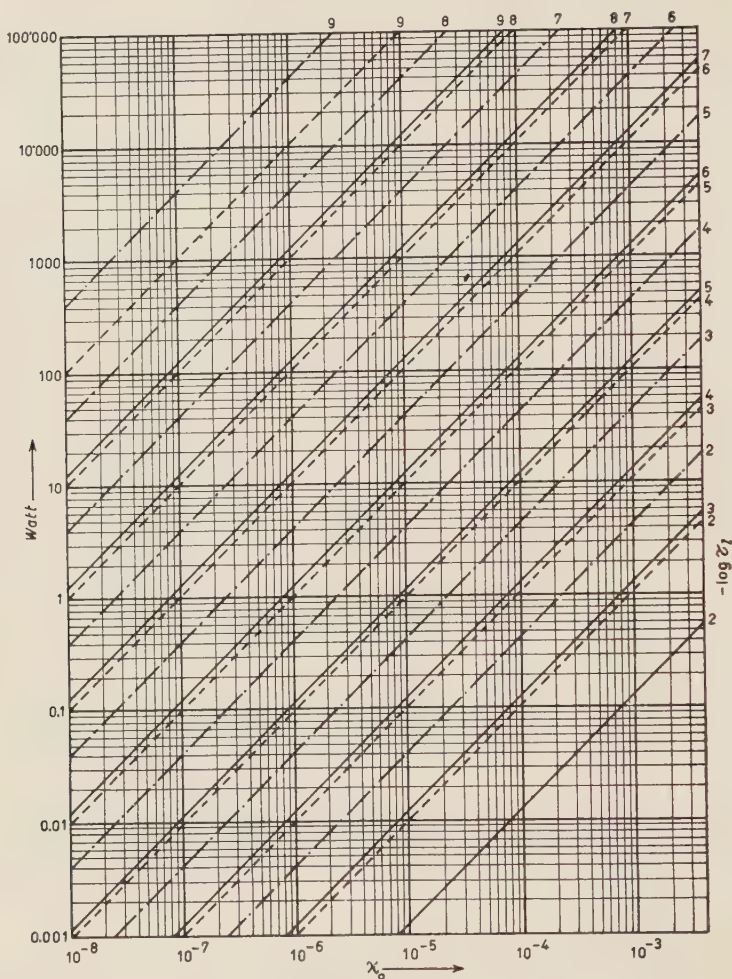


Fig. 2 Power absorbed versus specific susceptibility, for different values of τ_i , H_0 and for $s=0.9$. Curve ——— refers to $H_0=1070$; Curve - - - - - refers to $H_0=3570$; Curve - . - . - refers to $H_0=10700$ Gauss.

long (generally $\tau_i \sim 10^{-3} \div 10^{-2}$ s) and χ_0 has values ⁽³⁾ of the order of $10^{-4} \div 10^{-3}$, the power, required to obtain high saturation of the paramagnetic resonance ($s=0.9$), is of the order of 1 W.

We shall now investigate the dynamical process which tends to restore the

⁽³⁾ R. J. BENZIE and A. H. COOKE: *Proc. Phys. Soc.*, **63**, A 210 (1950).

nuclear system to its equilibrium state, when electron resonance is turned off. OVERHAUSER ⁽²⁾ by taking into account only one interaction of the electron spins, namely the one with nuclei, in the case $S = I = \frac{1}{2}$, writes the following equations:

$$\dot{M}_z = \dot{\mathcal{M}}_z = \frac{M_0 - M_z}{\tau_1} + \frac{\mathcal{M}_0 - \mathcal{M}_z}{\tau_n},$$

where \mathcal{M}_z and \mathcal{M}_0 refer to the nuclei.

Taking into account also the interactions between electron and lattice with relaxation time τ_2 , the foregoing equations become:

$$(8) \quad \begin{cases} \dot{M}_z = \frac{M_0 - M_z}{\tau_l} + \frac{\mathcal{M}_0 - \mathcal{M}_z}{\tau_n} \\ \dot{\mathcal{M}}_z = \frac{\mathcal{M}_0 - \mathcal{M}_z}{\tau_n} + \frac{M_0 - M_z}{\tau_1} \end{cases},$$

where $1/\tau_l = 1/\tau_1 + 1/\tau_2$. From eqs. (8) one finds:

$$\mathcal{M}_z - \mathcal{M}_0 = A \exp[\alpha_- t] + B \exp[\alpha_+ t]$$

where:

$$\alpha_{\pm} = -\frac{1}{2} \left(\frac{1}{\tau_n} + \frac{1}{\tau_l} \right) \pm \frac{1}{2} \left[\left(\frac{1}{\tau_n} - \frac{1}{\tau_l} \right)^2 + \frac{4}{\tau_1 \tau_n} \right]^{\frac{1}{2}}$$

and A, B , are constants which can be determined by means of the initial values of \mathcal{M}_z and M_z . As $1/\tau_l$ generally is predominant as compared to the other terms we have $\alpha_+ \cong 0$, $\alpha_- \cong -1/\tau_l$. It follows that nuclear and electronic depolarization occur at the same rate.

We must recall that the foregoing results are only approximate because they are based on the relaxation time theory. However we can conclude that the power required to obtain values of s near 1 is not very high and can easily be emitted by a usual generator of microwaves.

The nuclear polarization achieved will last until the alternating field is on; for this reason it is necessary to use unmodulated generators.

Low temperatures of the order of 1°K can be reached by means of liquid Helium. The Helium which will evaporate while the substance is at this temperature, is approximately 1,1 l per hour, when 1 watt is absorbed, neglecting losses due to a bad thermal insulation of the equipment.

We conclude that the biggest experimental difficulty we have to face in order to obtain high nuclear polarization comes from the low value of the

specific heat and of the thermal conductivity of the paramagnetic substances in the liquid helium thermostat. These low values, because of the heat produced in the microwaves absorption, make it difficult to maintain low temperatures.

RIASSUNTO

In questa nota si discutono le principali modalità pratiche per l'impiego dell'effetto Overhauser come tecnica per ottenere altre polarizzazioni nucleari.

Relativistic Treatment of the Vector Meson Field.

R. J. N. PHILLIPS

Trinity College, Cambridge, England

(ricevuto il 18 Ottobre 1954)

Summary. — A covariant theory for the quantized vector meson field is formulated, using Dirac's Hamiltonian formalism, and is compared with a theory due to Stückelberg. The latter theory cannot be generalized to a similar manifestly covariant form, but is found to give the same results as the former.

1. — Introduction.

DIRAC's relativistic treatment of Hamiltonian field dynamics ⁽¹⁾ enables one to state Hamiltonian field theories in a manifestly covariant form in all representations. As it is possible to consider arbitrary changes of a spacelike surface, on which field operators are defined, one no longer needs to consider the difficult problem of rotations of an infinite flat surface in four dimensions to verify the covariance of a theory in this form.

As it is possible to transform in a relativistic manner between different representations, one can pass to the Interaction Representation, and a covariant consideration of the transformation operators there, without reference to Tomonaga-Schwinger theory and the attendant complications. One avoids fresh considerations of integrability, and the difficulties connected with the possible « surface-dependence » of Interaction Representation operators ⁽²⁾. Furthermore, the surfaces need not be restricted by the « scale form flat » condition of KANESAWA and TOMONAGA.

⁽¹⁾ P. A. M. DIRAC: *Phys. Rev.*, **73**, 1002 (1948); *Can. Journ. Math.*, **2**, 129 (1950); **3**, 1 (1951); also developed in a slightly different form by T. S. CHANG: *Phys. Rev.*, **78**, 592 (1949), and other papers.

⁽²⁾ F. J. BELINFANTE: *Phys. Rev.*, **76**, 66 (1949).

Another advantage of the Dirac formalism is the consistent means it provides for dealing with dependences between the field variables (and their space-like derivatives). These are accounted for either by eliminating redundant variables by a redefinition of Poisson Brackets (P. B.), or by adding to the Hamiltonian fresh terms, multiplied by arbitrary velocities, according to whether the dependence is «second class» or «first class». In particular, one is able to treat those fields for which some of the field momenta vanish identically — cases in which the ordinary theory fails, and special expedients are required.

In the present note we describe a relativistic treatment of the quantized Proca field and compare it with the well-known treatment due to STÜCKELBERG. It transpires that the latter treatment cannot be adapted to general spacelike surfaces so that this method for verifying covariance fails. However, covariance can be proved indirectly, for on flat surfaces it gives the same results as the first theory.

We shall use throughout the notation of the second and third papers of reference ⁽¹⁾, which is specialized and in some ways unusual. In particular, the diagonal elements of the metric tensor are taken to be $(1, -1, -1, -1)$.

2. — Relativistic Hamiltonian Field Dynamics.

We consider a spacelike surface in four dimensions, $y_\mu = y_\mu(u)$, which can vary arbitrarily with an independent variable τ , and on which dynamical field variables are defined. $u = (u_1, u_2, u_3)$ is a parametrization of the surface, which can also vary arbitrarily. Using the homogeneous velocity formulation of the dynamical equations, Dirac has shown the Hamiltonian to be

$$(2.1) \quad H \equiv \int \dot{y}_\mu(u) \varphi_\mu(u) d^3u,$$

with $\varphi_\mu(u)$ some function of the dynamic variables that vanishes weakly, (where dots denote differentiation with respect to τ). If there are other quantities that vary arbitrarily with τ , further terms appear in H .

The Heisenberg equations of motion for a dynamical variable α are now

$$(2.2) \quad \dot{\alpha} = \int \dot{y}_\mu [\alpha, \varphi_\mu(u)] d^3u.$$

The condition for integrability is that the φ_μ (and any further φ -factors in a general H) shall have zero P.B.s with each other.

To pass to the quantum theory, we interpret P.B.s in terms of commutators in the usual way. For this to be consistent, all dependence conditions

(known as φ -equations) between field variables must have zero P.B. with each other and with H ; a redefinition of P.B.s may therefore have to be made first.

The Hamiltonian is a surface functional and depends on τ indirectly through the surface variables. To emphasise its form and for ease of comparison with other formalisms, we write

$$(2.3) \quad H \equiv H[\sigma(\tau)]$$

$$(2.4) \quad \equiv \int_{\sigma} H(\sigma, u) d^3u .$$

In the Heisenberg representation we have, for a dynamical variable $\alpha(u, \sigma)$, defined on the surface σ at the point u ,

$$(2.5) \quad \dot{\alpha}(\sigma, u) = \int_{\sigma} [\alpha(\sigma, u), H(\sigma, u')] d^3u'$$

and for the state vector, which is constant for the motion,

$$(2.6) \quad \dot{\Phi} = 0 .$$

We may transform to a generalized Schrödinger Representation by writing

$$(2.7) \quad \Psi_s[\sigma] = W[\sigma]\Phi ,$$

where W is defined by the (integrable) equation

$$(2.8) \quad i\hbar \dot{W}[\sigma] = W[\sigma]H[\sigma] .$$

The new equations of motion are

$$(2.9) \quad \left\{ \begin{array}{l} i\hbar \dot{\Psi}_s[\sigma] = H_s[\sigma]\Psi_s[\sigma] \\ \dot{\alpha}_s[\sigma, u] = 0 . \end{array} \right.$$

$$(2.10)$$

Similarly we may transform to the Interaction Representation by means of

$$(2.11) \quad \Psi_I[\sigma] = U[\sigma]\Phi ,$$

where

$$(2.12) \quad i\hbar \dot{U}[\sigma] = U[\sigma]H'[\sigma]$$

in an obvious notation. The equations of motion are

$$(2.13) \quad \left\{ \begin{array}{l} i\hbar\dot{\Psi}_I[\sigma] = H'_I[\sigma]\Psi_I[\sigma] \end{array} \right.$$

$$(2.14) \quad \left\{ \begin{array}{l} \dot{\alpha}_I[\sigma, u] = [\alpha_I[\sigma, u], H^0_I[\sigma]] \end{array} \right.$$

A perturbation solution of (2.13) gives the following expression for the transformation operator between two surfaces σ_1 and σ_0 ,

$$(2.15) \quad S[\sigma_1, \sigma_0] = \sum_{n=0}^{\infty} \left(-\frac{i}{\hbar} \right)^n \frac{1}{n!} \int_{\sigma_0}^{\sigma_1} d\tau_1 \dots d\tau_n P(H'_I[\sigma(\tau_1)] \dots H'_I[\sigma(\tau_n)]) .$$

In practice, for convenience, one takes all surfaces to be flat and parallel. Thus we arrive at the usual transformation operators in a fully covariant way and independently of the Tomonaga-Schwinger theory ⁽³⁾. This is important because, in our formalism, when redundant field variables have been eliminated, the interaction Hamiltonian may appear different from the usual one and it may be difficult to prove directly that the Tomonaga-Schwinger equation is integrable.

3. - The Proca Field.

Our treatment of the Proca field A_μ , with rest-mass $\hbar\kappa$, is very similar to that of the electromagnetic field already published by DIRAC ⁽⁴⁾. Our considerations will be brief and confined to the free-field case.

The Lagrangian is taken to be

$$(3.1) \quad L \equiv \int \mathcal{L} \Gamma d^3u \equiv \int \left(-\frac{1}{4} f_{\mu\nu} f_{\mu\nu} + \frac{1}{2} \kappa^2 A_\mu A_\mu \right) \Gamma d^3u ,$$

where $f_{\mu\nu} = A_{\nu\mu} - A_{\mu\nu}$. Varying only the velocities A_μ and \dot{y}_μ , we may calculate the variation in L and hence find the momenta. In the present treatment we take the components A_t, A^r to be basic rather than A_μ . The conjugate momenta are

$$(3.2) \quad B_t = 0$$

$$(3.3) \quad B_r = f_{\mu\nu} l_\nu y_{\mu r} \Gamma .$$

⁽³⁾ This formalism can, if necessary, be deduced from ours. See CHANG, ref. ⁽¹⁾

⁽⁴⁾ P. A. M. DIRAC: *Nuovo Cimento*, **7**, 925 (1950).

Hence the Hamiltonian is

$$\begin{aligned}
 (3.4) \quad H &\equiv \int (w_\sigma + B_l A_{l\sigma} + B_r A^r_\sigma - l_\sigma \mathcal{L}) \dot{y}_\sigma d^3u \\
 &\equiv \int (w_l + B_l A_{ll} + \tfrac{1}{4} f_{rs} f^{rs} \Gamma - \tfrac{1}{2} B_r B^r \Gamma^{-1} - B_s^s A_l - \tfrac{1}{2} \kappa^2 A_\mu A_\mu \Gamma) \cdot \dot{y}_l d^3u \\
 &\quad + \int (w^r + B_s A^{sr} + B_l A_l^r - (B_s A^r)^s) \dot{y}_r d^3u,
 \end{aligned}$$

where w_σ is conjugate to y_σ , and we have used reductions of $(B_r A^r_l + \tfrac{1}{4} f_{\mu\nu} f^{\mu\nu})$ and $\int B_s A^s_\nu t_{\mu}^s y_\nu^s \dot{y}_l d^3u$ which are derived in ref. (4). The term $B_l A_{ll} \dot{y}_l$, however, still contains velocities other than surface velocities and must be reduced by means of strong equations. Since $B_l = 0$, and we can deduce $A_{\mu\mu} = 0$ from the equations of motion, it follows that

$$(3.5) \quad B_l A_{vv} = 0$$

is a strong equation. From this we infer, after some manipulation, that

$$(3.6) \quad \int B_l A_{ll} \dot{y}_l d^3u \equiv \int \dot{y}_l (B_l^r A_r - B_l A_{lr} y_v^r - B_l A_r y_v^{rs} y_{vs}) d^3u.$$

Hence H is expressed in the form (2.1), where φ^r, φ_l contain no velocities.

However, the theory cannot yet be quantized as there are two «second class» φ -equations

$$(3.7) \quad B_l = 0$$

$$(3.8) \quad B_s^s + \kappa^2 A_l \Gamma = 0$$

which do not have zero P.B.s with each other, although they have zero P.B. with the φ 's which appear in H — as is indeed necessary for consistency. We have already derived (3.7); (3.8) can be deduced from the equation of motion

$$(3.9) \quad (F_{\nu\mu})_\mu = \kappa^2 A_\nu$$

with the help of (3.3). We therefore redefine P.B.s in the usual way⁽¹⁾, so that (3.7) and (3.8) shall hold as strong equations, and then use these strong equations to eliminate B_l, A_l completely from the theory. We now have a theory suitable for quantization, with

$$\begin{aligned}
 (3.10) \quad H &\equiv \int (w_l + \tfrac{1}{4} f_{rs} f^{rs} \Gamma - \tfrac{1}{2} B_r B^r \Gamma^{-1} - \tfrac{1}{2} \kappa^2 A_r A^r \Gamma + \tfrac{1}{2} \kappa^{-2} (B_s^s)^2 \Gamma^{-1}) \dot{y}_l d^3u \\
 &\quad + \int (w^r + B_s A^{sr} - (B_s A^r)^s) \dot{y}_r d^3u \\
 &\equiv \int (\varphi_l \dot{y}_l + \varphi^r \dot{y}_r) d^3u,
 \end{aligned}$$

say.

When this is used in the Heisenberg equation (2.2), φ_i describes changes due to motion of the surface normal to itself and the φ^r describe changes due to changes of parametrization on the surface. In the particular case of a flat surface, with uniform rectangular parametrization and $\dot{y}_i = 1$, this Hamiltonian reduces to that of the ordinary theory ⁽⁵⁾ which is thus proved to be covariant.

The generalization to charged and symmetric vector meson fields is straightforward.

When interaction terms appear in \mathcal{L} , a similar treatment can be used; the second-class φ -equations (3.7, 8) will, of course, be different.

We note in passing a case ⁽⁶⁾ with interesting properties, that of interaction with Pauli-Weisskopf particles of rest-mass $\hbar\mu$. Because of the gauge-invariance of the Lagrangian, we may describe the complex Pauli-Weisskopf field ψ by the two real fields R, θ , putting

$$(3.11) \quad \psi \equiv R \exp[-i\theta].$$

To our present \mathcal{L} we add

$$(3.12) \quad \mathcal{L}' \equiv R_\mu R_\mu + R^2(\theta_\mu - gA_\mu)(\theta_\mu - gA_\mu) - \mu^2 R^2$$

and proceed in the usual way. In this case it is found that (3.7) is unchanged but (3.8) is replaced by

$$(3.13) \quad B_s^s + \Gamma A_i - g\varrho = 0,$$

where ϱ is the momentum conjugate to θ . After re-defining P.B.s, we clearly can use these two equations to eliminate B_i and ϱ instead of B_i and A_i . This leads to the appearance of negative as well as positive powers of the coupling constant g in H , presenting a problem that cannot be solved by perturbation methods.

For a general interaction, using the φ -equations to eliminate B_i and A_i , we notice from the way that (3.8) and (3.13) are derived that the momenta B_s will appear in the interaction Hamiltonian only in the combination (B_s^s) . Taking, for convenience, all surfaces to be flat and restricted as above, we can use (3.10) to find the free-field commutation rules between the four quantities A^r, B_s^s ; they prove to be precisely the same as those between the quantities $C^r + (1/\kappa)E^r$ and $-\kappa^2[C_i + (1/\kappa)\dot{E}]$ respectively, where C_μ and E are a vector and a scalar field obeying the equations

$$(3.14) \quad (\square + \kappa^2)C_\mu = (\square + \kappa^2)E = 0, \quad (\square = \partial_\mu \partial_\mu).$$

⁽⁵⁾ See, for example, G. WENTZEL: *Quantum Theory of Fields* (New York, 1949).

⁽⁶⁾ In close analogy to a case studied by DIRAC, ref. (4).

For many purposes (e.g. the calculation of virtual processes in the S -matrix), we may therefore replace the first set of variables by the second, which are easier to handle.

4. – Stückelberg's Formulation.

STÜCKELBERG has shown ⁽⁷⁾ how to describe the Proca field, of rest-mass $h\kappa$, in terms of a vector field C_μ and a scalar field E , which are subject to auxiliary conditions. It is sufficient, at present, to consider the free-field case for which the Lagrangian density is

$$(4.1) \quad \mathcal{L} \equiv \frac{1}{2}(-C_{\mu\nu}C_{\mu\nu} + \kappa^2 C_\mu C_\mu + E_\nu E_\nu - \kappa^2 E^2)$$

and the auxiliary conditions are

$$(4.2) \quad C_{\mu\mu} - \kappa E = 0$$

and its time-derivative. If we now write

$$(4.3) \quad A_\mu = C_\mu + \frac{1}{\kappa} E_{,\mu}$$

it can be shown that A_μ obeys the Proca field equations and that the C_μ - and E -fields can be eliminated completely from the Hamiltonian to give the usual Proca field Hamiltonian.

Some authors ⁽⁸⁾ have preferred to use (4.2) and its time-derivative merely as auxiliary conditions on the state vector, keeping the components of C_μ and E independent, although this was not Stückelberg's original intention. We see later, however, that both forms of the theory give the same results in the S -matrix.

When we try to re-write Stückelberg's theory in terms of Dirac's Hamiltonian dynamics, difficulties arise. We shall find it is sufficient to consider the case in which the components C_μ are taken as basic. Using the Lagrangian density (4.1) we can construct the Hamiltonian

$$(4.4) \quad \begin{aligned} H &\equiv \int (w_t - \frac{1}{2} D_\mu D_\mu \Gamma^{-1} + \frac{1}{2} F^2 \Gamma^{-1} + \frac{1}{2} C_{\mu r} C_\mu^r \Gamma - \frac{1}{2} E^r E^r \Gamma + \\ &\quad + \frac{1}{2} \kappa^2 E^2 \Gamma - \frac{1}{2} \kappa^2 C_\mu C_\mu \Gamma) \dot{y}_t d^3u + \int (w^r + D_\mu C_\mu^r + F E^r) \dot{y}_r d^3u \\ &\equiv \int (\varphi_t \dot{y}_t + \varphi^r \dot{y}_r) d^3u, \end{aligned}$$

say.

⁽⁷⁾ E. C. G. STÜCKELBERG: *Helv. Phys. Acta*, **11**, 299 (1938).

⁽⁸⁾ E.g., Y. MIYAMOTO: *Prog. Theor. Phys.*, **3**, 124 (1948).

The auxiliary condition (4.2) must be written in a form free from time-like derivatives,

$$(4.5) \quad \varphi^{(1)} \equiv C_{\mu-\mu} - \Gamma^{-1} D_{\mu} l_{\mu} - \frac{1}{\kappa} E = 0.$$

This is a φ -equation in the sense used earlier. However, for consistency it must have zero P.B. with H , and we therefore postulate

$$(4.6) \quad [\varphi^{(1)}(u), \varphi^r(u')] = 0,$$

$$(4.7) \quad [\varphi^{(1)}(u), \varphi_i(u')] = 0.$$

Using the rules for the P.B.s of surface variables tabulated in the third paper of ref. (1), we find that (4.6) is satisfied and that

$$(4.8) \quad [\varphi^{(1)}(u), \varphi_i(u')] \equiv C_{\mu i} y_{\mu s} \delta^s(u - u') - \left[y_{\mu s} (D_{\mu} \Gamma^{-1})^s - D_i \Gamma^{-1} l_{\nu-\nu} + \right. \\ \left. + l_{\mu} \Gamma^{-1} (C_{\mu s} \Gamma)^s + \kappa^2 C_i + \frac{1}{\kappa} F \Gamma^{-1} \right] \delta(u - u') \\ \equiv \varphi^{(3s)} \delta^s(u - u') + \varphi^{(2)} \delta(u - u').$$

We must postulate, therefore, that the coefficients $\varphi^{(2)}$ and $\varphi^{(3s)}$ vanish. The former is simply Stückelberg's second condition, that the time-derivative of $\varphi^{(1)}$ vanishes, in a general form and written as a φ -equation. The other conditions are equivalent to

$$(4.9) \quad \varphi^{(3,\mu)} \equiv D_{-\mu} = 0.$$

There is no equivalent to this in Stückelberg's work. It may be thought of as an additional restriction due to the possible curvature of the surface. $\varphi^{(3\mu)}$ has zero P.B. with q^r but not with φ_i , and we thus need more consistency conditions,

$$(4.10) \quad [\varphi^{(3\mu)}(u), \varphi_i(u')] \equiv (D_{\nu} l_{\nu} y_{\mu s} + C_{\nu s} y_{\nu r} y_{\mu}^r) \delta^s(u - u') + \\ + y_{\nu r} y_{\mu}^r [(C_{\nu s} \Gamma)^s + \kappa^2 C_{\nu} \Gamma] \delta(u - u') = 0.$$

These new conditions give rise to still more consistency conditions, of greater complexity. However, we can already see that Stückelberg's work has no analogue in our theory for general surfaces for, taking the particular case of flat parallel surfaces, the conditions derived so far permit us, after

re-defining P.B.s, to eliminate D_μ , E and F in terms of C_μ and its space-like derivatives.

We cannot choose some other generalization of (4.2) in such a way that these difficulties are avoided, for $\varphi^{(1)}$ must be some multiple of a u -scalar (to insure a vanishing P.B. with φ^r), and we can quickly see that any alternative linear expression in the field variables would have to contain (4.5) as a factor and would suffer from the same defects. In the same way we see that nothing is to be gained by working with the components C_i , C^r instead of C_μ , although at first sight such an approach would suggest a different generalization of (4.2).

Stückelberg's method may be incorporated in Dirac's formalism but only under the severe restriction that all the surfaces used be flat and parallel. In this case, (4.4) is replaced by

$$(4.11) \quad H = \Phi_i \dot{y}_i + \int \Phi^r \dot{y}_r \, d^3u$$

where

$$(4.12) \quad \Phi_i = \int \varphi_i(u) \, d^3u$$

and the conditions

$$(4.13) \quad \varphi^{(1)} = \varphi^{(2)} = 0$$

prove to be consistent. Since, further, the two conditions commute, they are first-class and the appropriate Hamiltonian, taking them into account, is

$$(4.14) \quad H = \Phi_i \dot{y}_i + \int \varphi^r \dot{y}_r \, d^3u + \int v^{(1)} \varphi^{(1)} \, d^3u + \int v^{(2)} \varphi^{(2)} \, d^3u,$$

where $v^{(1)}$ and $v^{(2)}$ are arbitrary velocities and are at our disposal. To describe the Proca field, we choose $v^{(1)}$ and $v^{(2)}$ in such a way that, using (4.3), H contains only A_μ and B_μ (in fact, only $A_{-\mu}$ and $B_{-\mu}$). This elimination is precisely the same as that in the original formalism mentioned earlier.

The relativistic covariance of Stückelberg's theory does not follow at once because of the restriction to flat surfaces. However, for flat surfaces it gives the same results as the ordinary theory ⁽⁵⁾ and the theory of Section 3, and it must therefore be covariant.

The modified form of Stückelberg's theory ⁽⁸⁾ has been stated relativistically in the Tomonaga-Schwinger formalism. There is no exact counterpart in the Dirac theory to an auxiliary condition applied to the state-vector alone. It is interesting to note, however, that the free-field commutation rules in this case are precisely those stated at the end of Section 3 and that, as a result,

all S -matrix elements are the same in this theory and in the other two which we have considered.

In conclusion I should like to thank Professor P. A. M. DIRAC for much help and encouragement in this and other work.

RIASSUNTO (*)

Servendosi del formalismo dell'hamiltoniana di Dirac, si formula una teoria covariante per il campo vettoriale mesonico quantizzato e la si confronta con una teoria proposta da STÜCKELBERG. Quest'ultima teoria non può essere generalizzata riducendola ad una simile forma manifestamente covariante, ma dà gli stessi risultati della precedente.

(*) *Traduzione a cura della Redazione.*

Formative Time of the Cathodic Space Charge.

D. BRINI, O. RIMONDI and P. VERONESI

Istituto di Fisica dell'Università - Bologna

(ricevuto il 26 Ottobre 1954)

Summary. — The present paper sets forth a criterion for the evaluation of the formative time of the cathodic space charge, beginning with the moment at which the discharge becomes self-standing. Such a criterion is based on two facts to be observed in the study of intermittent discharges with a low-pressure gas: 1) it is possible to note a rise time of the oscillation pulse at the beginning of the first kind which is independent of the external circuit. 2) in these conditions a notable overtension exists at the start of the intermittent discharges in respect to the initial tension of Townsend's phase. From an evaluation of the pulse rise time and overtension value a calculation of the formative time of the cathodic space charge is possible. At the end, moreover, a general picture of the different kinds of intermittent discharges and conditions of their existence is drawn.

1. — Introduction.

In previous papers ^(1,2) we measured the decay time of the cathodic space charge in a discharge tube containing a low-pressure gas, when the tube was made to function in a condition of intermittent discharges. We then pointed out the existence of a minimum value, independent of the external circuit, of the oscillation pulse rise time in conditions of intermittent discharges at the end of the first kind. We assumed such a time to be the superior limit of the decay time of a cathodic space charge.

During these experiments we had occasion to observe the existence of overtensions at the start of the first kind discharges. Qualitative observations

⁽¹⁾ D. BRINI and P. VERONESI: *Nuovo Cimento*, **10**, 1662 (1953).

⁽²⁾ D. BRINI, O. RIMONDI and P. VERONESI: *Nuovo Cimento*, **12**, 413 (1954).

permitted us to conclude that such overtensions do not have values which vary from a statistical point of view, but that they assume a value which is well determined and constant for every functioning condition of the tube in the region of intermittent discharges of the first kind. Such a value, moreover, for every given discharge tube, depends on E , R and C values compatible with periodic discharges of the first kind. In the present paper we have taken up these experiments again for the purpose of measuring the formative time of the cathodic space charge.

For the measurements we used the equipment already adopted in the previous experiments, and as discharge tubes commercial ones were employed. It is useful to remember that in these tubes the geometric shape and arrangement of the electrodes are not very good; it is, however, possible to obtain satisfactorily reproducible measurements.

2. — Measurement of the Formative Time of the Cathodic Space Charge.

It is our present purpose to describe the criterion followed in determining the formative time of the cathodic space charge. This criterion is based on the behaviour of the discharge tube when this is functioning in the region of intermittent discharges at the beginning of the first kind. In these conditions two observations are evident.

1) The transition from the counter region to the beginning of the first-kind discharge conditions is characterized by the disappearance of the statistic behaviour at the starting of the discharges and by the fact that the oscillations

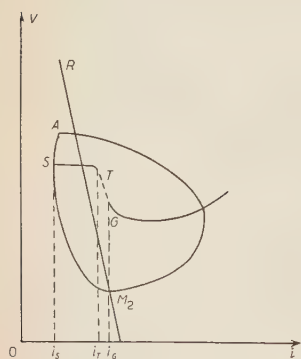


Fig. 1.

become rigorously periodic, with a well-determined and constant amplitude. It is possible to observe this situation experimentally by sending the oscillation pulse to an oscilloscope in which the sweep is absent. It is then easy to see, within a small percentage (5%), the condition in which the oscillation amplitude becomes regular and constant and to assume such a condition as that corresponding to the discharges at the beginning of the first kind. We consider that the verifying of this situation corresponds to the fact that, in every discharge, the dynamic characteristic intercepts the static one at the point where Townsend's

phase begins. The process is illustrated schematically in Fig. 1 where we have, at the same time, shown, in arbitrary units, the static characteristic of the tube and the dynamic one of an oscillation in discharge conditions at the beginning of the first kind.

2) The starting tension of the discharges at the beginning of the first kind is superior to the one corresponding to the beginning of Townsend's phase. This fact can be easily verified by observing the static characteristic of the tube

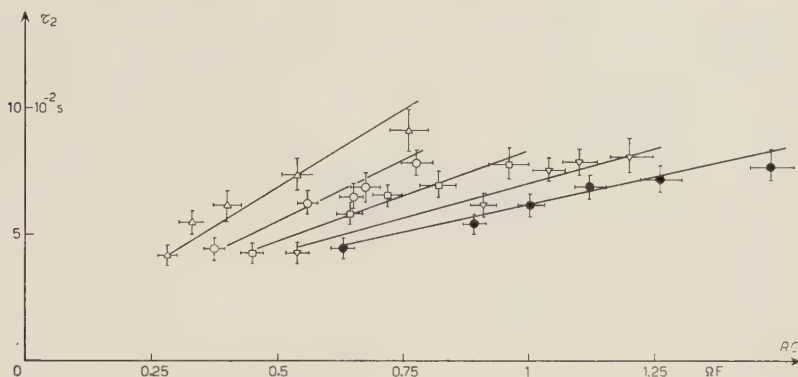


Fig. 2. a) - Tube STV 140 N. 1. R from 10 to 180 M Ω ; C from 3 000 to 80 000 pF.

Δ $E = 400$ V \circ $E = 500$ V \square $E = 600$ V ∇ $E = 700$ V \bullet $E = 800$ V

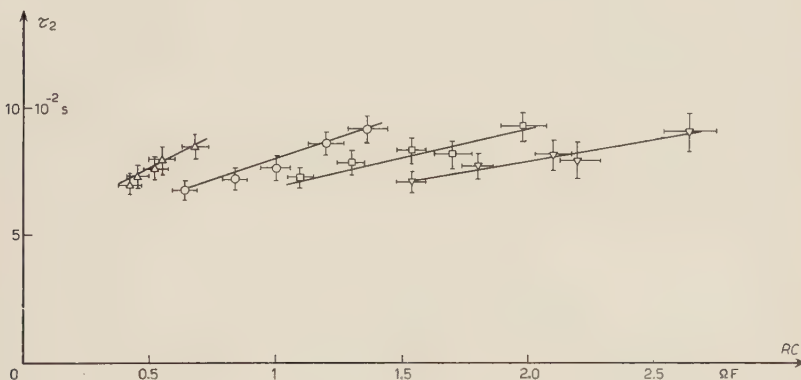


Fig. 2. b) - Tube STV 140 N. 2. R from 40 to 220 M Ω ; C from 35 000 to 45 000 pF.

Δ $E = 400$ V \circ $E = 600$ V \square $E = 800$ V ∇ $E = 1000$ V

in Townsend's region and measuring the absolute value of the peak tension of the oscillations of each discharge. This last parameter was measured by us with the device already described in the previous papers.

In conditions of intermittent discharges at the beginning of the first kind we made the following measurements:

- a) τ_2 , tension rise time at the tube electrodes
- b) $A - M_2$, oscillation amplitudes,
- c) A , initial discharge tension.

On the static characteristic, moreover, the values of the following parameters were observed:

- d) S , initial tension of Townsend phase,
- f) i_s , current at the beginning of Townsend phase.

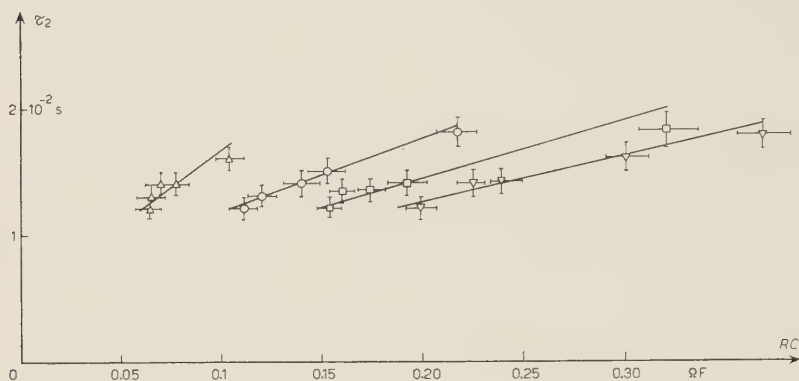


Fig. 2. e) - Tube STV 140 N. 3. R from 20 to 220 M Ω ; C from 800 to 8000 pF.

Δ $E = 400$ V \circ $E = 600$ V \square $E = 800$ V ∇ $E = 1000$ V

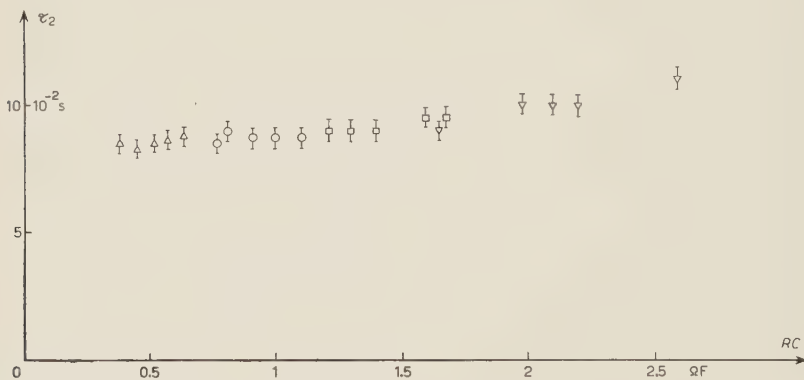


Fig. 2. d) - Tube 85A1. R from 60 to 220 M Ω ; C from 2000 to 30000 pF.

Δ $E = 400$ V \circ $E = 600$ V \square $E = 800$ V ∇ $E = 1000$ V.

The symbols used to indicate the various parameters are the same as those adopted in the above-mentioned papers.

For the measurement a) we looked for the dependence of τ_2 on the external circuit. The experimental conclusions reported in Fig. 2 put clearly in evidence the existence of a minimum value of τ_2 , for every type of tube, which is both sufficiently well defined, independent of the external circuit and characteristic of the tube itself. In the figure the ranges of the values used of R and C are also reported. In the case of tube 85 A I the errors on the RC

axis have not been reported in order to maintain clarity, nor has the line of behaviour of τ_2 as a function of RC , this latter being extremely uncertain owing to experimental errors.

As a consequence of 1) and 2) we were able to evaluate the formative time of the cathodic space charge.

Let us look in fact at Fig. 1. The fraction of the dynamic characteristic M_2S represents the part of the process which corresponds to the decay of the space charge and which is characterized by the relation

$$\mu = \gamma \left(\exp \int \alpha dx - 1 \right) < 1.$$

During this process we assumed, as in previous experiments, that the current decreases in a manner represented by the relation

$$(1) \quad -di = Ki dV.$$

In the fraction SA of the dynamic characteristic the discharge is characterized by the condition $\mu > 1$, and the multiplication processes of the ions cause a strong increase in ionic density in the tube. We admit that such an increase continues until the positive ionic density is sufficient to determine the cathodic space charge. The duration of such a process, which is indicated by τ_g , corresponds to the time in which the fraction SA on the dynamic characteristic is covered. We may therefore put

$$\tau_g = \tau_2 - \bar{\tau}_2,$$

where $\bar{\tau}_2$ represents the time necessary for the discharge process to complete the fraction M_2S of the dynamic characteristic. By using (1) and making our calculations with the same criteria used in the above-mentioned paper ⁽²⁾, it is immediately apparent that

$$(3) \quad \bar{\tau}_2 = RC_2 \ln \frac{E - M_2 - v_2}{E - S - v_2},$$

where

$$v_2 = R\bar{i}_2; \quad \bar{i}_2 = \frac{i_{M_2}}{\ln(i_{M_2}/i_S)} \left(1 - \frac{i_S}{i_{M_2}} \right); \quad i_{M_2} = \frac{E - M_2}{R}.$$

Table I reports the values of τ_g taken from (2) and (3) for the tube STV 140 No. 1. The different values for τ_g are compatible with the errors in the measurements, whence we can assume their mean value as the formative time of the cathodic space charge. We estimate such a value of τ_g , however, to be exact within 15%.

TABLE I.

E (V)	C (pF)	R (M Ω)	$A-M_2$ (V)	A (V)	S (V)	i_s (μ A)	τ_2 (ms)	$\bar{\tau}_2$ (ms)	τ_g (ms)
400	4000	70	22	158	151	0.05	42	21	21
500	3700	100	22	158	151	0.05	45	21	24
600	3200	140	22	158	151	0.05	43	19	24
700	3400	160	22	158	151	0.05	43	19	24
800	3500	180	22	158	151	0.05	45	20	25

The time τ_g could also be assumed as the time lag of spark breakdown. In this case, however, the initial current in the tube being sufficiently great, the spark takes place without statistical behaviour.

Similar measurements of the time lag in intermittent discharges were carried out by MAUZ and SEELIGER ⁽³⁾. The experimental conditions in which these authors worked were not, however, so well defined as those described in the present paper; therefore, the results which they obtained are not directly comparable with ours.

The present results could be compared and agree with those of TILLES ⁽⁴⁾, if the correspondence between τ_g and the time indicated by the author as *formative* time lag, is assumed. In our case, the so-called *initiator* time lag is not present because the initial current is great.

In every discussion on the time lag of spark Loeb's ⁽⁵⁾ analysis of this phenomenon must be clearly borne in mind.

The experiments of those authors mentioned by LOEB and other more recent ones ⁽⁶⁻⁸⁾, show a large variety of results because of the widely different exper-

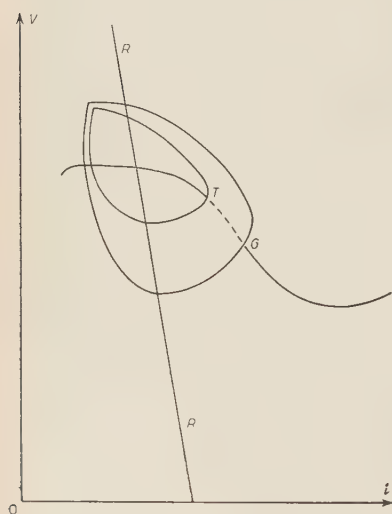


Fig. 3.

⁽³⁾ E. MAUZ and R. SEELIGER: *Phys. Zeits.*, **26**, 47 (1925).

⁽⁴⁾ A. TILLES: *Phys. Rev.*, **46**, 1015 (1934).

⁽⁵⁾ L. B. LOEB: *Fundamental processes of electrical discharge in gases* (New York, 1947), Chapter X.

⁽⁶⁾ G. A. KACHICKAS and L. H. FISHER: *Phys. Rev.*, **82**, 562 (1951).

⁽⁷⁾ G. A. KACHICKAS and L. H. FISHER: *Phys. Rev.*, **91**, 775 (1953).

⁽⁸⁾ B. BEDERSON and L. H. FISHER: *Phys. Rev.*, **81**, 109 (1951).

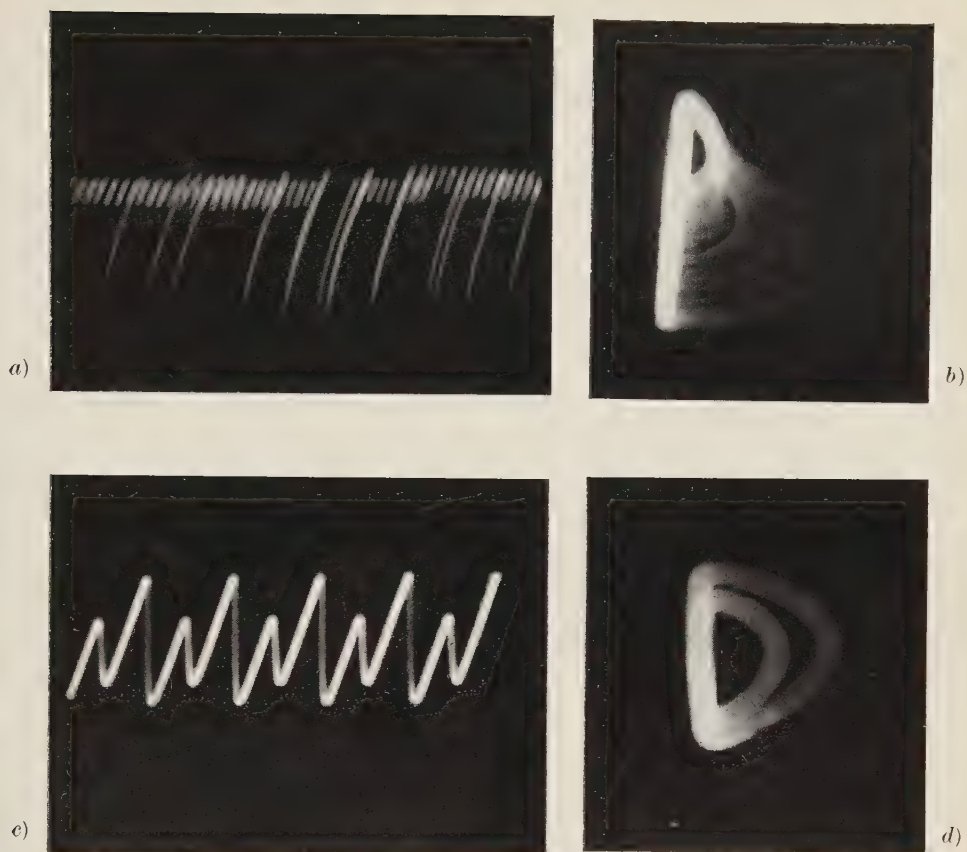


Fig. 4.

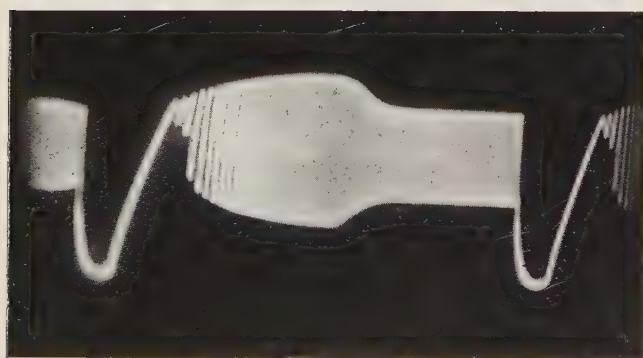


Fig. 5.

imental conditions and procedures. A comparison among all the results is possible, only if this circumstance is taken into account.

3. — Different Types of Intermittent Discharges.

Another condition of relaxation oscillations with tubes containing a low-pressure gas was observed by us during these measurements. Using convenient values of E and R , such that E/R is sufficiently small, it can be seen that oscillations develop in such a way that their dynamic characteristic interests Townsend's phase alone. If the condition that E/R is sufficiently small is satisfied, it is possible to pass from the intermittent discharges of the first kind to the intermittent discharges of Townsend's phase, reducing the value of C . Fig. 3 shows schematically, in arbitrary units, the dynamic characteristics relative to the two kinds of discharges. The transition from one to the other condition always takes place across group discharges so that oscillations in Townsend's phase alternate with those of the first kind. It must be noted, however, that the substitution of one kind of discharge for another does not take place in a regular manner, as is the case on the contrary in group discharges between the first and second kinds.

In Fig. 4 oscillographic photographs of the two types of phenomena are shown. In 4 *a*), the transition from the first kind oscillations to those in Townsend's phase is reported as $V=V(t)$. The irregularity of this condition of functioning did not permit us to take a very clear photograph. It is nevertheless possible to observe the tension A ; in the two cases this does not vary very greatly, while strong variations appear in the value of M . In 4 *b*) the dynamic characteristics of the same discharges, i.e. $V=V(i)$, are reported. 4 *c*) and 4 *d*) refer instead to $V=V(t)$ and $V=V(i)$ of the group discharges between the first and second kind respectively.

It is easy to see that in these last cases the two kinds of oscillations assume very different values of A , which correspond to the lowering of the operating tension of the tube at the transition of Townsend's phase to the glow one.

The occurrence of the intermittent discharges in Townsend's phase can also be observed visually. Unlike first kind discharges in which the cathodic glow is marked, the anodic glow only is observed in this case.

Fig. 5 summarizes all these conditions. It was obtained by one of the methods already described in ⁽¹⁾; the three different conditions of oscillation which take place when E increases are distinctly visible. The oscillations in Townsend's phase take place first, then those of the first kind, and, lastly, the second kind ones.

At the end it was possible to establish some conditions for fixing the extreme limits for the existence of the different kinds of discharges. Observing Fig. 1

it is apparent that:

- a) if $(E - G)/R \leq i_g$ second kind discharges cannot exist,
- b) if $(E - S)/R \leq i_s$ first kind discharges cannot exist,
- c) if $(E - S)/R \leq i_s$ or $(E - T)/R \geq i_t$ intermittent discharges in Townsend's phase cannot exist.

These conditions also show that for a given pair of values for E and R compatible with the existence of intermittent discharges of the second kind, pischarges in Townsend's phase cannot exist and vice versa.

Our thanks are due to Mr. L. PARISINI for help given in the measurements.

RIASSUNTO

Nel presente lavoro viene proposto un criterio per la valutazione del tempo di formazione della carica spaziale catodica, a partire dall'istante in cui la scarica diviene automantenentesi. Tale criterio si basa su due constatazioni, che si possono fare nello studio delle scariche intermittenti con gas a bassa pressione: 1) è possibile mettere in evidenza un tempo di salita dell'impulso di oscillazione di inizio prima specie, indipendente dal circuito esterno; 2) esiste una notevole sovratensione nella partenza delle scariche intermittenti, in queste condizioni, rispetto alla tensione di inizio della fase di Townsend. Dalla valutazione del tempo di salita dell'impulso e del valore della sovratensione è possibile calcolare un tempo di formazione della carica spaziale catodica. In fine viene formulato un quadro generale sui diversi tipi di scariche intermittenti e sulle condizioni della loro esistenza.

Time Variations of Cosmic Ray Intensity.

F. BACHELET and A. M. CONFORTO

Istituto di Fisica dell'Università - Roma

Istituto Nazionale di Fisica Nucleare - Sezione di Roma

(ricevuto il 3 Novembre 1954)

Summary. — An apparatus for the continuous registration of the total ionization component of cosmic rays at sea level has been set up at Rome. The purpose is to study the correlations between cosmic ray intensity and atmospheric, geomagnetic and solar phenomena. The apparatus consists of telescopes of Geiger-Müller counters in triple coincidence, directed vertically, and inclined at 30° to the vertical in the direction South and North respectively. The difference between the diurnal variations in two inclined directions is considered free from atmospheric effects and is thus able to show up an anisotropy of the primary radiation. There are four independent telescopes in each direction, with a total of about 27 000 coine./h in North and South directions respectively, and about 48 000 coine./h in the vertical. The counters are held thermostatically at $(30 \pm 1)^\circ\text{C}$. The methods used to reduce the instrumental inequalities and to obtain the maximum operational stability and continuity are described. The preliminary results obtained in the first counting period, from January to March 1954, are presented.

1. — Introduction.

An apparatus for the continuous recording of the total ionizing component of the cosmic radiation at sea level has been set up in Rome (41.9° N , 12.5° E geogr.; 47.4° N geom.), in connection with an international program of studies on the time variations of the cosmic ray intensity.

The purpose is that of bringing to light: *a*) the anisotropy of the primary radiation and, *b*) the correlation between cosmic rays and atmospheric, geomagnetic and solar phenomena.

The apparatus, designed on the pattern of those already operating in

Stockholm ⁽¹⁾ and Manchester ⁽²⁾, consists of telescopes of G-M counters in triple coincidence, symmetrically inclined with respect to the vertical plane. A means is thus provided to reveal the lack of isotropy of the primary radiation, since the difference between the solar daily variations as measured by two directional arrays of this kind is free from atmospheric effects. The residual wave observed, with an amplitude of the order of 0.1%, is generally taken as an index of such an anisotropy.

The vertical radiation is also detected, in order to improve the statistics in the study of the geophysical and solar correlations of cosmic rays.

Data of atmospheric pressure at sea level, as well as of temperature and height of the isobaric levels near the meson producing layer (200, 100 and possibly 50 mbar) are systematically given by the Ministero della Difesa Aeronautica (Aeroporto di Ciampino). The Istituto Nazionale di Geofisica provides the geomagnetic (Osservatori di Corinaldo e di Gibilmanna) and ionospheric (Stazione di Roma) information. Finally, for the solar data we refer to the Osservatori Astronomico di Roma and Astrofisico di Arcetri, as well as to the Fraunhofer Institut of Freiburg i.B..

2. - Experimental Apparatus.

The apparatus is operated on the top floor of the Physics Department, under a thin roof of light material (about 3 g/cm² air equivalent).

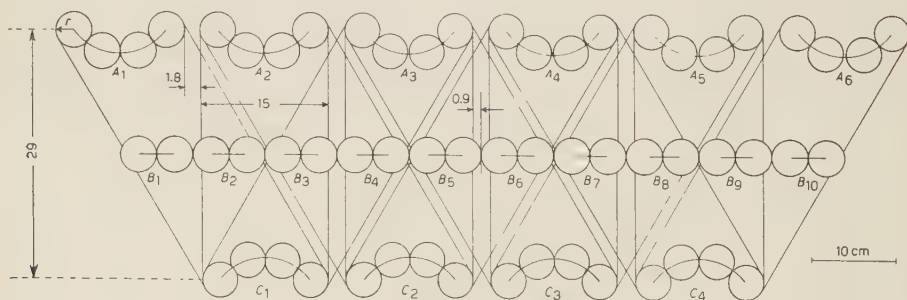


Fig. 1.

Fig. 1 gives a cross-section view of the geometry presently corresponding to a meridian plane. The inclined telescopes point therefore North and South respectively, with a mean angle of 30° to the vertical. This is also the direction of maximum sensitivity, if the sensitivity in a particular direction is defined

⁽¹⁾ K. G. MALFORMS: *Tellus*, 1, 55 (1949).

⁽²⁾ H. ELLIOT and D. W. N. DOLBEAR: *Journ. Atm. Terr. Phys.*, 1, 205 (1951).

enough (80 V) to prevent counting of two-fold coincidence pulses. The counting units include chains of scale-of-two circuits, with a scaling factor 8. A coupling stage between the final scaler unit and the 6V6 driver circuit gives pulses of suitable length for reliable operation of the electromechanical registers. The electromechanical registers and driver circuits are selected on the requirement of handling more than 10 regularly spaced pulses per second. The plate voltage for the driver stage is taken from an independent part of the power supply.

The power supply for all the apparatus is independent of the a.c. mains, whose frequent failures are thus avoided; it is obtained by means of stationary batteries and of a 1.5 kW d.c. generator and an electronic system for the voltage stabilization within $\pm 2\%$.

The recording equipment includes a 16 mm film camera, by which the dials of the electromechanical registers and a clock for the time reference are automatically photographed every 15 minutes. This operation is initiated with the precision of one second by a spring driven clock which is temperature compensated and maintains an accuracy of better than ± 3 s per day.

Most important for this type of measurements are clearly the requirements of operational stability and continuity as well as the limitation of all possible errors. It has been seen above that various methods have been adopted to secure the best operational conditions and the means to keep the apparatus under continuous control. It is perhaps worth noting that the arrangement of the telescopes in four independent groups for each direction provides a means for checking the counting rates by comparison and for securing the continuity of the measurements as well as possible. At the same time, the interdependence of the South, North and Vertical sets, up to the coincidence stages, helps to identify certain operational failures occurring in elements in common. Aside from the general weekly controls, a quick check of the scaling units is available, by inspection of the interpolation indicators (neon lamps), set on each scale of two; the interpolation is not recorded by the camera, but the error arising in this way is purely statistical and cannot be more than $\pm 0.05\%$ in the case of the bihourly rates.

A few remarks should be made on the problem of systematical errors. As already mentioned, interchange between the two groups of North and South pointing telescopes was devised in order to eliminate the geometrical and instrumental inequalities and to level off the spurious effects. In particular, it is clear that, when the South minus North differences are computed, also this common background vanishes. However, we are aware that all spurious effects which might be different for the various instruments and moreover periodical could still affect the interpretation of the data.

Sources of systematical errors are in general spurious coincidences due for instance to accidental side showers, and multiple pulses of the counters, as well as counting losses. The background of all spurious coincidences, checked experimentally, is of the order of 1%. Variations of the accidentals due to instrumental causes are certainly insignificant on account of the operational stability of the electronic circuits. The effects of the multiple pulses in the G-M tubes might be related to inadequate external conditions. The temper-

ature stabilization is expected to render these uniform enough; it serves also to prevent possible temperature variations of the counter efficiency.

In any case, multiple counting of individual pulses having minor oscillations superposed on them would be reduced by a « dead » time of about 600 μ s of the circuit following the coincidence stage. While, as is known, the efficiency of the scaler itself is thus increased, the fractional counting losses remain altogether of the order of 0.2% ⁽³⁾.

We shall here remark that the counting losses would increase if a multivibrator quenching stage, as used elsewhere ⁽⁴⁾, were connected to each of the 60 G-M tubes (it should be remembered that the S, N and V telescopes are partly interdependent). Moreover, because of the short rise times involved ($< 1 \mu$ s), a large expenditure of power would be required. It was therefore preferred not to adopt such input circuits, at least for the moment, and to keep instead the voltage characteristics of the G-M counters under control. Our counters are operated at as low voltages as possible; their mean life is about 7 months. It should be added that all types of trigger circuits based on multivibrators are generally avoided in our electronic apparatus, in order to prevent possible sources of instability.

3. — Preliminary Results.

A group of the first results, for the period December 31, 1953, to March 13, 1954, a total of 50 days of effective data, has been examined.

Combining the counting rates of the four parallel telescopes in each direction, we get on the average about 27 000 counts/h North and South respectively, and about 48 000 counts/h in the vertical direction.

The statistical analysis (χ^2 -test) of a good part of the hourly data, taken channel by channel and day by day, has constituted a guide for the checking and selection of the results.

A further check of the internal consistency of the data was provided by the study of the correlation with the atmospheric pressure: the agreement was very good when the rates of equivalent groups of counter telescopes were taken separately.

A mean value for the barometer coefficient has been derived in the inclined directions, from the daily means through the whole period of measurements, of $(-2.49 \pm 0.04)\%$ /cm Hg ⁽⁵⁾. This value refers to the total regression coefficient between cosmic rays and pressure, i.e. the correlations with temperature and height of the upper air layer have been temporarily neglected. A rough estimate of the contributions of these two variables to the intensity

⁽³⁾ L. ALAOGH and N. M. SMITH: *Phys. Rev.*, **53**, 832 (1938); E. BALDINGER and R. CASALE: *Helv. Phys. Acta*, **21**, 117, (1948).

⁽⁴⁾ H. ELLIOT: *Proc. Phys. Soc.*, A **92**, 369 (1949).

⁽⁵⁾ For the error used see M. G. KENDALL: *The Advanced Theory of Statistics*, II (1952), p. 156. Our barometer data have an accuracy of 0.1 mbar.

variations can be made by taking into account their maximum ranges during this time together with the order of magnitude of the two temperature coefficients as obtained by other workers ⁽⁶⁾; the effect seems quite negligible compared to that of the pressure changes, so that the above value for the barometer coefficient should be reliable enough. This is confirmed by the high total correlation coefficient found, $r = -0.96_{-0.08}^{+0.02}$ (the errors being the 99.7% fiducial limits computed by means of Fisher's z -function) ⁽⁷⁾.

As regards the solar diurnal effect, the South minus North differences between the percentage variations from the respective means have been computed on the basis of the two-hourly values. Despite the poor statistics of the single points, evidence for a residual diurnal wave is given by their sequence distribution. The first harmonic of this wave exhibits a maximum around 3 p.m., with an amplitude of $(1.46 \pm 0.49) \cdot 10^{-3}$.

The experimental data are generally examined as hourly or bihourly values; however a finer control of the various channels is available, when necessary, since recording is constantly made every 15 minutes. That would permit, furthermore, to follow sudden intensity variations of the cosmic rays, possibly accompanying strong magnetic storms or solar flares.

χ^2 -tests were carried out mostly on the days after some operational failures had occurred, in order to ascertain that no particular trend of the counting rates appeared. The same procedure was followed on the occasions when the rates of one or more channels seemed to present some peculiarities and still there were no objective reasons for rejecting them. Clearly, a strict comparison of the experimental χ^2 -distribution with that expected is possible only on the assumption of data affected by purely random fluctuations. Therefore, when a systematic effect due to pressure changes during the day was superimposed and became significant, the probability of the relative χ^2 -distribution was valued accordingly.

On the days with a very steep pressure gradient the barometer coefficient was also computed on the basis of threehourly values. This was done mainly as a means of comparison through the 24 hours between the two recording arrays which are expected to be equivalent, the left- and right-hand telescopes respectively. The results are in good agreement with one another, within the limits of accuracy, as well as with the more dependable values derived from the daily means through the whole period of data. Also in this case, the pressure coefficients were tentatively calculated by neglecting the multiple correlation, this time because only two data a day (at 3 a.m. and p.m.) of temperature and height of the upper air layers are available. On the other hand, the total regression coefficients happen to be all quite high, ranging from 0.86 to 0.98.

⁽⁶⁾ B. TRUMPY and H. TREFALL: *Physica*, **19**, 636 (1953).

⁽⁷⁾ R. A. FISHER: *Statistical Methods for Research Workers* (1944).

Acknowledgments.

We are deeply indebted to Dr. F. LEPRI for the design of the electronic circuits and for all his contributions to their adjustment.

Special thank are due to the Ispettorato delle Telecomunicazioni e Assistenza al Volo for the meteorological data kindly supplied every month.

The assistance and the cooperation of the technical staff of this Laboratory, where most of the equipment was constructed, is very gratefully acknowledged.

Finally we should like to thank Prof. B. FERRETTI for the very helpful discussions.

RIASSUNTO

Si descrive un apparecchio per la registrazione continua della totale ionizzante dei raggi cosmici al livello del mare, messo in funzione a Roma per lo studio delle correlazioni tra l'intensità dei raggi cosmici e fenomeni atmosferici, geomagnetici, solari. L'apparecchio è costituito da telescopi di contatori G-M in coincidenze triple, sia diretti secondo la verticale che inclinati di 30° rispetto a questa, nelle direzioni Sud e Nord rispettivamente. La differenza tra le variazioni diurne nelle due direzioni inclinate si ritiene esente da effetti atmosferici e perciò in grado di mettere in evidenza una anisotropia della radiazione primaria. A ciascuna direzione competono 4 telescopi indipendenti, con un totale di circa 27 000 coine./h a Nord e a Sud rispettivamente, e di circa 48 000 coine./h in verticale. I contatori sono tenuti in termostato a $(30 \pm 1)^\circ\text{C}$. Si espongono i metodi seguiti per ridurre le differenze strumentali e per ottenere la massima stabilità e continuità di funzionamento. Si presentano i risultati preliminari ottenuti in un primo periodo di misure, dal Gennaio al Marzo 1954.

Nuclear Collisions of High Energy Protons, Mesons and α -Particles.

A. ENGLER, U. HABER-SCHAIM and W. WINKLER

Physikalisches Institut der Universität Bern, Switzerland

(ricevuto il 3 Novembre 1954)

Summary. — The results of a systematic scanning of nuclear emulsions flown at high altitude are presented and analyzed. It is found that at high energies the size of the target-nucleus is not of major importance with regard to the number of shower particles produced. Also, the multiplicity of mesons for α -particles is about the same as for protons. The angular distribution of shower particles in the c.m. system is described and evidence is presented for the asymmetry of mesons nucleus collisions. Finally, the elasticity of nucleon-nucleus collisions is briefly discussed.

1. — Introduction.

There exists a considerable amount of experimental material concerning stars with collimated shower tracks produced in photographic emulsions ⁽¹⁻¹¹⁾.

⁽¹⁾ J. J. LORD, J. FAINBERG and M. SCHEIN: *Phys. Rev.*, **70**, 970 (1950).

⁽²⁾ E. PICKUP and L. VOIVODIC: *Phys. Rev.*, **84**, 1191 (1951).

⁽³⁾ H. L. BRADT, M. F. KAPLON and B. PETERS: *Helv. Phys. Acta*, **23**, 24 (1950).

⁽⁴⁾ V. D. HOPPER, S. BISWAS and J. F. DARLY: *Phys. Rev.*, **87**, 545 (1952).

⁽⁵⁾ R. R. DANIEL, J. H. DAVIES, J. H. MULVEY and D. H. PERKINS: *Phil. Mag.*, **43**, 753 (1952).

⁽⁶⁾ M. DEMEUR, C. C. DILWORTH and M. SCHÖNBERG: *Nuovo Cimento*, **9**, 92 (1952).

⁽⁷⁾ C. C. DILWORTH, S. J. GOLDSACK, T. F. HOANG and L. SCARSI: *Compt. Rend.*, (20 Aprile 1952); *Nuovo Cimento*, **10**, 1201 (1953).

⁽⁸⁾ T. F. HOANG: *Journ. de Phys. et le Rad.*, **14**, 395 (1953); **15**, 337 (1954).

⁽⁹⁾ K. GOTTSTEIN and M. TEUCHER: *Naturforschung*, **8a**, 120 (1953).

⁽¹⁰⁾ C. CASTAGNOLI, G. CORTINI, C. FRANZINETTI, A. MANFREDINI and D. MORENO: *Nuovo Cimento*, **10**, 1539 (1953).

⁽¹¹⁾ G. BERTOLINO and D. PESCE: *Nuovo Cimento*, **12**, 630 (1954). We are indebted to the authors for making their paper available to us prior to publication.

Most of this material is limited, however, to stars with no more than 4 evaporation tracks which are sometimes interpreted as due to glancing collisions.

In the present paper we make use of the fact that the photographic emulsion contains hydrogen, light and heavy elements and study the effect of the size of the target nucleus on meson production. Since our plates were flown at high altitude we have a reasonable number of stars produced by α -particles to enable us to compare these stars with those due to singly charged particles.

In the next section the experimental procedure is outlined. In section 3 the average multiplicity of shower particles is presented as function of the energy and the number of black prongs for both singly charged and α -primaries. Although the energy of the star producing particles is determined by the half angle method which assumes the existence of a c.m. system, the angular distribution of the secondaries still gives an estimate of the energy also under more general conditions. It is only in section 4 where the existence of a c.m. system is essential. There the angular distribution of the shower particles in that system initiated by singly charged particles is compared with those initiated by alphas. It is suggested that the difference between the two distributions is due to meson produced stars.

Finally, in section 5 the elasticity of the nucleon-nucleus collision is discussed in relation to the ratio of neutral to charged star producing particles.

2. — Experimental Procedure.

In the present experiment 18 emulsions with a volume of 95.5 cm^3 were scanned. These emulsions were obtained from two different flights at $\sim 30 \text{ km}$ altitude, exposed, for ~ 4 and ~ 7 hours respectively. From all the stars found in the scanned volume those produced by singly charged, neutral or α -particles satisfying the following conditions were accepted for our analysis: *a*) at least 5 shower particles, *b*) half the shower particles have a projected angle of $\leq 10^\circ$ with the primary. The conditions for α -produced stars were $n_s \geq 5$ and a projected half angle of $\leq 14^\circ$. No restriction was imposed on the number of black and grey prongs. The true half angle is usually greater than the projected half angle because of the dip of the tracks. We believe, therefore, that all the stars from the scanned volume having a true half angle $\leq 10^\circ$ for singly charged and $\leq 14^\circ$ for α -primaries were actually selected (*). The half angle of the n -stars was taken with respect to the axis of the shower.

(*) The plates were scanned with a magnification of $200\times$ without oil. The emulsions were very clear due to the excellent processing of Dr. MERLIN in Padua. It seems very unlikely that a considerable fraction of stars was lost during the scanning because we found 5 shower stars without heavy prongs (compare section 3).

Two formulae have been used to determine $\gamma_c = (1 - \beta_c^2)^{-\frac{1}{2}}$ where β_c is the velocity of the center of mass system relative to the laboratory system. Both are based on the same well known assumptions of symmetry ^(3,7,11),

$$(1) \quad \gamma_c = \text{ctg } \theta'_{\frac{1}{2}},$$

where $\theta'_{\frac{1}{2}}$ is the median angle of the shower.

$$(2) \quad \log \gamma_c = -\frac{1}{n_s} \sum_{i=1}^{n_s} \log \text{tg } \theta'_i,$$

as suggested by the Rome-group ⁽¹⁰⁾. In most cases the values of γ_c given by the two formulae differ only slightly. Yet both have inherent deficiencies which are best seen by superposing the resulting angular distributions in the c.m. system. Using (1) a peak is found at 90° ⁽¹¹⁾. This is due to the following. Most stars are to some degree asymmetric in the c.m. system due to fluctuations. By using (1) one forces at least one track (namely the median) into the vicinity of 90° thus yielding a fictitious peak around that point. It can also be shown that (1) will rather overestimate γ_c than underestimate it which results in an asymmetry between 0° and 180° in the c.m. system. This asymmetry (high peak at 180°) may also be partially due to the increase of large angles by secondary interactions.

When plotting the angles in the c.m. with (2) both the peak at 90° and the asymmetry between 0° and 180° disappear. But (2) attaches a large weight to large angles which results in a slight underestimate of γ_c causing more particles to go forward in the c.m. than backwards.

The energy of the primary particle is given (in nuclear mass units) by

$$(3) \quad E = \frac{2k}{\text{tg}^2 \theta'_{\frac{1}{2}}} = 2k\gamma_c^2.$$

We also define a quantity

$$(3') \quad \gamma = 2\gamma_c^2.$$

Here k is the number of nucleons at rest which participate in the collision. A similar formula holds also for the general case when the k nucleons are not hit simultaneously. Although we cannot determine k without using a definite model ⁽¹²⁾ we can still use γ as a measure of the energy as long as the probability of hitting a given number of nucleons is energy independent. This is the case, for example, in the tunnel model of ROESLER and MCCUSKER ⁽¹³⁾.

⁽¹²⁾ G. COCCONI: *Phys. Rev.*, **93**, 1107 (1954).

⁽¹³⁾ F. C. ROESLER and C. B. A. MCCUSKER: *Nuovo Cimento*, **10**, 127 (1953).

Therefore, a quantity which is expected to be a function of energy (e.g. n_s) should also be a function of γ though generally a different one ⁽¹⁴⁾.

For the collision of α -particles it seems reasonable to put $k = 4$. Then γ is the energy per nucleon. This would remain unaltered also for a stripping collision when, say, one nucleon of the α -particle strikes one nucleon of the target nucleus and the other three fly on undisturbed. If one chooses $k = 1$, then γ will be the total energy of the α -particle, since at high energies (3) holds irrespective of the mass of the primary particle.

3. - The Multiplicity of Shower Tracks.

Frequency histograms of the number of shower particles (n_s) and slow particles (N_h) per star are shown in Figs. 1 and 2. Stars with $20 < \gamma < 65$ are shown in dotted lines. Since not all of these stars which were found in the scanned volume have been measured their frequency should not be com-

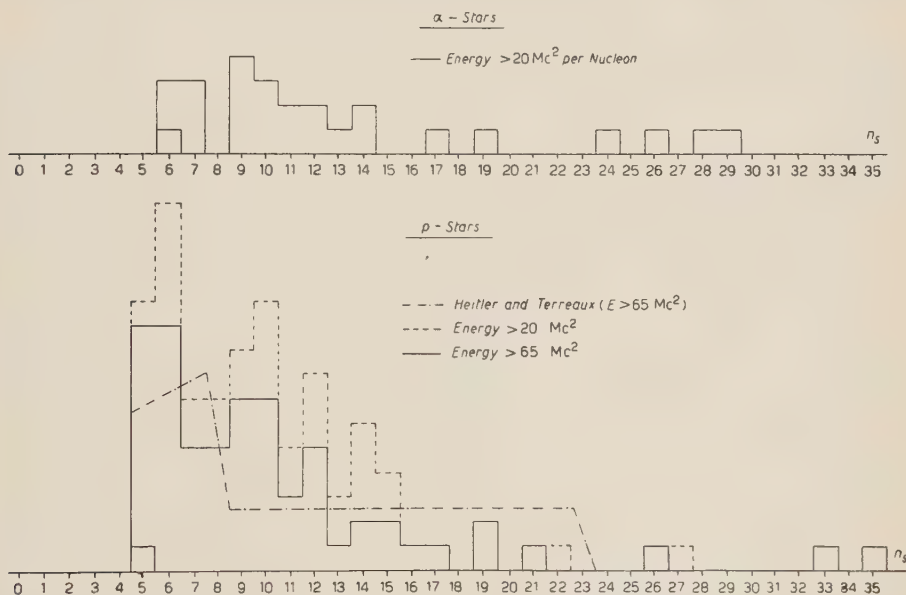


Fig. 1. - Frequency histogram of n_s for stars produced by α - and singly charged particles.

pared with that of the stars with $\gamma > 65$. The third line in Fig. 1 shows the frequency distribution of shower tracks according to the Heitler-Therreux theory ⁽¹⁵⁾ for primaries of $\gamma > 65$. The theoretical curve has been normalized

⁽¹⁴⁾ A. ENGLER and U. HABER-SCHAIM: *Phys. Rev.*, **95**, 1700 (1954).

⁽¹⁵⁾ W. HEITLER and CH. THERREAUX: *Proc. Phys. Soc.*, A **66**, 929 (1953).

to the total number of stars observed (65) and is apparently in disagreement with the experimental curve.

We characterize the distributions of the various quantities by their mean value $\bar{n} = (1/\nu) \sum n f(n)$, and their median value \tilde{n} defined by $f(n < \tilde{n}) =$

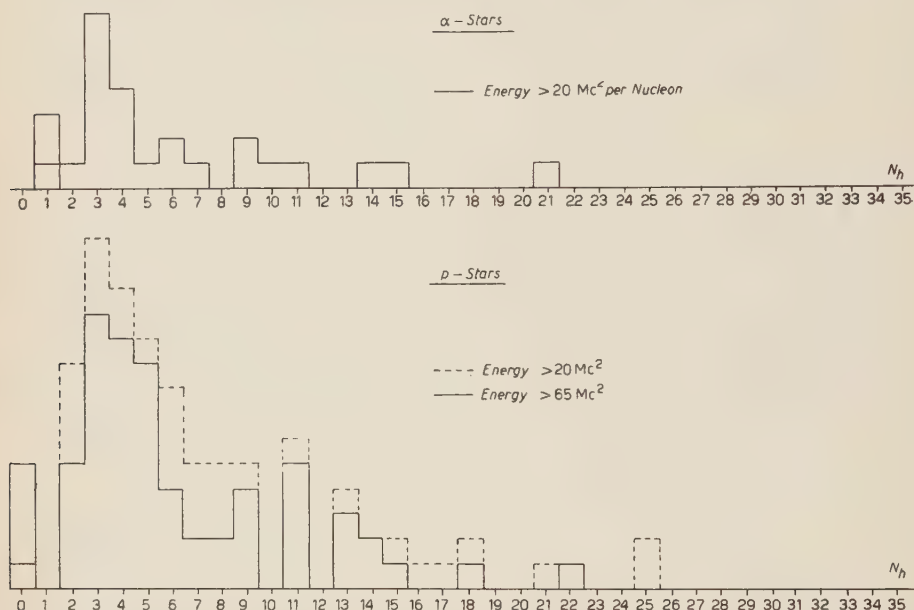


Fig. 2. - Frequency histogram of N_h for stars produced by α - and singly charged particles.

$= f(n > \tilde{n})$. $f(n)$ is the number of stars with given n , and ν the total number of stars of a certain category. With limited statistics such as in our case the median value is not as sensitive to single but large fluctuations as is the mean value. Therefore it may be a somewhat better indicator for the general trends than the mean value.

Tables I and II show the multiplicity of shower particles as function of the energy. The first column gives the energy of the primary as described in the previous section. The second column shows the number of cases and the third to sixth give the mean and median values for the minimum ionization and heavy tracks respectively.

TABLE I.

γ	ν	\bar{n}_s	\tilde{n}_s	\bar{N}_h	\tilde{N}_h
20 - 65	31	11	10	9	7
65 - 100	24	8.9	8	6.4	5
100 - 300	31	10.2	8	5.1	4
> 300	10	13.5	10.5	7.3	6.5

TABLE II.

γ	ν	\bar{n}_s	\tilde{n}_s	\bar{N}_h	\tilde{N}_h
20-65	18	12.5	11	6.5	3.5
> 65	8	13.8	10	4.4	4

We notice immediately that the mean (or median) number of shower particles does not change significantly with energy. There may be two factors responsible for the constancy of \bar{n}_s :

a) One may assume that for each energy there exists a distribution of n_s which shifts to the right along the n_s axis with increasing energy. Since we make a cut-off at $n_s = 5$ we possibly take only the upper fraction of the distribution as we go down with energy. Hence around $\gamma = 65$ we calculate the mean value of n_s not over the whole distribution but only over its upper fraction which yields a larger mean value.

b) The values of \bar{n}_s at energies 20-100 Mc² may really be fairly constant due to an increasing interference effect in the development of the cascade inside the nucleus. At low energies particles are produced with a relatively wide angular distribution and one may consider them as continuing their way inside the nucleus independently. With increasing energy the angular distribution becomes more and more peaked in the forward direction and the various particles in the «core» cannot act independently. Instead of adding the output of separate collisions one should probably add the energy of those particles and consider them to collide simultaneously^(16,17). Since the multiplicity of meson production in a nucleon-nucleon collision increases slower than the first power of the energy, the effect of the collimation will tend to decrease the multiplicity in the nucleon-nucleus collision thus balancing (or out-balancing) the increase due to possible independent secondary collisions.

TABLE III.

N_h	ν	\bar{n}_s	\tilde{n}_s
0	5	10	10
1-3	17	8.4	9
4-6	23	8.4	8
7-9	8	10.7	10.5
> 10	12	16.3	13

TABLE IV.

N_h	ν	\bar{n}_s	\tilde{n}_s
0-3	11	11	9
4-6	7	15.7	11
> 7	8	13.3	11

⁽¹⁶⁾ U. HABER-SCHAIM: *Phys. Rev.*, **84**, 1199 (1951).

⁽¹⁷⁾ M. F. KAPLON and D. M. RITSON: *Phys. Rev.*, **85**, 932 (1952).

Tables III and IV show the mean and median multiplicities of shower tracks as a function of N_h for stars produced by singly charged and α -particles respectively. Let us consider first Table III and start with the stars with $N_h = 0$. All our five stars have an even number of prongs and can therefore be due to proton-proton collisions. Adding up published stars from other laboratories (¹⁸⁻²⁰) we find a ratio of even to odd stars without heavy prongs of 18:9. This suggests that about one third of all the stars with $N_h = 0$ are due to proton-proton collisions (all even) and two thirds are due to proton-nucleus collisions (about half even and half odd). Similar results were found for the interactions of π^- in photographic emulsions at 1.5 GeV (²¹). The partial (geometric) cross-section for hydrogen in the G5 emulsion is 5.6%. We observe 5 stars with $N_h = 0$ out of 65 which is 7.8%. Hence it is very probable that 2 or 3 of these stars are due to proton-proton collisions.

We cannot make any definite statement about the groups of stars with $1 \leq N_h \leq 6$. They certainly contain a mixture of collisions with light and heavy elements. We can only observe that if stars with $N_h \leq 3$ are interpreted as coming from the HCNO-group and those with $N_h \geq 4$ from the SAgBrI-group the result is in agreement with the partial cross-section for both proton- and α -stars. Above $N_h \geq 7$ all stars are produced in heavy elements. We wish to conclude from our results that the size of the target nucleus is only a minor factor in the production of mesons at the energies under consideration. The dependence of the multiplicity on the nuclear radius is certainly much weaker than the quadratic dependence predicted by the Heitler-Therreaux-model (¹⁵) and possibly also weaker than the linear dependence suggested by McCUSKER and ROESLER (^{13,22}).

Comparing Tables I and II (or III and IV) we notice that the mean number of shower particles in the « α » stars is only slightly higher than in the «p» stars. This fact becomes more striking if we compare $\bar{n}_s - \frac{1}{2}$ for «p» stars with $\bar{n}_s - 2$ for « α » stars which one should do if one is interested in comparing the number of mesons produced in both types of showers: $(\bar{n}_s^\alpha - 2)/(\bar{n}_s^p - \frac{1}{2}) = 1.13$. As has been mentioned already there may exist a tail on the left side of the distribution given in Fig. 1. This tail may be considerably larger for protons than for α -particles in particular at the lower end of our energy band. It is difficult to calculate or measure this tail exactly, but it seems to us that adding 10 stars of $n_s = 4$ and 10 stars of $n_s = 3$ to the distribution of «p»

(¹⁸) M. F. KAPLON, D. M. RITSON and W. D. WALKER: *Phys. Rev.*, **90**, 716 (1953).

(¹⁹) D. LAL, YASH PAL, B. PETERS and D. S. SWAMI: *Proc. Ind. Acad. Science*, **39**, 75 (1952).

(²⁰) W. HEISENBERG: *Kosmische Strahlung* (1953), p. 150 and ref. 4, 5, 8-10.

(²¹) J. CRUSSERD, W. D. WALKER and M. KOSHIBA: *Phys. Rev.*, **94**, 736 (1954).

(²²) C. B. A. McCUSKER and F. C. ROESLER: *Phys. Rev.*, **91**, 769 (1953).

stars for $\gamma > 65$ and *none* to the α distribution would be a generous correction. We then obtain $(\bar{n}_s^x - 2)/(\bar{n}_s^p - \frac{1}{2}) = 1.37$ ⁽²³⁾. We believe that this result presents strong evidences for the view that the meson production in the collision of an α -particle with a nucleus cannot be considered as a superposition of 4 nucleon collisions but should rather be considered like the nucleon-nucleus collision as a single complex event ⁽¹³⁾.

The mean (and median) number of black prongs is lower for α -stars than for «p» stars as shown in Tables I and II. This is in accordance with the increase of the partial cross-section for a collision with light elements in the emulsion for α -particles as compared to protons (70% AgBrIS and 30% HCNO for protons and 60% AgBrIS and 40% HCNO for alphas).

4. - The Angular Distribution in the c.m. System.

Once we consider the showers to be produced in a single collision there arises the question of the isotropy of the angular distribution in the center of mass system. As a suitable measure of the degree of isotropy of a star, we take the ratio $u = n_s(|\eta| \geq 0.5)/n_{s\text{total}}$, where $\eta = \cos\theta$ in the c.m. system, i.e. the fraction of shower particles contained in the half solid angle around

the direction of the primary. We plotted the frequency histogram of u for both sets of γ_c as explained in section 2. Although some stars did shift the

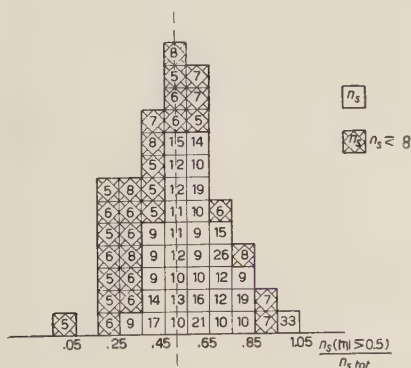


Fig. 3. - Frequency histogram of $u = n_s(|\eta| \geq 0.5)/n_{s\text{tot}}$ for stars produced by singly charged particles.

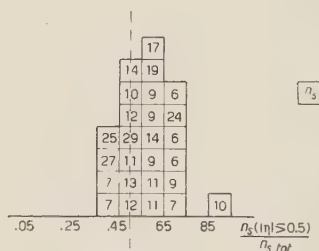
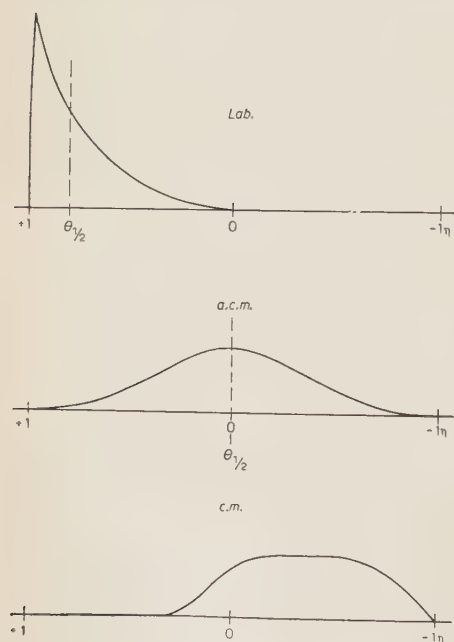


Fig. 4. - Frequency histogram of $u = n_s(|\eta| \geq 0.5)/n_{s\text{tot}}$ for stars produced by α -particles.

picture as a whole remained the same and is therefore not sensitive to small errors in γ_c . Fig. 3 shows the result for «p» stars and Fig. 4 for α -stars.

⁽²³⁾ One cannot make this tail much larger without changing the energy spectrum of cosmic ray primaries in such a way that it will be steeper around 65-100 then below and above this region.

Stars for which the angular distribution favors the forward and backward directions are on the right side of Figs. 3 and 4 ($u > 0.5$). Those with an isotropic angular distribution are in the middle and those favoring 90° are at the left side ($u < 0.5$). The number in each square is n_s of that particular star. One would be inclined on first look to conclude that the collisions are isotropic within statistical fluctuations. We then observe, however, that the stars with low multiplicities in Fig. 3 are concentrated on the left side of the histogram whereas those of high multiplicity are to be found at the center and on the right side of it. For illustration stars with $n_s \leq 8$ are specially marked. We observe further that the histogram of *all* α -stars resembles that of the high multiplicity part of the «p» stars but is qualitatively different from the total «p» histogram. This leads us to the conclusion that the «p» histogram contains two types of stars one of which is concentrated on the left side. It is plausible to attribute a part of these stars to mesons. Indeed, according to the Bombay group (¹⁹), mesons from meson-nucleus-collisions are preferentially produced in the backward direction in the c.m. system. Since we defined the c.m. system through the symmetry requirement our γ_c will be too small and will project the laboratory angles only half way back thus giving rise to the observed angular distribution. This process is schematically indicated in Fig. 5. From geometrical consideration of our stack we should expect about 10-15 stars out of our 65 to be due to mesons; so that the meson hypothesis is also quantitatively adequate to explain the extreme left part



of the histogram. As an additional check we looked at the stars produced by neutral particles. Our statistics is too poor to enable us to make a significant statement but the indication is that these stars look rather like « α » stars and not like «p» stars.

The possible existence of two types of stars (e.g. proton and meson stars) has first been put forward by DILWORTH *et al.* (⁷) and later by HOANG (⁸) and BERTOLINO and PESCEITI (¹¹). However, their suggestions that the two types

Fig. 5. - Schematic [representation of the transformation of angles for meson produced stars. a.c.m.=apparent c.m. as obtained by the symmetry requirement.

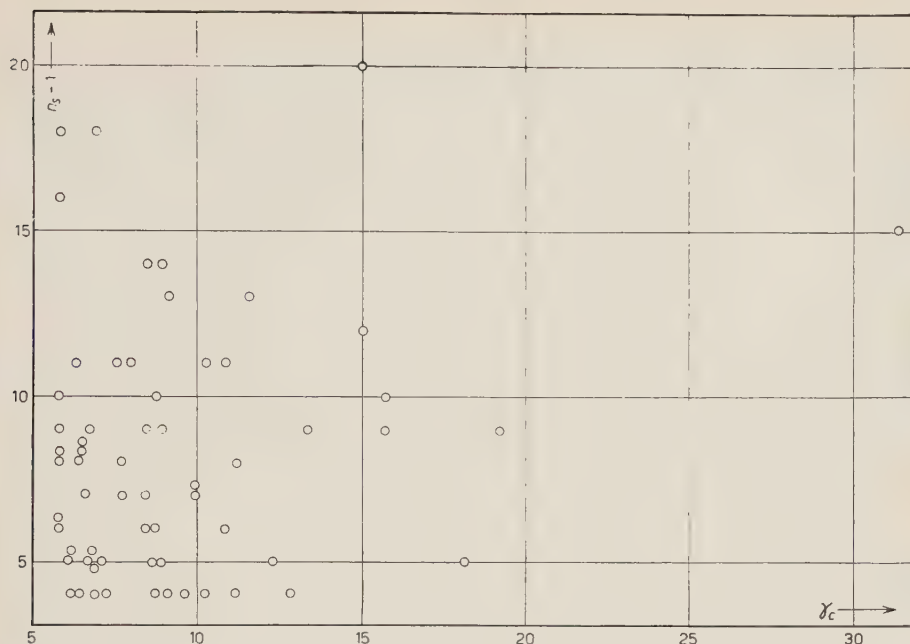


Fig. 6. — A plot of $(n_s - 1)$ versus γ_c as defined by the median angle. Two stars of $n_s = 33$ and 35 are not shown.

of stars appear as separate groups on a n_s versus γ_c plot is not supported by our data (Fig. 6).

It is of interest to note that if we accept the meson hypothesis then the mean multiplicity of the bona fide proton stars will increase and be even closer to that of the α -stars.

There are two different theoretical approaches to the question of anisotropy in the c.m. system. According to FERMI⁽²⁴⁾ the anisotropy is a result of the conservation of angular momentum only. Strong anisotropy should go together with low multiplicity; i.e., stars with low multiplicity should be found on the right side of Figs. 3 and 4. This is not confirmed by our data. According to HEISENBERG⁽²⁵⁾ and LANDAU⁽²⁶⁾ also central collision should show an anisotropy due to the interactions of the mesons in the Lorentz contracted hot volume. Here the anisotropy should be an increasing function of γ_c . We cannot detect such an increase but more data are required to draw a definite conclusion. Further work on this point is in progress.

⁽²⁴⁾ E. FERMI: *Phys. Rev.*, **81**, 683 (1951).

⁽²⁵⁾ W. HEISENBERG: *Zeits. f. Phys.*, **133**, 65 (1952).

⁽²⁶⁾ L. D. LANDAU: *Izv. Akad. Nauk SSSR, Ser. Fiz.*, **17**, n. 1 (1953).

5. - The Elasticity of Nucleon-Nucleus Collisions.

The elasticity ε i.e. the fraction of energy retained by the nucleons in nuclear collisions is a parameter of great interest. HOANG⁽⁸⁾ suggested a method for the determination of the elasticity in the c.m. system. His method is based on the following assumptions:

- 1) All mesons have the same energy in the center of mass system, i.e. the same velocity β_0 .
- 2) This $\beta_0 < \beta_c$. Hence there exists a maximum observable angle in the laboratory system θ'_{\max} for the shower particles.
- 3) The largest angle observed in the laboratory system is identified with θ'_{\max} .

It is mainly the third assumption which in our opinion makes this method somewhat questionable. The angular distribution in the laboratory system is strongly peaked in the forward direction and tails off towards larger angles. It is evident, therefore, that for a given energy the probability of finding a track in the tail of the distribution increases with the multiplicity. Using the largest angle of the shower as a measure for the elasticity one then finds that it decreases with n_s . This in itself is a reasonable result but one cannot conclude from this trend the existence of a θ'_{\max} in particular since the largest observed angle is subject to great fluctuations.

A different method for determining the average elasticity directly in the laboratory system has been suggested by WALKER and GREISEN⁽²⁷⁾. They use as a measure of the elasticity the ratio of the number of stars produced by neutrons (N) to that of singly charged particles (C) at or above a certain energy. This ratio depends on the elasticity of the collision, the primary spectrum and the multiplicity of meson production. In reality these quantities depend on the energy. But one may try to obtain some rough estimates by taking reasonable average values. WALKER and GREISEN applied this method to a counter experiment and had introduced many corrections to the measured values of N and C . The advantage of the Walker-Greisen experiment is that it was made at mountain altitudes and therefore the results are independent of the conditions at the top of the atmosphere.

We wish to use the ratio of N/C obtained from photographic emulsions. This has several advantages and disadvantages compared with the W.G.-experiment.

⁽²⁷⁾ K. GREISEN and W. D. WALKER: *Phys. Rev.*, **90**, 915 (1953).

1) No corrections are required for the experimental values. At the energies under consideration ($\gamma > 65$) the identification of p and n stars is assured.

2) In the upper atmosphere the ratio N/C depends only weakly on the multiplicity of pion production and their subsequent probability of colliding with air nuclei since the main contribution to the excess of C over N comes from the primary protons.

3) In our particular case the flight level was too high (16 g/cm^2). We obtained the values $N/C = (10 \pm 4)\%$. In addition the result is predominantly dependent on the relative flux of primary protons, α -particles and heavier nuclei. Using the model of α air nucleus collisions suggested by HABER-SCHAIM and YEKUTIELI⁽²⁸⁾ and a relative flux of 10:1 of protons to α -particles we find $N/C = 9.4\%$ with an elasticity of $\varepsilon = 0.17$ and $N/C = 15\%$ with $\varepsilon = 0.5$ as suggested by WALKER-GREISEN. The effect of primaries heavier than α -particles was only approximately taken into account. An exact treatment would have increased the value of N/C in both cases.

This method would give more reliable results when applied to a flight at $\sim 70 \text{ g/cm}^2$ residual pressure (22 km) because at that altitude the importance of the primary α -particles will be reduced and the sensitivity to the meson multiplicity will still be small.

The measured value is also in agreement with that calculated by HABER-SCHAIM and YEKUTIELI⁽²⁸⁾ on the basis of the Fermi theory⁽²⁴⁾.

6. — Acknowledgments.

It is a pleasure to express our gratitude to Prof. F. G. HOUTERMANS who suggested the investigation of the α -stars and to Prof. CH. PEYROU for their interest and encouragement. Drs. M. TEUCHER and W. THIRRING have contributed generously of their time for many valuable discussions. Finally we are indebted to Mrs. B. MESMER, R. MÜLLER and T. RIESEN for the careful scanning of the plates and to Miss H. HUWYLER and Mrs. H. THIRRING for general technical assistance.

This work was supported by the Schweizerischer Nationalfonds zur Förderung der Wissenschaftlichen Forschung.

⁽²⁸⁾ U. HABER-SCHAIM and G. YEKUTIELI: *Nuovo Cimento*, **11**, 172 (1954).

RIASSUNTO (*)

Si presentano e analizzano i risultati di una ricerca sistematica eseguita su emulsioni nucleari esposte in voli a grande altezza. Si trova che alle alte energie il volume del nucleo colpito non riveste grande importanza per quanto riguarda il numero di particelle dello sciame generato. Anche la molteplicità dei mesoni prodotti è uguale sia per le particelle α che per i protoni. Si descrive la distribuzione angolare delle particelle dello sciame nel sistema del c.m. e si portano prove a sostegno dell'asimmetria delle collisioni mesoni-nucleo. Si discute infine brevemente l'elasticità delle collisioni nucleone-nucleo.

(*) *Traduzione a cura della Redazione.*

LETTERE ALLA REDAZIONE

(La responsabilità scientifica degli scritti inseriti in questa rubrica è completamente lasciata dalla Direzione del periodico ai singoli autori)

Λ^0 Excited State (*).

D. C. PEASLEE

Purdue University - Lafayette, Ind.

(ricevuto il 26 Ottobre 1954)

Among charged hyperon decays the best-supported experimentally ⁽¹⁾ appear to be the following:

$$(1) \quad \Lambda^- \rightarrow \pi^- + \Lambda^0 + Q_1 \quad Q_1 \sim 60 \text{ MeV}$$

$$(2) \quad \begin{cases} Y^\pm \rightarrow \pi^\pm + n + Q_2 \\ Y^+ \rightarrow \pi^0 + p + Q_2 \end{cases} \quad Q_2 \sim 120 \text{ MeV}$$

The decay (1) is in accord with a general scheme ⁽²⁾ of V-particles. The present note suggests that decay (2) is most readily incorporated into this scheme by taking the Y^\pm to be an excited state of the Λ^0 . It is of the same generic type

as the Λ^0 , being a fermion with integer isotopic spin and charge number t_z . The ground state of the Λ^0 has $t=0$, and the excited state Y evidently has $t=1$. The excitation energy is $(Y - \Lambda^0) = Q_2 - Q_0 = 120 - 37 \approx 85 \text{ MeV}$, so that the Y^\pm states cannot decay to Λ^0 by rapid emission of a π ; they must decay to a nucleon plus π by a weak interaction of the same sort that induces Λ^0 decay. The state Y^0 does not have this metastability, since it decays to Λ^0 by rapid γ emission.

Indirect evidence in support of this interpretation comes from observations ⁽³⁾ on the nuclear capture of τ^- -mesons with subsequent Λ^0 production. The observations indicate that this process occurs predominantly with production of a single π -meson. We suppose that a single nucleon in the nucleus absorbs the τ^- yielding a shortlived hyperon state of the Λ^0 class with some 310 MeV excitation above the ground state. If the excited state has $t=0$ (Λ^0 -type), it can decay to the Λ^0 ground state by emission of 0, 2, ... π -mesons. If it has $t=1$ (Y -type), it decays to Λ^0 by emis-

(*) After this was written, Prof. E. GUTH kindly showed the author a preprint of M. GELL-MANN and A. PAIS, *Glasgow Conference Proceedings* (1954), where the discussion of « Model II » coincides in part with the present note.

⁽¹⁾ A partial list of references is: R. ARMENTEROS, K. BARKER, C. BUTLER, A. CACHON and C. YORK: *Phil. Mag.*, **43**, 597 (1952); A. BONETTI, R. LEVI SETTI, M. PANETTI and G. TOMASINI: *Nuovo Cimento*, **10**, 1736 (1953); C. D. ANDERSON, E. W. COWAN, R. B. LEIGHTON and C. A. van LINT: *Phys. Rev.*, **92**, 1089 (1953); C. CASTAGNOLI, G. CORTINI e A. MANFREDINI: *Nuovo Cimento*, **12**, 464 (1954); E. W. COWAN: *Phys. Rev.*, **94**, 161 (1954); further references are in some of these articles.

⁽²⁾ M. GELL-MANN: *Phys. Rev.*, **92**, 833 (1953).

⁽³⁾ H. DE STAEBLER: *Phys. Rev.*, **95**, 1110 (1954); J. E. NAUGLE, E. P. NEY, P. S. FREIER and W. B. CHESTON: *Phys. Rev.* (in press).

sion of 1, 3, ... π -mesons. The observations therefore indicate that $\tau^- + N \rightarrow Y^*$ exceeds $\tau^- + N \rightarrow \Lambda^{0*}$. There are two reasons to expect this predominance: (i) the nucleon N can be either n or p for Y^* production but can be only p for Λ^{0*} production. For the excitation energy available here, Y^{0*} decay will proceed predominantly by π^0 rather than Y emission. (ii) The behavior of a complex system at energy E is dominated by the eigenstate of the system with energy E_0 nearest to E . If the only states involved are $t=0$ at $E_0=0$ and $t=1$ at $E_0 \approx 85$ MeV, this rule somewhat favors a Y -type state at $E \approx 310$ MeV.

According to this interpretation the production rates of Y and Λ^0 mesons by cosmic radiation should not differ by many orders of magnitude. Some bias in favor of Λ^0 production is presumably associated with the fact that the Y is stable by only ~ 55 MeV against rapid decay into a Λ^0 by π -emission, while the Λ^0 is stable by ~ 225 MeV against rapid π -decay into a Y .

The bound excited state of the Λ^0 is

reminiscent of the virtual «excited state» of the nucleon, with one important difference: the «resonance» in π -nucleon scattering does not absolutely require description in terms of a phenomenological excited state; it can be obtained from field theoretical calculations in which the nucleon is a fundamental particle without intrinsic isobars⁽⁴⁾. This second alternative is not possible for Λ^0 if it really has $t=0$, as single emission of a π cannot occur with isotopic spin conservation, in contrast to the nucleon case. It therefore seems that the Y states can have only a phenomenological description at present.

Pair emission of π -mesons is of course possible for the Λ^0 . The relatively weak and constant binding of the Λ^0 in light nuclei — of order 2 ± 2 MeV for all known cases — is apparently a measure of the meson-pair contribution to nuclear forces, if the τ -exchange forces between a Λ^0 and a nucleus are taken to be non-repulsive.

(4) E. g., G. F. CHEW: *Phys. Rev.*, **94**, 1755 (1954); L. SARTORI and V. WATAGHIN: *Nuovo Cimento*, **12**, 260 (1954).

On a Systematization of Heavy Mesons and Hyperons.

J. RAYSKI

Department of Physics, Nicholas Copernicus University, Toruń

(ricevuto il 3 Novembre 1954)

The best known particles (e.g. pions, nucleons) are characterized by means of some irreducible representations (single or double valued) of the group of rotations and reflections. But it is the group that is all important so that it must appear strange why only some and not all irreducible representations should be realized in physics. This defect of the contemporary field theory will be removed if we assume that to every irreducible representation corresponds a field. Then the situation will be more satisfactory from a group-theoretical viewpoint, moreover, we shall possess a clue for understanding the existence of various types of particles and their properties.

For a systematization of heavy particles we may limit ourselves to the 3-dimensional euclidean space. The intrinsic properties should manifest themselves also in the state of rest so that they are not expected to have anything to do with the time variable. The interesting group is that of rotations (including reflections) and the unitary unimodular group.

We propose tentatively the following assignments:

Pion family (*ps*-tensor).

spin	0	1	2	3
parity	—	+	—	+
name	π	τ	?	?

Nucleon family

spin	1/2	3/2	5/2
relative parity	+	—	+
	(—)	(+)	(—)
name	N^+	Y^-	?

Theton family (tensor)

spin	1	2	3
parity	—	+	—
name	$\theta(\chi)$	κ	?

Λ -family

spin	1/2	3/2	5/2
relative parity	—	+	—
	(+)	(—)	(+)
name	$\Lambda^0(\Omega^\pm)$?	?

The above classification is consistent with the following postulate: To every irreducible representation of the group of rotations and reflections corresponds a particle type, except for the trivial representation by unit matrices (non-existence of a scalar particle).

The combined laws of conservation of angular momentum and parity yield absolute selection rules forbidding the decay of τ into two pions and a decay of Y^- into a nucleon and a pion.

The apparent contradiction between long life times (10^{-8} - 10^{-16} s) of heavy particles and their copious production seems to be resolved by the «two coupling constants hypothesis». We assume the usual type of coupling between bosons and fermions $g\bar{\psi}\psi\varphi$ (where the Dirac matrices, symmetrization, etc., have been disregarded for simplicity). The value of g may depend upon the type of field quantities involved in the interaction. We distinguish:

I) Interaction involving the ps -tensor (pion) family.

II) Interaction involving the tensor (theton) family.

In each case we distinguish two alternatives:

A) Both spinor field quantities belong to the same family.

B) Both spinor field quantities belong to two different families.

Then, each of the four cases may be subdivided according to parities of the fields in question:

a) Both ψ and $\bar{\psi}$ have the same (opposite) relative parities which will be denoted by $+$ ($-$).

b) The boson field quantity φ possesses an even (odd) parity denoted again by $+$ ($-$).

There are 16 cases altogether and to each case we attach either a large (G)

or a small (g) coupling constant to account for the long life time and copious production of heavy particles:

IA				IB			
1	2	3	4	1	2	3	4
a	+	+	-	a	+	+	-
b	-	+	-	b	-	+	+
G	g	g	?	g	$g?$	g	$g?$

IIA				IIB			
1	2	3	4	1	2	3	4
a	+	+	-	a	+	+	-
b	-	+	+	b	-	+	+
g	g	?	?	?	?	G	$G?$

Let us discuss a few of them. A large coupling constant must be assumed in the case I A1 to account for the

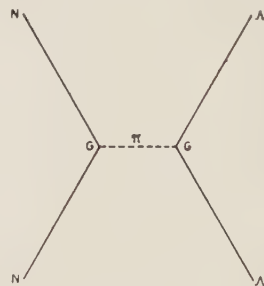


Fig. 1.

(usual) nuclear forces. But then we have automatically the same situation if replacing a nucleon by a hyperon. This accounts immediately for the Danysz effect (Λ -nucleus) (Fig. 1). Small values g in the cases I A2, II A1, II A2, I B1, and I B3 account for the long life times of τ , θ , κ , Y and $\Lambda(\Omega)$ respectively. A small g in I A3 prevents a rapid decay of Y directly into a proton and two

pions. The reversed process to IB3 cannot yield a copious production of Λ . The only way to account for its copious production is to assume a large value G either in the case IIB3, or IIB4, or IB4. But then we have a simultaneous production of a hyperon together with a heavy meson (Fig. 2). Cosmotron evidence shows that this is actually the

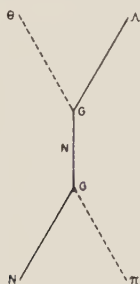


Fig. 2.

case in IIB3 (and IIB4?) but not in IB4 (there has never been observed a simultaneous production of Λ and τ .)

Concluding it may be stated that all the experimental facts known at present are consistent with the above scheme. Two striking facts: the Λ -nuclei, and a simultaneous production of hyperons and heavy mesons, follow compulsorily from the hypothesis of two coupling constants. The cascade particle Y could be predicted if it were not known yet.

Further facts can be predicted: 1) A simultaneous production of pairs of hyperons (Fig. 3). 2) The existence of a long

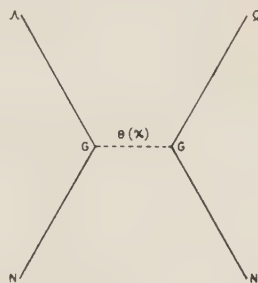


Fig. 3.

lived meson belonging to the pion family with spin 3 (mass about 1500). 3) The existence of a long lived hyperon belonging to the Λ -family with spin 3/2 (mass about 3000).

The values of the masses can be predicted from the formulae (10) and (12) given in our previous note ⁽¹⁾. In particular, assuming that the field mass is negligible in comparison with the total nucleonic mass, $M_{\frac{3}{2}} = \sqrt{2} M_{\frac{1}{2}} = 2597$ in good agreement with the mass value of the cascade hyperon Y^- . To account for the masses of the Λ -family we have to assume a field mass $\kappa/2 \cong 350$.

A full account will be published in *Acta Phys. Polonica*.

⁽¹⁾ J. RAYSKI: *Nuovo Cimento*, **12**, 815 (1954).

On Intermittent Discharges in Air at Low Pressure.

D. BRINI, O. RIMONDI and P. VERONESI

Istituto di Fisica dell'Università - Bologna

(ricevuto l'8 Novembre 1954)

With the experimental equipment and discharge tube described in a previous paper ⁽¹⁾ we have measured the frequencies of the intermittent discharges at the end of the first kind and the beginning of the second in air at low pressure. The measurements were carried out for the purpose of investigating the behaviour of such frequencies with variations in the pressure of the gas contained in the tube and the distance between the electrodes.

The results, which are briefly reported here, were obtained for one value only of E and R ; namely $E=1\,050$ V, $R=1$ M Ω . The transitions from the end of the first kind to the beginning of the second were obtained by varying C . Fig. 1a and b which summarizes these results, reports the frequencies of the intermittent discharges at the end of the first kind and the beginning of the second as a function of the pressure for different values of the distance between the electrodes. In both cases it is possible to see that, for each value of the distance between the electrodes, there exists a sufficiently well-defined pressure range, within which the

frequencies fall abruptly. Such a pressure range is the better defined as the distance between the electrodes is shorter; its definition is more marked in the discharges at the beginning of the second kind than in those at the end of the first kind. In the case of the second kind it is also possible to see that the product of the distance between the electrodes by pressure value, to which the maximum frequency corresponds, is constant within the limits of error; i.e.

$$p_M d = \text{const},$$

where with p_M we have indicated the maximum frequency pressure. The ratio between the frequencies at the beginning of the second kind and those at the end of the first kind, for values of pressure corresponding to the flat parts of the curves of the figure, diminishes slowly. We think, however, that these results are not so significant as might seem at first sight; in fact they refer to one value only of E and R . To obtain information which is much more strictly dependent on the discharge tube and not influenced by the external circuit, it would be necessary to look for the maximum frequency obtainable for the variations of E and R for every value of p and d .

⁽¹⁾ D. BRINI and P. VERONESI: *Nuovo Cimento*, **10**, 1662 (1953).

A sufficiently plausible explanation of the experimental results obtained can be given in the following manner.

The frequency of the intermittent

breakdown tension increases, the frequencies diminish and vice versa. A verification of this hypothesis, carried out by taking up two Paschen's curves

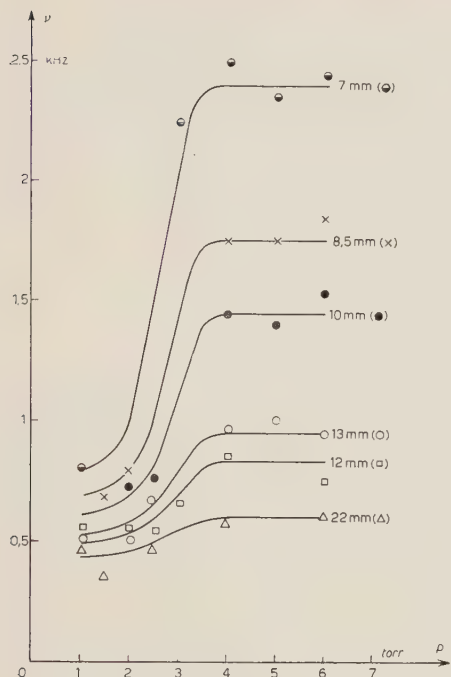


Fig. 1-a - First kind.

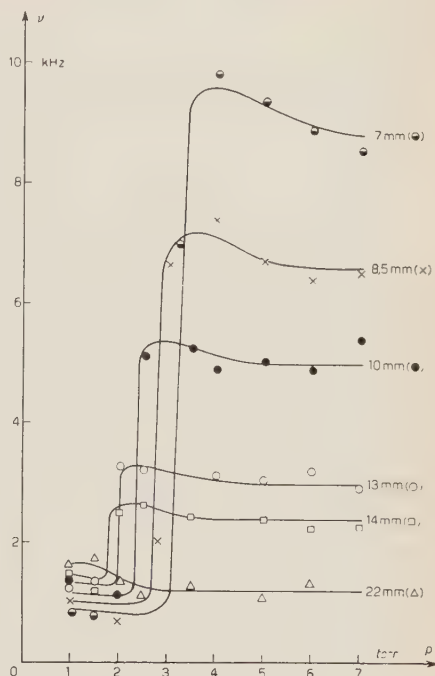


Fig. 1-b - Second kind.

periodic discharges depends in a marked manner on the difference between the applied tension and the corresponding one at the end of Townsend's phase. This last is not very different from that of the spark breakdown of Paschen's law. In the conditions of pressure and distance between the electrodes, in which the

corresponding to two different pressures and varying the distance between the electrodes, showed a qualitative agreement with the experimental results.

Such a conclusion, however, might seem satisfying, but needs further experimental verification in order to be accepted as a whole.

Sul contributo del campo elettrostatico alla quantizzazione della massa.

E. MINARDI

Aosta

(ricevuto il 10 Novembre 1954)

In una precedente nota ⁽¹⁾ si è presentato un esempio di quantizzazione della massa nel caso di particelle neutre. Per quanto, come già si è osservato, non vi siano finora sufficienti argomenti per accettare gli operatori di massa proposti nella suddetta nota e il metodo presentato possa essere considerato soltanto come un esempio di particolare semplicità di quantizzazione della massa, è forse interessante notare alcuni particolari aspetti che appaiono nella teoria quando si voglia tener conto dell'interazione tra il campo φ descrivente le proprietà interne delle particelle e il campo elettrostatico creato dalla distribuzione di carica associata alla particella stessa.

Limitandoci al caso di una particella spinoriale si ha, com'è noto, nel sistema del suo baricentro

$$(1) \quad -\alpha \cdot \mathbf{p}^{(\eta)} = m.$$

Sembra naturale assumere che la densità di carica nell'interno della sfera di raggio l considerata nella precedente

nota sia $\varphi = e\varphi^*\varphi$ e che per tener conto dell'interazione con il campo elettrostatico si debba sommare al primo membro della (1) la energia mutua elettrostatica U relativa alla distribuzione di carica di densità ϱ :

$$(2) \quad U = \frac{1}{2} \int e\varphi^*\varphi V(\eta) d\tau_\eta.$$

Pertanto il potenziale elettrostatico $V(\eta)$ soddisfa all'equazione di Poisson

$$(3) \quad \Delta_\eta V(\eta) = -4\pi e\varphi^*(\eta)\varphi(\eta).$$

Con ciò, ed effettuando la sostituzione operatoriale $p_\nu^{(\eta)} \rightarrow -i(\partial/\partial\eta_\nu)$, passando inoltre in coordinate polari e ponendo

$$(4) \quad \varphi(r) = \begin{pmatrix} Z(r) \\ Y(r) \end{pmatrix},$$

con $r = (\eta_1^2 + \eta_2^2 + \eta_3^2)^{\frac{1}{2}}$, si ottiene dalla (1):

$$(5a) \quad \frac{d^2 Y}{dr^2} + \frac{2}{r} \frac{dY}{dr} + \left[\left((m - U)^2 - \frac{k(k+1)}{r^2} \right) Y = 0, \right.$$

⁽¹⁾ E. MINARDI: *Nuovo Cimento*, **11**, 694 (1954). Approfittiamo di questo riferimento per correggere alcuni errori della suddetta nota. La formula (5) deve scriversi: $P_\nu^{(2)}\eta^\nu\varphi = 0$; il secondo membro della (10) e della (11) deve essere cambiato di segno.

$$(5b) \quad Z = c - \int_0^r \left[(m - U)^2 Y - \frac{k-1}{r(m-U)} \left(Y' + \frac{1+k}{r} Y \right) \right] dr.$$

La condizione $Y(l)=0$ fornisce per la massa m la seguente equazione, analoga alla (19) della nota precedente:

$$(6) \quad J_{k+\frac{1}{2}}[(m-U)l] = 0.$$

La soluzione è

$$(7) \quad m = m_{0n} + U,$$

ove m_{0n} è la massa della particella neutra descritta dalla n -esima radice dell'equazione $J_{k+\frac{1}{2}}(ml)=0$, e U è calcolata con la (2) e con l'equazione di Poisson (3). Si ha così un esempio del modo con cui si può tener conto del contributo del campo elettrostatico al valore della massa.

Se come valore di m_{0n} si prende la massa del neutrino si ottiene semplicemente dalla (7) che la massa è eguale all'energia elettrostatica. In questo caso il sistema della (3) e (5) è rigorosamente

risolvibile. Si ha infatti

$$(8) \quad \varphi = \begin{pmatrix} c \\ 0 \end{pmatrix},$$

cosicchè le densità di massa e di carica sono omogenee entro la sfera e cadono bruscamente a zero in $r=l$. Una tale particella deve considerarsi particella « classica », poichè nell'espressione di U non entra la costante di Planck; le altre particelle ottenute dalla (7) devono invece considerarsi di origine quantistica poichè m_{0n} tende a zero se $\hbar \rightarrow 0$. Notiamo che nella teoria classica dell'elettrone di Lorentz, nel caso di una densità di carica omogenea, la massa è ottenuta con un raggio della particella uguale al valore $l=2,29 \cdot 10^{-13}$ cm usato nella precedente nota. Notiamo inoltre che l'esistenza di una particella descritta dalla (8) appare nel presente formalismo come una conseguenza dell'operatore di massa per particelle con spin 1/2 poichè le stesse proprietà non possono essere ottenute partendo dall'invariante $p_\nu^{(\eta)} p^{(\eta)\nu} = m^2$.

Queste considerazioni sembrano indicare che una teoria relativistica non locale degli elettroni in interazione con il campo elettromagnetico, svolta in questa direzione, possa essere interessante.

A Negative Hyperon Decaying in Flight.

A. DEBENEDETTI, C. M. GARELLI, L. TALLONE and M. VIGONE

Istituto di Fisica dell'Università - Torino

Istituto Nazionale di Fisica Nucleare - Sezione di Torino

(ricevuto il 16 Novembre 1954)

An example of a negative hyperon decaying in flight has been observed in a nuclear emulsion. The event has been found during the regular scanning of a plate flown at 80 000 ft: from a star of the type $11+14\alpha$ is emitted a grey track which travels 927μ ; from point A (fig.1) starts a track of lower ionization which, after 16590μ comes to rest and gives rise to a σ -star.

The hypothesis of the scattering of a π -meson emitted from the star can be excluded because of the change of ionization. On the other hand, no recoil track is visible at point A . Therefore it seems reasonable to think that an unstable heavy particle decays in flight at point A , giving rise to a negative π -meson.

The direct determination of the mass of the primary particle is affected by a large error due to the short range of the track. However the value obtained from ionisation-scattering measurements, $2300 \pm_{-640}^{+270} m_e$, suggests the hypothesis that the heavy primary is probably a hyperon.

The $p\beta$ of the unstable primary is $250 \pm 82 \text{ MeV}/c$.

The secondary particle is emitted at an angle of $147^\circ 16' \pm 15'$ with the direction of the primary. The energy of

the π -meson can be obtained from its range:

$$E_{\pi^-} = 30.54 \pm 0.88 \text{ MeV}.$$

This event can be interpreted according to two schemes of decay:

$$(a) \quad Y^- \rightarrow \Lambda^0 + \pi^- + Q$$

$$(b) \quad Y^- \rightarrow n + \pi^- + Q'.$$

If we assume that the neutral particle is a Λ^0 , we find:

$$Q = 97 \pm 15 \text{ MeV},$$

if we assume that the neutral secondary is a neutron, we find:

$$Q' = 107 \pm 15 \text{ MeV}.$$

All data on charged hyperons whose charged secondary is a light meson can be summarized in the following way:

— there is some evidence of events of the type (a) in cloud chamber experiments, and the Q value is about $67 \text{ MeV}^{(1,2)}$;

⁽¹⁾ C. D. ANDERSON, E. W. COWAN, R. B. LEIGHTON and V. A. J. VAN LINT: *Phys. Rev.*, **92**, 1089 (1953).

⁽²⁾ E. W. COWAN: *Phys. Rev.*, **94**, 161 (1954).



Fig. 1.

— the evidence of the positive hyperons decaying in a neutron and a π^+ with a Q value of about 110 MeV is well established from the results of cloud chamber and nuclear emulsions work;

— only one case of negative hyperon, found in cloud chamber, has been

interpreted following the scheme (b) ⁽³⁾.

We think that our results are in better agreement with the second scheme of decay, so that they support the hypothesis of the existence of a negative counterpart of the $Y^+ \rightarrow n + \pi^+ + Q$ with the same energy release.

⁽³⁾ W. B. FOWLER, R. P. SHUTT, M. THORNDIKE and W. L. WHITTERMORE: *Phys. Rev.*, **93**, 861 (1954).

On Narrow Showers of Pairs of Charged Particles.

A. DEBENEDETTI, C. M. GARELLI, L. TALLONE, M. VIGONE and G. WATAGHIN

Istituto di Fisica dell'Università - Torino

Istituto Nazionale di Fisica Nucleare - Sezione di Torino

(ricevuto il 16 Novembre 1954)

The purpose of the present note is to make a preliminary report on two high energy events of pair production observed in a stack of stripped nuclear emulsions Ilford G5, 600 μ thick, 4" \times 6", flown at 80 000 ft during the Sardinia expedition 1953. These events seem to be of the same type as the one described recently by SCHEIN *et al.* ⁽¹⁾. The common feature of these events is that the whole picture consists of very energetic pairs of charged particles (presumably pairs of electrons), and no other charged track or prong is observed in the neighbourhood. The number of these pairs is rapidly increasing on a path of the order of few cm; the half cone enclosing all the tracks is of about 10^{-3} rad. In both cases the point of production of the first pair is inside the emulsion; we are making a special scanning in the backward direction: till now we did not find any event related with the pair showers.

Recently, during the regular scanning, two other events have been found that look very similar to the cases described in this paper (one in the same

stack and the other in another). They will be studied as soon as possible.

The data till now available on the two events are the following:

	Event 1	Event 2
Zenith angle	61°	32°
Angle to the emulsion surfaces	31°	16°
Total length	3 cm	5 cm

We tried to measure the angle between the tracks of each pair; under the assumption that they are electron pairs, we calculated the energy of the parent photons from the formula given by STEARNS ⁽²⁾ for the equipartition of the energy. These values are probably underestimated if the separation is due to the multiple scattering and if the energy of the photon is not equally divided.

The distance between the second pair and the third one of the event 2 is very difficult to explain if the parent photons are directly produced in some explosive

⁽¹⁾ M. SCHEIN, D. M. HASKIN and R. G. GLASSER: *Phys. Rev.*, **95**, 855 (1954).

⁽²⁾ M. STEARNS: *Phys. Rev.*, **76**, 836 (1949).

Event 1.

Pair	Distance to the point of production of the first pair (μ)	Angle of the pair (rad.)	Minimum energy of the photon (GeV)
1	—	$2 \cdot 10^{-4}$	55
2	760	$2 \cdot 10^{-4}$	55
3	2 200	10^{-3}	10
4	5 030	10^{-3}	10
5	6 800	10^{-3}	10
6	11 820	10^{-2}	0.7
7	12 160	$6 \cdot 10^{-4}$	17
8	16 560	10^{-2}	0.7
9	18 670	$6 \cdot 10^{-4}$	17
10	19 500	10^{-3}	10
11	19 850	$2 \cdot 00^{-3}$	4
12	20 000	10^{-3}	10
			199.4 GeV

Event 2.

Pair	Distance to the point of production of the first pair (μ)	Angle of the pair (rad.)	Minimum energy of the photon (GeV)
1	—	10^{-3}	10
2	550	$2 \cdot 10^{-4}$	55
3	27 240	10^{-3}	10
4	27 440	$6 \cdot 10^{-4}$	17
5	27 690	$2 \cdot 10^{-3}$	4
6	30 510	10^{-2}	0.7
7	32 990	—	—
8	35 660	$2.5 \cdot 10^{-2}$	0.25
9	36 420	10^{-3}	10
10	37 240	$4 \cdot 10^{-4}$	27
11	37 290	$4 \cdot 10^{-4}$	27
12	39 160	$5 \cdot 10^{-4}$	20
13	39 560	10^{-2}	0.7
14	39 760	10^{-3}	10
15	41 110	$3 \cdot 10^{-3}$	3
16	41 510	$2 \cdot 10^{-3}$	4
17	42 760	10^{-3}	10
			208.65 GeV

process; the interpretation is easier if we think that they come from the decay of several neutral unstable particles (π_0 , and other particles having a slightly greater lifetime), and assume that the measured energies are underestimated.

A plausible interpretation of these events on the basis of the presently available data could be derived assuming that a very energetic neutral unstable particle is decaying or annihilating in flight. The assumption of SCHEIN *et al.* ⁽¹⁾ of a shower of pure photons produced in an annihilation process becomes compatible with the event 2, if one supposes that the neutral unstable particle suffers

a transition with emission of two photons before the explosion.

Another plausible interpretation is that a glancing collision of two neutrons gave rise to the formation of π_0 and other neutral particles with an extremely anisotropic distribution in the center of mass system.

The measurements are in progress and we hope to be able to report on new results and their interpretation in a forthcoming paper.

We are glad to acknowledge the constant help and interest of Professor R. DEAGLIO.

Sullo spettro della componente fotonica nella bassa atmosfera.

C. CERNIGOI e G. POIANI

Istituto di Fisica dell'Università - Trieste

Istituto Nazionale di Fisica Nucleare - Sezione di Padova

(ricevuto il 18 Novembre 1954)

È noto che la componente fotonica nell'atmosfera viene alimentata principalmente da tre processi distinti e cioè: dai processi d'urto delle particelle μ cariche, dai processi di disintegrazione delle stesse e dai processi di disintegrazione dei mesoni π^0 . Lo spettro della fotonica è pertanto formato dalla sovrapposizione di tre spettri derivanti ciascuno dai tre menzionati processi. È tuttavia alquanto difficile valutare sperimentalmente l'andamento dello spettro ed il contributo che ad esso portano i tre processi.

In questi ultimi tempi sono state fatte alcune ricerche al livello del mare con contatori di G. e M. ⁽¹⁻³⁾ e con dispositivi misti comprendenti contatori a scintillazione ⁽⁴⁾, per misurare l'andamento dello spettro; altre ricerche sono state fatte in quota con lastre, per valutare prevalentemente il contributo a detta radiazione dei processi di disintegrazione dei mesoni π neutri, attraverso

la produzione di coppie ⁽⁵⁾. I risultati sono abbastanza concordanti per poter affermare che lo spettro della fotonica, verso le alte energie, è uno spettro di potenza, ma per quanto riguarda l'esponente dello spettro, i valori ottenuti non sono in grande accordo, andando, per lo spettro integrale da un minimo di 1,07 ⁽¹⁾ al l.d.m., ad un massimo intorno a due, in quota ⁽⁵⁾. È certo che una tale dispersione di valori è dovuta sia alla diversa sensibilità dei dispositivi sperimentali, sia ad un'effettiva variazione dell'esponente dello spettro con l'energia dei fotoni.

La provenienza dei fotoni contemporaneamente dalle particelle μ cariche e dai mesoni π neutri comporta la formazione di un miscuglio la cui composizione dovrebbe modificarsi con l'altezza, in quanto variano diversamente con l'altezza gli spettri dei due primari. Per indagare su questo punto abbiamo voluto portare al Laboratorio dei Raggi Cosmici della Marmolada (2050 m sul l.d.m) il dispositivo che ci era servito per valu-

⁽¹⁾ J. CLAY: *Physica*, **14**, 569 (1949).

⁽²⁾ E. D. PALMATIER: *Phys. Rev.*, **83**, 197 (1951).

⁽³⁾ C. CERNIGOI e G. POIANI: *Nuovo Cimento*, **11**, 41 (1954).

⁽⁴⁾ C. N. CHOU: *Phys. Rev.*, **90**, 473 (1953).

⁽⁵⁾ A. G. CARLSON, J. E. HOOPER e D. T. KING: *Phil. Mag.*, **41**, 701 (1950); G. BARONI, G. CORTINI, A. MILONE, L. SCARSI e G. VANDERHAEGE: *Nuovo Cimento*, **9**, 867 (1952); K. HINTERMANN: *Helv. Phys. Acta*, **27**, 125 (1954).

tare lo spettro di potenza della componente fotonica al livello del mare ⁽³⁾. Tale impianto, che ripete sostanzialmente la disposizione di JÁNOSY e ROSSI ⁽⁶⁾, consente di misurare l'assorbimento in piombo della fotonica attraverso un telescopio di contatori in coincidenza tripla, coperta da un piatto di contatori in anticoincidenza. Per i dettagli rimandiamo alla precedente nota ⁽³⁾.

Nella figura sono riportati i dati relativi all'assorbimento in piombo della fotonica, al livello del mare (90 m sul l.d.m.) ed alla Marmolada. Esclusa la parte iniziale, i punti suggeriscono un assorbimento essenzialmente esponenziale in entrambe le quote. Usando il metodo dei minimi quadrati abbiamo tracciato le rette che meglio si adattano ai dati sperimentali, limitandoci alla parte centrale dell'assorbimento. L'andamento di quest'ultimo è rappresentabile con la relazione:

$$T(x) = \int_{E_1(x)}^{\infty} \varrho(W) F[W, E_1(x), x_0] dW,$$

in cui $\varrho(W)$ è lo spettro fotonico incidente sull'assorbitore, F una funzione calcolata nel precedente lavoro, $E_1(x)$ l'energia media che gli elettroni di conversione debbono possedere per poter attraversare lo spessore assegnato di piombo e che è indipendente dalla quota. Si vede così che la forma dello spettro influisce sulla curva di assorbimento, e cioè, essendo questa una retta, sulla sua inclinazione. L'aumento dell'intensità della fotonica dalla quota inferiore a quella superiore si riflette in proporzione nel maggior numero di particelle che prendono parte al processo di assorbimento in piombo: la retta superiore indica ri-

spetto a quella inferiore un aumento medio dell'intensità pari a 2,26 volte, di altrettanto dovrebbe essere quindi incrementata l'attività della fotonica. Questo valore è in ottimo accordo con quello

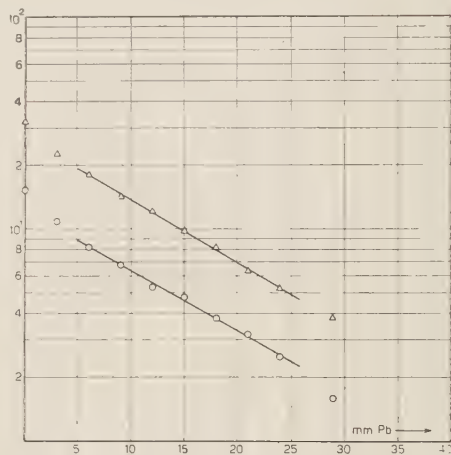


Fig. 1. - Assorbimento della fotonica in Pb. Ascisse: spessori dell'assorbitore; ordinate: numero di impulsi all'ora.

a 90 m. sul l. d. m.: \circ a 2050 m sul l. d. m.: \triangle

ricavabile, per la molle, dalle curve di Rossi ⁽⁷⁾. La retta superiore risulta inoltre leggermente più inclinata rispetto a quella inferiore: infatti il suo coefficiente angolare presenta un aumento del 5%. Anche questo fatto rientra nelle previsioni, in quanto alla maggior quota risulta percentualmente più elevata la partecipazione dei processi di decadimento dai mesoni neutri che, com'è noto, risentono di un assorbimento maggiore di quello presentato dalle particelle μ .

Desideriamo ringraziare sentitamente il prof. A. ROSTAGNI per averci concesso di eseguire le misure nel Laboratorio dei Raggi Cosmici della Marmolada.

⁽⁶⁾ L. JÁNOSY e B. ROSSI: *Proc. Phys. Soc.*, A **175**, 88 (1940).

⁽⁷⁾ B. ROSSI: *Rev. Mod. Phys.*, **20**, 537 (1948).

A. DAUVILLIER — *Le magnétisme des corps Célestes*, nn. 1208 e 1209 delle « Actualités Scient. et Industr. », Hermann, Paris, 1954, con pag. 171 e 161 risp., più alcune tavole fuori testo.

Questi due fascicoli, che fanno parte di una serie di quattro, destinati a questioni di Fisica cosmica, seguono al 1°, dedicato alla genesi, natura ed evoluzione dei pianeti, e trattano del magnetismo dei vari corpi celesti nei suoi vari aspetti e conseguenze.

Il geomagnetismo, del resto esaurientemente trattato in opere come quella di S. CHAPMAN e J. BARTELS (Oxford, 1940), sebbene possa interessarci più da vicino, è qui trattato alla stregua di tanti altri fenomeni nei quali si ravvisa oggi una manifestazione del magnetismo cosmico; ma appunto per questo i libri di DAUVILLIER appaiono più interessanti ed utili, in quanto condensano in un numero non eccessivo di pagine le idee ed i fatti fondamentali inerenti a questo magnetismo.

Nel 1° dei due fascicoli in parola l'Autore, dopo aver richiamato i fondamenti della dinamica dell'elettrone e la teoria che lo Störmer ha sviluppato fin dal 1904 per calcolare la traiettoria seguita da una particella carica che si muove in vicinanza di un dipolo magnetico, passa a considerare il magnetismo stellare e quello solare: per quest'ultimo considera il problema generale, quello particolare delle macchie, e quello della

corona. Vengono infine messe a punto anche le questioni concernenti le onde elettromagnetiche di provenienza cosmica.

Un ultimo capitolo è dedicato alla luce zodiacale che, considerata dall'Autore come legata ai fenomeni della corona solare, sembra essa pure, secondo alcune teorie, manifestazione dei fenomeni magnetici del Sole.

Nel 2° volume sono richiamati invece i principali fatti del geomagnetismo, per dedurne anche la probabile sede. All'origine del geomagnetismo è dedicato un intero capitolo, e un altro è dedicato alle diverse variazioni di magnetismo sulla Terra, incluse quelle di origine extraterrestre, e ai loro effetti meteorologici, nonché alle tempeste magnetiche.

Negli ultimi tre capitoli sono infine trattati i rapporti tra geomagnetismo e raggi cosmici, il magnetismo della Luna e dei pianeti, e i fenomeni elettromagnetici legati alle comete.

Ci sembra che il pregio fondamentale del lavoro di DAUVILLIER, che dovrebbe ora essere completato da un fascicolo sulle aurore boreali e la luminescenza notturna, sia quello di aver raccolto in poca mole fatti e teorie concernenti una vastissima materia, realizzando un libro cui possono con vantaggio attingere i non specialisti anche perchè — sistema che vorremmo vedere più largamente seguito nei libri francesi — i vari argomenti sono stati dal DAUVILLIER corredati da copiose note bibliografiche.

ANGELO DRIGO

E. C. POLLARD - *The Physics of Viruses*. Academic Press Inc., New York, 1953.

L'interesse per la fisica dei sistemi viventi che era molto vivace nel secolo scorso (e basti ricordare l'opera di MAYER, HELMHOLTZ, TYNDALL) è diminuito poi fortemente e solo da circa un decennio si assiste ad un suo rifiorire.

Questo risveglio è giustificato storicamente da un duplice ordine di fattori. Da una parte una raggiunta parziale sistematicità della meccanica quantistica ha permesso l'estensione di questi metodi agli aggregati molecolari; dall'altra parte varie scoperte fondamentali (come, ad esempio, quella di STANLEY sulla produzione di paracrystalli del virus del mosaico del tabacco) hanno messo in luce taluni nessi importanti tra sistemi biologici e modelli fisico-chimici. Negli ultimi anni poi, la microscopia elettronica, i radioisotopi, le grandi macchine acceleratrici, ed i problemi di sicurezza del personale addetto ai reattori nucleari (unitamente ai problemi della valutazione dell'effetto patologico delle radiazioni connesse alle esplosioni atomiche) hanno contribuito ad indirizzare nuove forze alla biofisica.

Contemporaneamente, in sede speculativa i famosi scritti di JORDAN e SCHRÖDINGER sulla fisica delle unità biologiche elementari hanno servito ad orientare i biologi stessi ed a vivificarne gli interessi in questa direzione. Come risultato di questo ampio movimento sperimentale e teorico si ha che oggi gli studi sui geni, sui virus (specie i batteriofagi) e sui nuclei batterici compiuti con mezzi fisici (oltre che biologici e chimici) costituiscono, a detta di alcuni fra i maggiori biologi, il prolegomeno alla futura biologia generale.

Il libro del POLLARD si inserisce autorevolmente in questo quadro di nuovi interessi. Puntualizzando le attuali conoscenze sulla fisica dei virus, il libro si propone di servire come punto di par-

tenza per studi più penetranti e di dimostrare la potenza dei metodi finora usati.

Il POLLARD, professore allo Sloane Physics Laboratory della Yale University, limitando lo studio ai soli virus, differenzia il proprio libro da altri che considerano il più ampio problema della biofisica e dei suoi metodi (come, ad esempio, i noti testi dell'ÜBER e del WEISSLINGER), e ciò gli permette di approfondire la struttura delle unità biologiche elementari. Le conoscenze in questo campo si sono sviluppate molto rapidamente negli ultimi anni, ed è pregio, certo non secondario, del libro darne una sintesi, forse rapida ma esauriente, aggiornata praticamente a tutto il 1953.

Il libro si rivolge essenzialmente ai fisici (ed ai chimico-fisici) e quindi il primo capitolo contiene brevi cenni di virologia atti ad introdurre nell'argomento il lettore non familiarizzato con la biologia.

Nel capitolo successivo vengono studiate le dimensioni, la forma e l'idratazione dei virus alla luce dei più recenti mezzi di indagine. Sono poi raccolti cenni del tutto elementari di microscopia elettronica, e di ultrafiltrazione, diffusione, sedimentazione, viscosimetria, onde dimostrare il cammino fatto negli ultimi 15 anni nei vari campi. Nel caso del microscopio elettronico è forse da rimproverare l'eccessivo sforzo di sintesi che ha tolto la necessaria ampiezza di informazione sulle tecniche di misura e sui risultati. Molto utile risulta il paragrafo sullo scattering dei raggi X a piccolo angolo da parte dei virus. L'aspetto più importante di questa nuova difficile tecnica (richiedente virus molto purificati) è dovuto al fatto che esso permette uno studio differenziato del virus e dell'acqua ad esso associata.

Il III capitolo sui virus e le radiazioni ionizzanti tiene presente l'esistenza di altri libri sulla teoria dell'urto (come, ad esempio, quello del LEA e del TIMOFEEFF-RESSOVSKY), e cerca quindi di dare più che una sistematica dell'argomento quelle

nozioni e quei risultati che permettono di trarre deduzioni di carattere strutturale. Queste inferenze di strutturalistica virale ottenibili dall'analisi degli effetti biologici dell'esposizione a radiazioni ionizzanti costituiscono uno dei più interessanti pregi del libro del POLLARD.

Nel capitolo successivo viene data una descrizione della natura della inattivazione termica dei virus. Questo campo è poco noto, se non al ristretto gruppo degli specialisti, ed indica una buona e promettente linea di attacco, anche se i risultati sono fino ad oggi abbastanza scarsi. Le considerazioni teoriche sull'inattivazione termica degli enzimi e delle proteine sviluppate qualche anno fa sono di guida anche in questo studio.

L'azione biologica dell'ultravioletto, che è stata oggetto di molte ricerche, trova un'ampia descrizione nel cap. VI. I recenti progressi nella purificazione dei virus rendono possibili nuovi importanti risultati: tra l'altro, lo studio dell'assorbimento selettivo delle proteine e dell'acido nucleico, che contribuisce a stabilire l'importanza relativa, nei vari tipi di funzione, degli amino-acidi aromatici. Risultati promettenti si raggiungono combinando questi studi con studi di polarizzazione e di assorbimento a basse temperature.

I capitoli più originali sono indubbiamente il V e l'ultimo, dove si tratta la natura della superficie virale e si espongono i risultati ottenuti per via fisica sulla genetica dei virus e la loro moltiplicazione. Sono oggetto di particolare esame la descrizione dei virus, le forze operanti nella loro moltiplicazione, lo studio della atmosfera ionica; delle forze di doppio strato e di van der Waals, ecc.

Va pure notato che la bibliografia e la maggior parte dei lavori citati riguardano la produzione biofisica americana, mentre sono trascurati, in linea di massima, i contributi di altri paesi. Questo può essere forse giustificato dal grande numero di riviste in cui si trovano sparsi i lavori di biofisica, ciò che rende diffi-

cile il lavoro di sintesi e obbliga l'Autore ad una selezione non sempre felice.

Prima di chiudere questa breve recensione è forse utile ricordare alcune parole della prefazione: « It is significant that the author, starting as a physicist, has, through the study of viruses, developed an understanding of, and sympathy with, biologists, and heightened his already high respect for their penetrating discoveries ».

In questo spirito è da augurarsi che anche nel nostro paese si sviluppi una più intensa collaborazione tra fisici e biologi ed un rinnovato interesse per questo ordine di studi che ha permesso, secondo le parole di SCHRÖDINGER, scoperte che sono fra le più interessanti che la scienza abbia sino ad oggi rivelato.

CARLO CASTAGNOLI

F. TRICOMI - *Equazioni differenziali*. II ed., Einaudi, 1953.

Non è molto frequente il caso che un trattato di matematica pura, scritto con tutto il rigore che questa disciplina richiede, risulti di particolare utilità per un fisico; troppo spesso questi viene posto di fronte ad un linguaggio eccessivamente stenografico, ad elenchi interminabili di definizioni e teoremi senza che alcun cenno aiuti a discriminare il fondamentale dall'accessorio, per non parlare dell'orrore che molti autori mostrano di avere degli esempi riguardanti le applicazioni, che tanto giovano a comprendere le teorie generali a chi colle applicazioni è già familiare. Quando ciò non scoraggia il fisico, lo infastidisce; finisce coll'arrangiarsi da sé, alla garibaldina, col risultato che accanto alla « matematica vera » è nata e prospera tutta una nuova disciplina, la « matematica dei fisici », che purtroppo, bene spesso, ha assai poco in comune colla prima. Troppi sono i lavori di cosiddetta

« fisica teorica » originati esclusivamente da tale situazione, che non sempre trovano, con la dovuta rapidità, nel cestino la loro degna destinazione.

È perciò motivo di profonda soddisfazione leggere un'opera come questa del TRICOMI, che è anzitutto una brillante lezione di arte didattica; il linguaggio vi è piano ed accessibile; il lettore, a cui non si richiedono conoscenze superiori a quelle impartite nel primo biennio dei nostri corsi universitari, è condotto per mano dai primi principi agli sviluppi più avanzati — per accorgersi allora, con grata sorpresa, che non gli si è fatta leggere, in realtà, una sola pagina in più del necessario. Chi ha già conoscenza delle questioni trattate si trova spesso, di fronte all'eleganza e alla semplicità di talune dimostrazioni, ad invidiare il principiante, che può apprendere con assai meno fatica le stesse cose che a lui costarono più di un rompicapo.

Gli argomenti svolti, se certo non esauriscono quelli che un fisico dovrebbe conoscere, sono tuttavia di importanza fondamentale e, diremmo, preliminare: le equazioni differenziali vengono trattate sia nel campo reale che nel campo complesso, cosa quest'ultima di particolare utilità per lo studioso di meccanica quantica; i concetti relativi alle singolarità delle equazioni e dei loro integrali sono svolti con assoluta chiarezza; i metodi di integrazione asintotica vengono

discussi in un lungo ed esauriente capitolo, che in vari punti presenta felici innovazioni rispetto a trattazioni precedenti; lo studio dei problemi ai limiti, più di ogni altro forse importante per un fisico, risulta assai snellito per l'uso di un artificio introdotto dal PRÜFER nel 1926. Di quest'ultima parte si sarebbe forse desiderato uno svolgimento ancora più esteso, in ispecie per quanto concerne i legami colla teoria delle equazioni integrali, solo brevemente accennati; è questo, infatti, uno dei punti più importanti, e più trascurati, nella usuale preparazione matematica dei fisici; abbastanza è detto, tuttavia, perchè lo studioso possa poi muoversi da solo, con sicurezza, nella vasta letteratura sull'argomento.

Come commento finale, vorremmo dire che noi riteniamo assai più utile, per un giovane fisico, la lettura di poche opere su argomenti particolari, che vadano fino al fondo delle cose, che non la digestione di enciclopedici trattati in cui si toccano un po' tutti i soggetti, sempre supponendo però che un fisico non debba entrare nel *sancta sanctorum* dei matematici; la formazione matematica è, riteniamo, assai più importante per il fisico che non l'informazione sulle matematiche. Sotto tale riguardo, l'opera del TRICOMI è indubbiamente da prendersi a testò, ed a modello.

E. R. CAIANIELLO